IL
NUOVO CIMENTO
ORGANO DELLA SOCIETÀ ITALIANA DI FISICA
SOTTO GLI AUSPICI DEL CONSIGLIO NAZIONALE DELLE RICERCHE

VOL. XV, N. 2 *Serie decima* 16 Gennaio 1960

On the Role of the Intermediate Boson in $\mu \to e + \gamma$ Decay (*).

M. E. EBEL and F. J. ERNST
University of Wisconsin - Madison Wis.

(ricevuto il 21 Maggio 1959)

Summary. — The dependence of the branching ratio

$$R(\mu \to e + \gamma)/R(\mu \to e + \nu + \bar{\nu})$$

upon the ratio of cut-off to boson mass and upon a possible boson anomalous moment is discussed. Some of the properties of the boson are inferred from the present experimental data.

1. – Introduction.

It has been suggested that the universal V-A Fermi interaction, which has proven so successful in correlating the experimental facts of β and μ decay, arises via an intermediate charged vector boson which is coupled to fermion pairs. Such a mechanism would not lead to a Fermi interaction involving either four neutral fermions or four charged fermions, and consequently the decays $\mu \to 3e$ and $K^{\pm} \to \pi^{\pm} + 2\nu$ would be suppressed, in agreement with the experimental observations.

(*) Work supported in part by the U.S. Atomic Energy Commission and in part by the Alfred P. Sloan Foundation, Inc.

Whereas the decay $\mu \to e + \gamma$, which has never been observed experimentally, cannot arise from the usual direct four-fermion interaction, it would be possible under the intermediate boson hypothesis if the boson had a non-infinite mass. In fact, it has been asserted that the calculated branching ratio

$$\varrho = R(\mu \to e + \gamma)/R(\mu \to e + \nu + \bar{\nu})$$

turns out to be much too large [1], for an experimental upper limit on the branching ratio has been set by LOKANATHAN and STEINBERGER at $2 \cdot 10^{-5}$, by DAVIS, ROBERTS and ZIPF at 10^{-5}, and by BERLEY, LEE and BARDON at $2 \cdot 10^{-6}$ [2].

The calculation of the $\mu \to e + \gamma$ decay rate is not unambiguous, however, for the process involves divergent integrals, and hence any calculation requires that a high momentum cut-off be supplied. Although the divergence is only logarithmic, and hence for cut-offs *large* compared to the boson mass the branching ratio must be a slowly varying function of the cut-off, this need not be true for cut-offs of the order of magnitude of the boson mass or less. Indeed, it is not to be expected, for the principal contribution to the $\mu \to e + \gamma$ decay comes from radiation by the boson itself, a process which depends strongly upon the boson momentum. The major contribution to the decay rate comes from large momenta of the intermediate boson, and hence the process is sensitive to the magnitude of the cut-off to mass ratio. In particular, as the mass tends to infinity with the cut-off fixed, the branching ratio ϱ goes to zero in agreement with the direct four-fermion interaction hypothesis.

In the present article the dependence of the calculated branching ratio on the cut-off to mass ratio is studied in detail. If one assumes that the intermediate boson is quite massive, *e.g.* if it has a mass equal to five times the cut-off, then the calculated branching ratio is below $2 \cdot 10^{-6}$ for all values of the boson anomalous moment which are of the order of magnitude of a boson magneton.

A peculiar observation is that if the boson should happen to have an anomalous moment of approximately 0.7 boson magnetons, then for any boson mass greater than about one half the cut-off, the calculated branching ratio would be less than $2 \cdot 10^{-6}$. This might help explain why $\mu \to e + \gamma$ decay is not observed, and thus a study of the possible sources of a boson anomalous moment is clearly suggested.

---

[1] G. FEINBERG: *Phys. Rev.*, **110**, 1482 (1958). See also L. MICHEL: *Proc. Intern. Conference on High Energy Physics* 253 (1958), M. GELL-MANN: *Gatlinburg Conference* (1958).

[2] S. LOKANATHAN and J. STEINBERGER: *Phys. Rev.*, **98**, 240 (A) (1955); H. F. DAVIS, A. ROBERTS and T. F. ZIPF: *Phys. Rev. Lett.*, **2**, 211 (1959); D. BERLEY, J. LEE and M. BARDON: *Phys. Rev. Lett.*, **2**, 357 (1959).

2. – Branching ratio $\varrho = R(\mu \to e + \gamma)/R(\mu \to e + \nu + \bar{\nu})$.

The evaluation of the transition rate $R(\mu \to e + \gamma)$ proceeds from the Lagrangian density $\mathscr{L} = \mathscr{L}_0 + \mathscr{L}_{e.m.} + \mathscr{L}'$, where

$$\mathscr{L}_0 = -\frac{1}{2}[\bar{\psi}_\nu \delta \psi_\nu + \bar{\psi}_e(\delta + m_e)\psi_e + \bar{\psi}_\mu(\delta + m_\mu)\psi_\mu + \text{c.c.}] -$$

$$- \frac{1}{2}(\partial\bar{\varphi}_\nu/\partial x_\beta - \partial\bar{\varphi}_\beta/\partial x_\alpha)(\partial\varphi_\alpha/\partial x_\beta - \partial\varphi_\beta/\partial x_\alpha) - M^2\bar{\varphi}_\alpha\varphi_\nu ,$$

$$\mathscr{L}_{em} = \tfrac{1}{2} ie[\bar{\psi}_e, A\psi_e] + \tfrac{1}{2} ie[\bar{\psi}_\mu, A\psi_\mu] -$$

$$- ie\left[\left(\bar{\varphi}_\nu \overleftrightarrow{\frac{\partial}{\partial x_\beta}} \varphi_\alpha\right) A_\beta + \frac{\partial\bar{\varphi}_\alpha}{\partial x_\alpha} A_\beta \varphi_\beta - \bar{\varphi}_\alpha A_\alpha \frac{\partial\varphi_\beta}{\partial x_\beta} + (1+\mu)\bar{\varphi}_\alpha F_{\alpha\beta}\varphi_\beta\right],$$

and

$$\mathscr{L}' = ig\left[\bar{\psi}_e \varphi \frac{1+\gamma_5}{2}\psi_\nu + \bar{\psi}_\nu \frac{1-\gamma_5}{2}\bar{\varphi}\psi_e\right] - ig\left[\bar{\psi}_\mu \varphi \frac{1+\gamma_5}{2}\psi_\nu + \bar{\psi}_\nu \frac{1-\gamma_5}{2}\bar{\varphi}\psi_\mu\right].$$

Here ψ_ν, ψ_e, ψ_μ, A_α and φ_α are the neutrino, electron, muon, electromagnetic and vector boson field operators, respectively, $F_{\alpha\beta} = \partial A_\beta/\partial x_\alpha - \partial A_\alpha/\partial x_\beta$ and μ is the boson anomalous magnetic moment (in units of the vector boson magneton). The only unfamiliar aspect of the vector boson field is in the free-field commutation relations,

$$[\varphi_\alpha(x), \bar{\varphi}_\beta(x')] = -i\left[\delta_{\alpha\beta} - M^{-2}\frac{\partial^2}{\partial x_\alpha \partial x_\beta}\right]\Delta(x - x') ,$$

which are required by the demand for compatibility with the equations of motion derived from the Lagrangian density $\mathscr{L}_0$.

In the lowest order of perturbation theory three Feynman graphs contribute to the matrix element for $\mu \to e + \gamma$.

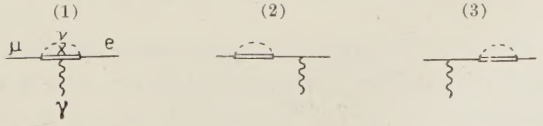

Letting q, q' and ω be the 4-momenta of the muon, electron and photon respectively and ε be the polarization vector of the photon, the S-matrix ele-

ments corresponding to the diagrams (1), (2) and (3) are:

$$S_1 = (2\pi)^{-9/2}\frac{ieg^2}{\sqrt{2\omega_0}}\sqrt{\frac{m_e m_\mu}{q_0' q_0}}\,\varepsilon_\lambda\cdot\bar{u}_e(q')\frac{1-\gamma_5}{2}\cdot$$
$$\cdot\int d^4k[\delta_{\alpha\beta}(q_\lambda' + q_\lambda - 2k_\lambda) - (q-k)_\alpha\delta_{\beta\lambda} - (q'-k)_\beta\delta_{\alpha\lambda} + (1+\mu)(\omega_\alpha\delta_{\beta\lambda} - \omega_\beta\delta_{\alpha\lambda})]\cdot$$
$$\cdot\left(\frac{\gamma_\beta + M^{-2}(q'-k)_\beta(q-k)}{(q'-k)^2+M^2}\right)\frac{k}{k^2}\left(\frac{\gamma_\alpha + M^{-2}(q-k)(q-k)_\alpha}{(q-k)^2+M^2}\right)u_\mu(q)\,,$$

$$S_2 = (2\pi)^{-9/2}\frac{eg^2}{\sqrt{2\omega_0}}\sqrt{\frac{m_e m_\mu}{q_0' q_0}}\,\bar{u}_e(q')\frac{1-\gamma_5}{2}K(q')\frac{i\not{q}' - m_\mu}{q'^2+m_\mu^2}\not{\varepsilon}\,u_\mu(q)\,,$$

and

$$S_3 = (2\pi)^{-9/2}\frac{eg^2}{\sqrt{2\omega_0}}\sqrt{\frac{m_e m_\mu}{q_0' q_0}}\;\bar{u}_e(q')\not{\varepsilon}\frac{i\not{q} - m_e}{q^2+m_e^2}K(q)\frac{1+\gamma_5}{2}u_\mu(q)\,,$$

where

$$K(p) = \int d^4k\,\frac{-2k + M^{-2}(p-k)k(p-k)}{[(p-k)^2+M^2]k^2}\,.$$

Although individually these contributions are not gauge invariant, the gauge invariance of the sum is reflected in the appearance of a factor

$$\bar{u}_e(q')\frac{1-\gamma_5}{2}\sigma_{\alpha\beta}(q_\beta - q_\beta')u_\mu(q)$$

in the final result. Assuming that $m_e \ll m_\mu$ and $(m_\mu/M)^2 \ll 1$ the S-matrix element may be found by expanding the denominators in S_1, S_2 and S_3 in powers of q and q'. The result is $S = 1 - i\mathcal{M}\,\delta^{(4)}(q - q' - \omega)$, where

$$(\mu \to e + \gamma) = -\frac{1}{2}\pi^2 i(2\pi)^{-9/2}e(g/M)^2\sqrt{\frac{m_e m_\mu}{q_0' q_0}}\cdot$$
$$\cdot\frac{\varepsilon_\alpha}{\sqrt{2\omega_0}}m_\mu\bar{u}_e(q')\frac{1-\gamma_5}{2}\sigma_{\alpha\beta}(q_\beta - q_\beta')u_\mu(q)N$$

and

$$N = (\mu-1)I_0 + (2\mu+1)I_1 - 3I_2\,,$$

where

$$I_n = \frac{M^{2n}}{\pi^2 i}\int\frac{d^4p}{(p^2+M^2)^{2+n}}\,.$$

The transition rate R is $(2\pi)^{-1}|\mathcal{M}|^2 \times$ density of states, and thus

$$R(\mu \to e + \gamma) = 2^{-14}\pi^{-5}e^2(g/M)^4 m_\mu^5 N^2\,,$$

which is to be compared with the corresponding rate for the normal decay mode of the muon

$$R(\mu \to e + \nu + \bar{\nu}) = \tfrac{1}{3}\, 2^{-9} \pi^{-3} (g/M)^4 m_\mu^5 .$$

Consequently the branching ratio is given by

$$\varrho = (3\alpha/8\pi) N^2 .$$

Since the integral I_0 diverges logarithmically, N converges only if the anomalous moment $\mu = 1$, in which case one obtains $N = +1$, corresponding to a branching ratio $\varrho = 0.870 \cdot 10^{-3}$, far above the experimental upper limit. However, if $\mu \neq 1$ a cut-off factor such as $\Lambda^2/(p^2 + \Lambda^2)$ must be introduced into each of the integrals I_n in order to obtain a finite branching ratio. Then it can be shown that

$$I_n(a) = J_n(a) - J_{n+1}(a) ,$$

where $a = (\Lambda^2/M^2)$ and

$$J_n(a) = \int_0^\infty \frac{\mathrm{d}y}{(1+y)^{1+n}} \left(\frac{a}{a+y} \right) .$$

Now in general the branching ratio can be expressed in the form

$$\varrho = \varrho_0 \left[1 - \frac{\mu}{\mu_0} \right]^2 ,$$

where

$$\varrho_0 = 0.890 \cdot 10^{-3} [I_0 - I_1 + 3 I_2]^2$$

is the branching ratio in the absence of any anomalous moment, and where

$$\mu_0 = 1 - 3 \left[\frac{I_1 - I_2}{I_0 + 2 I_1} \right] ,$$

is the value of the anomalous moment for which the branching ratio must necessarily vanish.

It is not difficult to determine the variation of ϱ_0 and μ_0 with the cut-off parameter $a = (\Lambda^2/M^2)$, for it can be easily verified that $J_0(a) = (a \ln a)/(a - 1)$, and $J_n(a)$ for $n \geq 0$ can be obtained by using the recurrence relation

$$J_{n+1}(a) = \frac{a}{a-1} \left[\frac{1}{1+n} - \frac{1}{a} J_n(a) \right] .$$

The case $a = 1$ is trivial, and we have $J_n(1) = 1/(1+n)$, from which it follows that $\varrho_0 = 2.95 \cdot 10^{-4}$ and $\mu_0 = 0.7$. Thus, whereas the branching ratio is abnormally high for the normal magnetic moment, it becomes zero at $\mu = 0.7$. Although one might suspect that the suppression of the $\mu \to e + \gamma$ decay for $\mu = 0.7$ is peculiar to this particular choice of cut-off, $\Lambda = M$, the constant μ_0 is actually very insensitive to the choice of cut-off.

First consider the case when $a = (\Lambda^2/M^2) \ll 1$. In this limit $J_0(a) \approx -a \ln a$, from which it can be shown that $I_n(a) \approx a/(1+n)$.

Therefore,

$$\varrho_0(a) = 1.95 \cdot 10^{-3} a^2 \qquad \text{and} \qquad \mu_0 = 0.75$$

whenever $a \ll 1$, and μ_0 is not greatly different from its value at $a = 1$.

In the opposite limit,

$$a = (\Lambda^2/M^2) \gg 1\,, \qquad \varrho_0(a) = 0.870 \cdot 10^{-3} (\ln a)^2 \qquad \text{and} \qquad \mu_0(a) = 1 - \frac{1}{(\ln a) + 1}\,.$$

For large values of a, ϱ_0 diverges and μ_0 approaches unity, as they must.

A number of individual points other than $a = 1$ have been calculated, and the results are summarized in the accompanying graphs. The first thing that should be noted is the slow variation of μ_0 as a function of Λ/M. It follows from this that if the boson should happen to have an anomalous moment $\mu = 0.7$ magnetons, the branching ratio would be small for a large range of values of Λ/M; specifically for any value of the boson mass M greater than one-half the cut-off Λ, the branching ratio ϱ would be less than $2 \cdot 10^{-6}$.

Although the case $\mu = 0.7$ is clearly the most favorable for the achievement of a small branching ratio, the rate for $\mu \to e + \gamma$ can be reduced to $2 \cdot 10^{-6}$ in general by letting the boson mass M exceed the cut-off Λ by a factor 5 or more. This hypothesis does not contradict the weak coupling approximation, for since $(g/M^2) \approx 10^{-5}/M_n^2$, where M_n is the nucleon mass, $M \approx 5\Lambda$ corresponds to a value of g considerably less than unity for any cut-off $\Lambda \leqslant 10 M_n$. By attributing to the intermediate charged boson a mass much larger than the cut-off, in effect it is prevented from emitting efficiently photons of energy $m_\mu c^2/2$.

Therefore, the conclusion is that one cannot rule out the possibility that the decay $\mu \to e + \gamma$ goes via a charged vector boson of very high mass; alternatively, if the boson should happen to have an anomalous moment near 0.7, its mass could be relatively small without contradicting the experimental data.

3. – Discussion.

It is apparent that the structure of the matrix element for $\mu \to e + \gamma$ decay is the same as that of the matrix element for the boson contribution to the muon or electron anomalous magnetic moment. Indeed, the only modi-

fication necessary in order to obtain the muon anomalous magnetic moment, for example, is to replace the electron in the final state by a μ-meson. This will change the numerical value of N, but it will not modify the general statements which have been made regarding the dependence of the matrix element upon the ratio of cut-off to boson mass. In particular, since the quadratically divergent part of S_1 is removed by a charge renormalization (coming from S_2 and S_3), the anomalous magnetic moment also is logarithmically divergent. Therefore, the selection of a cut-off necessary to give a small $\mu \to e + \gamma$ branching ratio will automatically guarantee a small contribution to the muon or electron anomalous magnetic moment; in fact, this contribution is about 10^{-9} muon magnetons for the μ-meson and hence is undetectable.

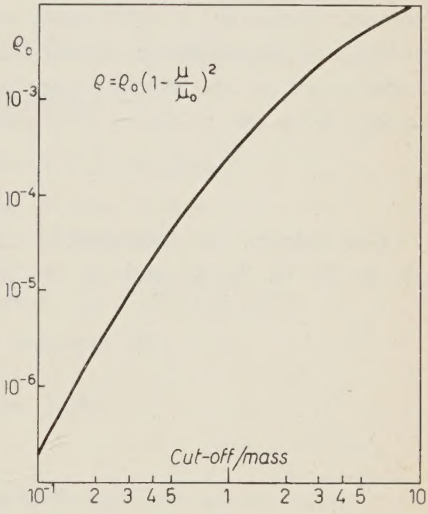

Fig. 1. – Branching ratio ϱ for intermediate boson with normal magnetic moment.

However, a different situation occurs in the case of the boson contribution to the self-energy of the muon or electron.

Here the divergence is quadratic, and hence there is the possibility of making this self-energy large and still keeping the branching ratio and hence the leptonic anomalous magnetic moments small. In fact, as the preceding

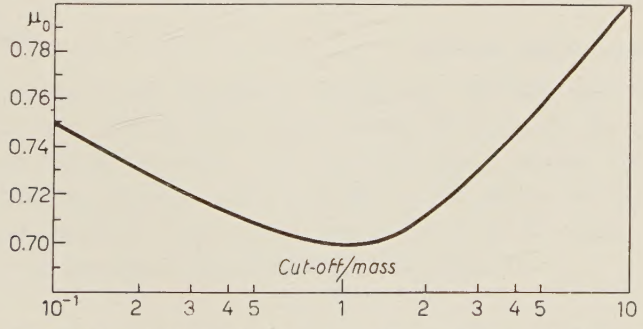

Fig. 2. – Cut-off dependence of the boson anomalous moment which must be postulated in order to obtain zero branching ratio ϱ.

section indicates, the Boson-lepton coupling may be made strong, with an associated self-energy of the order of magnitude of the muon mass, without contradicting any present experimental results.

It must be emphasized that this is not to be taken as suggesting that the $\mu - e$ mass difference could be accounted for by the interaction with the postulated intermediate Boson. Indeed, the present discussion has treated the muon and the electron symmetrically, and hence cannot give any mass difference. However, it does seem desirable to demonstrate that the different momentum dependences of the divergences in these various processes make it necessary to use extreme care in inferring the strength of the self-energy process from the $\mu \to e + \gamma$ branching ratio.

* * *

The authors are indebted to G. FEINBERG for a discussion of his work, and to R. G. SACHS and H. W. LEWIS for many helpful suggestions.

RIASSUNTO (*)

Si discute la dipendenza del rapporto di branching

$$R(\mu \to e + \gamma)/R(\mu \to e + \nu + \bar{\nu})$$

dal rapporto tra cut-off e massa del bosone e da un possibile momento anomalo del bosone. Dai dati sperimentali attualmente disponibili si deducono alcune proprietà del bosone.

(*) *Traduzione a cura della Redazione.*

Mesic Decays of Hypernuclei from K^--Capture.

I. - Binding Energies.

R. Ammar, R. Levi Setti and W. E. Slater (*)

The Enrico Fermi Institute for Nuclear Studies
The University of Chicago - Chicago, Ill.

S. Limentani, P. E. Schlein and P. H. Steinberg (**)

Northwestern University - Evanston, Ill.

(ricevuto il 23 Giugno 1959)

Summary. — The analysis of 134 uniquely identified mesic decays yields increased accuracy in the knowledge of the binding energies of the hypernuclides $^3H_\Lambda$, $^4H_\Lambda$ $^4He_\Lambda$, $^5He_\Lambda$, $^7Li_\Lambda$, $^8Li_\Lambda$, $^9Li_\Lambda$, and $^9Be_\Lambda$. In addition, individual examples of the new species $^7He_\Lambda$, $^{11}B_\Lambda$ and $^{12}B_\Lambda$ are described. The present data are combined with those collected in the EFINS survey. The isotopic spin multiplet structure of the light hypernuclei is discussed with reference to the information derived from the binding energies.

1. – Introduction.

Emulsion groups at the University of Chicago (EFINS) and Northwestern University (NU) are collaborating in the study of π^--mesic decays of hypernuclei produced by K^--capture. The present report covers the results on hypernuclear binding energies and is based on 265 mesic decays found in a first area scan of emulsion stacks containing about $4 \cdot 10^4$ K^--stars. Preliminary results of this collaboration were reported elsewhere [1].

(*) Research supported by the U. S. Air Force Office of Scientific Research, Contract no. AF 49(638)-209.

(**) Research supported by the National Science Foundation and by the U. S. Atomic Energy Commission through Argonne National Laboratory subcontract.

(1) R. Ammar, R. Levi Setti, S. Limentani, P. E. Schlein, W. E. Slater and P. H. Steinberg: *Annual Intern. Conf. on High Energy Physics at CERN* (1958); R. H. Dalitz and M. Kaplon: *Reports*, pp. 181, 200.

2. – Experimental details.

2·1. *Exposure and calibration of the stacks.* – Two stacks were exposed to the 300 MeV/c enriched K^- beam (ratio of minimum tracks to K^-, 800:1) at the Berkeley Bevatron. The EFINS stack consisted of 59 K-5 pellicles of dimensions 10 cm × 15 cm × 0.12 cm while the NU stack consisted of 59 K-5 and 71 L-4 pellicles both of dimensions 10 cm × 15 cm × 0.06 cm. The 0.12 cm pellicles were processed unmounted, while the 0.06 cm pellicles were processed mounted on glass. The mean thickness of each pellicle before processing was obtained from measurements in five to nine different regions. The lateral shrinkage of each unmounted pellicle was also determined. Details of the methods used have been described elsewhere [2].

A further stack, already processed and calibrated, was made available by the University of California Radiation Laboratory [*]. An average shrinkage factor was used for this stack, which yielded about 6% of our events.

The densities of the stacks were determined in two ways: *a*) for the EFINS stack, directly; *b*) for both the EFINS and the NU stacks, indirectly from proton ranges in Σ^+ decays (65 proton ranges in the EFINS stack, 33 and 26 proton ranges in the K-5 and L-4 parts of the NU stack). The mean range for each stack was compared with GILES' [3] value for emulsion of standard density (3.815 g/cm³); the densities of our stacks were then inferred following BARKAS *et al.* [4]. For the EFINS stack the indirect density value so obtained was in good agreement with the direct measurement. The corrections in reducing the ranges used in the present work to standard density amount to about 1%, with a statistical uncertainty of ± 0.5%.

2·2. *Analysis of events.* – For the purpose of analysis, the events may be divided into three classes

a) two-body decays of the type: $(A, Z) \to \pi^- + (Z+1, A)$ (π-r events).

b) three-body decays of the type: $(Z, A) \to \pi^- + p + (Z, A-1)$ (π-p-r events).

c) other decays, including those in which neutrons are emitted.

---

[2] W. E. SLATER: *Suppl. Nuovo Cimento*, **10**, 1 (1958).

[*] We are greatly indebted to Dr. W. H. BARKAS for the loan of this stack (Berkeley 1 U).

[3] P. C. GILES: UCRL Report no. 8007 (1957).

[4] W. H. BARKAS, P. H. BARRETT, P. CÜER, H. HECKMAN, F. M. SMITH and H. K. TICHO: *Nuovo Cimento*, **8**, 185 (1958)

a) According to the ranges of the decay products, the π-r decays fall into three main groups, as can be seen from Fig. 1. Among these, the $^3H_\Lambda$ and $^4H_\Lambda$ groups are readily identifiable, while the third group will be discussed later (Section 3·1).

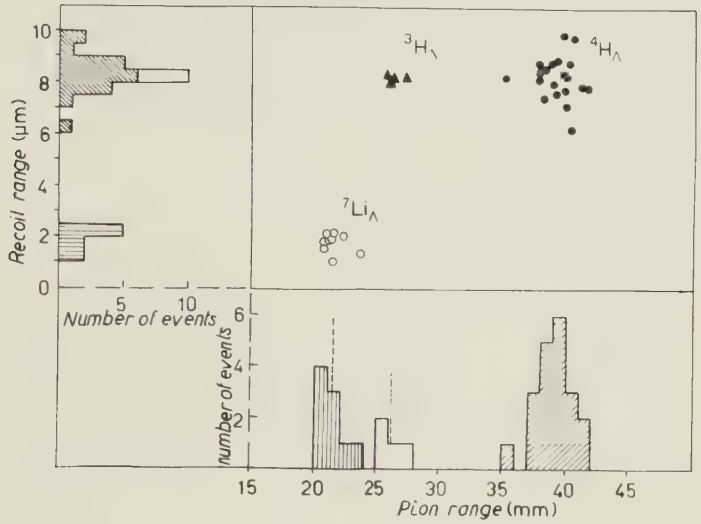

Fig. 1. – Pion and recoil ranges for π-r events.

b) The identities of the recoils in π-p-r decays are assigned on the basis of a comparison between their observed ranges and the ranges inferred from the vector sum $\boldsymbol{P}_{\pi p}$ of the π and p momenta. The procedure given by SLATER (2) was used; Fig. 2 is a plot of the range-momentum points obtained for events in which the recoil direction is collinear with $\boldsymbol{P}_{\pi p}$ within errors, and corresponds to Slater's Fig. 14. The curves drawn in Fig. 2 are those calculated by WILKINS (5), the curve for ^{4}He being displaced by 0.5 μm toward lower ranges to fit the calibration point from $^4H_\Lambda \rightarrow \pi^- + {}^4$He. The curve for ^{3}He was derived from the adjusted ^{4}He curve. This yields a very satisfactory fit to the ^{4}He points from $^5He_\Lambda$ decay over the range from 3 to 30 μm.

For ranges below 3 μm it is in general impossible to identify recoils uniquely. The separation between the range-momentum curves for different isotopes becomes at this range, even for flat tracks, smaller than the range measurement errors. Events with slightly larger recoils but large dip angles can also in some cases not be uniquely identified. (See Appendix I for further discussion.)

(5) J. J. WILKINS: A.E.R.E. G/R 664 (1951).

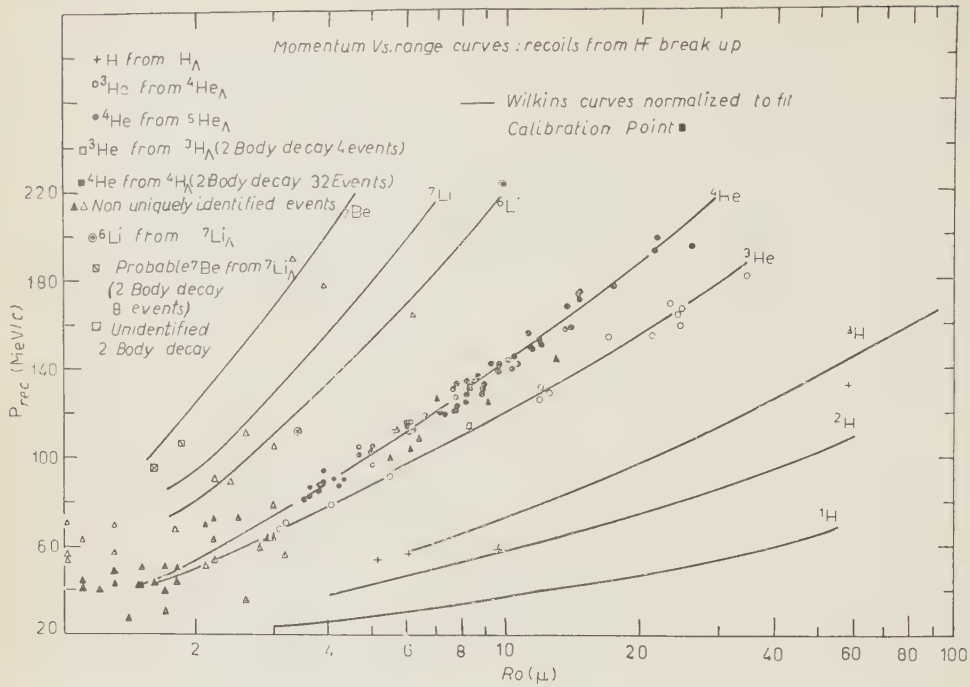

Fig. 2. – Range momentum curves for recoils from hyperfragment disintegration.

c) Events in this class, representing a small fraction of our data (~15%) were analyzed with an electronic computer programmed ([6,7]) for the permissible range of Z and A values for each prong. For every permutation of these (Z, A) assignments the computer printed out the Λ-binding energy (B_Λ) and the momentum unbalance (ΔP) for events yielding $-30 < B_\Lambda < 40$ MeV. An event is considered unique if there exists only one set of prong identities for which ΔP is zero within experimental error (*). This experimental error was calculated for *each* event from the assigned uncertainties in the measured input quantities (ranges, angles, etc.) by the electronic computer. For events assigned to a well-known hypernuclide, we require in addition that the calculated B_Λ be consistent with the known average B_Λ.

Non-colinear two-prong and non-coplanar three-prong decays which require at least one neutron are considered to be unique only if the analysis with a

([6]) E. M. Silverstein: *Suppl. Nuovo Cimento*, **10**, 41 (1958).

([7]) F. W. Inman: UCRL Report no. 3815 (1957).

(*) The spread of ΔP which may reasonably be expected can be seen from Sect. 3·3 where the ΔP-distributions for unique $^4H_\Lambda$ and $^5He_\Lambda$ are discussed.

single neutron yields a single positive binding energy. The identity of four-prong decays, where the emission of neutrons cannot be ruled out on the basis of coplanarity, will always be open to question. No attempt was made to establish any decay mode involving more than one neutron.

Finally, whenever possible, the charge of the hyperfragment was determined from profile ([8]) measurements on the connecting track.

For several events in which the kinematics yielded only two alternatives differing in Z, it was possible to establish a unique identity with the aid of such measurements. Details of the method are given in Appendix II.

2·3. *Conventions adopted.* – The binding energy of the Λ in a hypernucleus, B_Λ, is defined as the energy required to remove the Λ, leaving the residual core nucleus in its ground state.

$B_\Lambda(Z, A) = Q_0 - Q$, where Q is the total energy release and Q_0 is the difference between the sum of the Λ and core nucleus rest energies, and the sum of the decay product rest energies.

In the case of $^9Be_\Lambda$, where no stable core exists, the ground state of ^8Be (unstable against ^4He emission by 96 keV) is taken as the residual core.

The standards adopted for the determination of binding energies are the same as those described in ref. ([2]), except for Q_Λ, the energy release in the π^--decay mode of the free Λ.

The following values of Q_Λ, all obtained from K^--induced events, have been averaged: $((37.45 \pm 0.17)$ MeV) ([9]), $((37.58 \pm 0.18)$ MeV) ([10]) and $((37.71 \pm 0.16)$ MeV) ([11]). The adopted value is then (37.58 ± 0.15) MeV. The error assigned to this mean is considered more realistic than the one obtained from combining the three independent error estimates. Preliminary results of a new determination of Q_Λ at Berkeley ([12]) are consistent with the one adopted here.

2·4. *Errors.* – With the exception of the uncertainties in nuclear rest energies (of the order of 0.02 MeV), the error in Q_0 equals that in Q_Λ. An esti-

([8]) G. Alvial, A. Bonetti, C. Dilworth, M. Ladu, J. Morgan and G. Occhialini: *Suppl. Nuovo Cimento*, **4**, 244 (1956).

([9]) W. H. Barkas, P. C. Giles, H. H. Heckman, F. W. Inman, C. J. Mason and F. M. Smith: *Padua-Venice Conference Report* (1957), p. VI-41.

([10]) J. Bogdanowicz, M. Danysz, A. Filipkowsky, E. Marquit, E. Skrzypczak, A. Wroblewski and J. Zakrzewski: *Nuovo Cimento*, **11**, 727 (1959).

([11]) B. Brucker, F. Anderson, J. Lodge and A. Pevsner: kindly communicated to us by A. Pevsner (1959).

([12]) Kindly communicated to us by W. H. Barkas.

mate of the errors in $\bar{B}_\Lambda\ (Z, A) = Q_0 - \bar{Q}$ can be obtained from the following compilation:

Source	Error in Q_Λ (MeV)	Error in $\bar{Q}$ (MeV)	Correlated
(*a*) *R-E* relation	0.10÷0.20	0.10÷0.20	yes
(*b*) Stopping power	0.05÷0.10	0.05÷0.10	no
(*c*) Emulsion shrinkage	~ 0.05	~ 0.05	no
(*d*) Random errors	~ 0.08	0.08÷0.60	no

Since the same range-energy relation is used in determining both Q_Λ and $\bar{Q}$, the error propagated to $\bar{B}_\Lambda$ is negligible for most hypernuclear species. The entire set of $\bar{B}_\Lambda$'s could be shifted by a concomitance of errors *b*), *c*) and *d*) in Q_Λ and of errors *b*) and *c*) on $\bar{Q}$ by a total of about 0.2 MeV.

For events not involving a neutron, the random error in $\bar{B}_\Lambda$ is derived from the standard deviation σ of the experimental distributions for uniquely identified decays: these are displayed in Fig. 3, where B_Λ-histograms for the most abundant species are plotted. The quoted error in $\bar{B}_\Lambda$ for a given hypernuclide, σ_{av}, is $\sigma/\sqrt{n}$, where n is the number of events. The variation of σ with Q is shown in Fig. 4. For the non-abundant species where it is not possible to obtain σ in this way reliably, a value appropriate to the energy release was inferred from Fig. 4. In those cases where a neutron was emitted, the B_Λ error was inferred from a knowledge of the straggling and measurement errors.

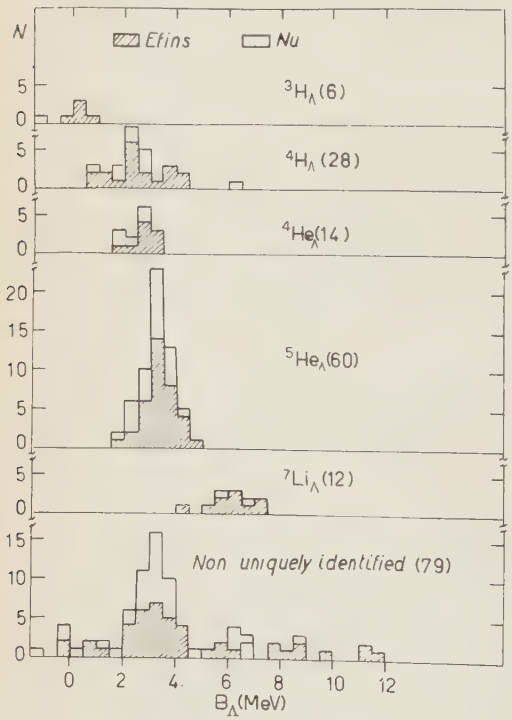

Fig. 3. – Binding energy histograms for the most abundant hypernuclear species.

Sources which contribute to the spread of the B_Λ-distribution include range straggling, measurement errors, distortion of the emulsion and uncertainties in the shrinkage factors ([2]). Our overall experimental error from these sour-

ces probably does not exceed 1%. In fact the range stragglings obtained compare with the theoretical one as follows: protons from Σ^+-decays, (1.9 ± 0.2)%, *vs.* 1.4%; pions from π-r decays of $^4H_\Lambda$, (2.7 ± 0.5)% *vs.* 2.7%.

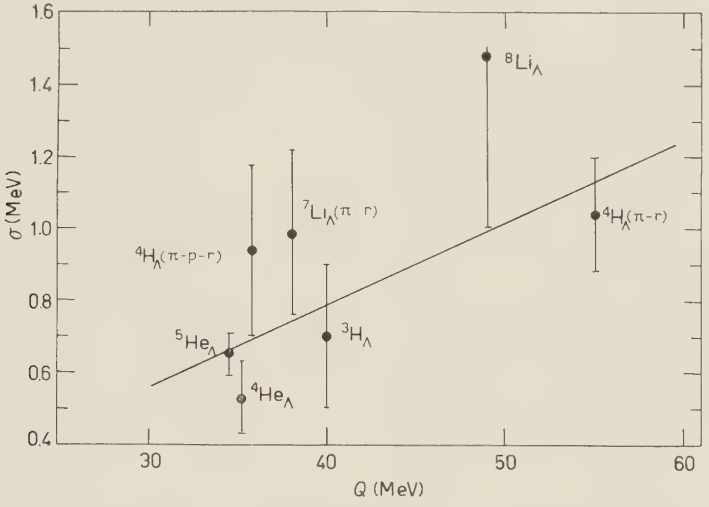

Fig. 4. – Variation of σ, experimental spread of B_Λ distributions, with the energy release, Q.

3. – Results.

3·1. *Uniquely identified events.* – The binding energies presented here were all deduced from « uniquely » identified events in which all decay tracks stopped in the emulsion (134 out of 214 complete events). With the exception of one decay in flight of $^3H_\Lambda$ (B_Λ not included in the average), all the decays occurred at rest.

Although the B_Λ value of an individual event in no case formed the basis for identification, those events with B_Λ departing by more than 3σ from the mean, $(\bar{B}_\Lambda)$, were rejected; this was only done for the species represented by more than ten events. One $^4H_\Lambda$ with $B_\Lambda = 6.1$ MeV and decaying by the mode $\pi^- + ^4He$ was rejected on this basis.

Table I gives a breakdown of the data used in the binding energy determinations. Since only complete events are considered, the frequencies do not represent the true relative abundances.

There appears to exist a small systematic difference (of order 0.6% Q) between the EFINS and NU results, as can be seen from the data for $^3H_\Lambda$, $^4He_\Lambda$ and $^5He_\Lambda$. This difference however is of the order of magnitude of the uncertainties in the stopping power calibrations, although it may arise from

TABLE I. – *Mesic hyperfragments from* K^-*-capture decay modes of uniquely identified events.*

Decay mode	EFINS		NU		Total
	B_Λ (MeV)	No. of events	B_Λ (MeV)	No. of events	
$^3H_\Lambda \to \pi^- + {}^3He$	0.06	3	−1.28	1	4
$\to \pi^- + {}^1H + {}^2H$	0.05	1	—	—	1
$\to \pi^- + n + 2\,{}^1H$	0.79	1	—	—	1
$^4H_\Lambda \to \pi^- + {}^4He$	2.58	12	2.13	7	19
$\to \pi^- + n + {}^3He$	1.61	2	—	—	2
$\to \pi^- + {}^1H + {}^3H$	2.05	4	0.66	1	5
$\to \pi^- + 2\,{}^2H$	2.21	1	—	—	1 (*)
$^4He_\Lambda \to \pi^- + {}^1H + {}^3He$	2.44	8	2.15	5	13
$\to \pi^- + 2\,{}^1H + {}^2H$	3.09	1	—	—	1
$^5He_\Lambda \to \pi^- + {}^1H + {}^4He$	3.13	35	2.95	25	60
$^7He_\Lambda \to \pi^- + {}^3H + {}^4He$	3.04	1	—	—	1 (*)
$^7Li_\Lambda \to \pi^- + {}^7Be$ (prob.)	6.02	8	6.57	1	9
$\to \pi^- + {}^1H + {}^6Li$	5.68	1	5.44	1	2
$\to \pi^- + {}^3He + {}^4He$	5.47	1	—	—	1
$^8Li_\Lambda \to \pi^- + 2\,{}^4He$	5.97	2	6.59	3	5
$^9Li_\Lambda \to \pi^- + n + 2\,{}^4He$	7.95	2	6.41	1	3
$^9Be_\Lambda \to \pi^- + {}^1H + 2\,{}^4He$	6.07	1	6.48	2	3
$^{11}B_\Lambda \to \pi^- + {}^3He + 2\,{}^4He$	9.93	1	—	—	1 (*)
$^{12}B_\Lambda \to \pi^- + 3\,{}^4He$	—	—	9.55	1	1 (*)

(*) Heretofore unobserved.

other sources. The averages of the results from both laboratories are, in our opinion, the best estimates of the binding energies $\bar{B}_\Lambda$. These $\bar{B}_\Lambda$'s are given in Table II, where the $\bar{B}_\Lambda$'s from the EFINS survey ([13]) are included for comparison; good consistency between both sets is apparent. The final column of Table II gives the grand averages.

A preliminary report of this experiment ([1]) quoted a *negative* value of B_Λ for $^3H_\Lambda$, suggesting that the value of Q_Λ adopted at that time, that is (37.22 ± 0.20) MeV, might be too low. The Q_Λ value here adopted on the basis of new evidence, together with an increased accuracy in the stopping power calibration of the present stacks, now yields a $\bar{B}_\Lambda$ for $^3H_\Lambda$ which is consistent with a small *positive* value.

([13]) R. LEVI SETTI, W. E. SLATER and V. L. TELEGDI: *Suppl. Nuovo Cimento*, **10**, 68 (1958).

TABLE II. – *Binding energies from uniquely identified mesic decays.* The value $Q_\Lambda = (37.58 \pm 0.15)$ MeV is adopted in the present compilation. See text for discussion and references.

Identity	EFINS survey May 1958			EFINS-NU collaboration			Average of survey and collaboration		
	B_Λ (MeV)	σ_{av} [a] (MeV)	No. of events	B_Λ (MeV)	σ_{av} [a] (MeV)	No. of events	B_Λ (MeV)	σ_{av} [a] (MeV)	No. of events
$^3H_\Lambda$	0.56	0.50	7	−0.06	0.30	6	0.12	0.26	13
$^4H_\Lambda$	2.17	0.20	21	2.23	0.19	27	2.20	0.14	48
$^4He_\Lambda$	2.35	0.20	9	2.38	0.15	14	2.36	0.12	23
$^5He_\Lambda$	3.18	0.20	17	3.06	0.10	60	3.08	0.09	77
$^7He_\Lambda$	—	—	—	3.0	0.7	1	3.0	0.7	1
$^7Li_\Lambda$ [b] 2-body	4.8	0.8	1	6.08	0.33	9	5.96	0.30	10
$^7Li_\Lambda$ [b] other	5.4	0.6	2	5.51	0.40	3	5.46	0.33	5
$^8Li_\Lambda$	6.0	0.4	3	6.34	0.67	5	6.11	0.35	8
$^9Li_\Lambda$	7,1	0,7	1	7.4	1.6	3	7.2	0.6	4
$^8Be_\Lambda$	6.6	0.6	1	—	—	—	6.6	0.6	1
$^9Be_\Lambda$	6.8	0.4	3	6.4	0.5	3	6.60	0.31	6
$^{11}B_\Lambda$	—	—	—	9.9	0.6	1	9.9	0.6	1
$^{12}B_\Lambda$	—	—	—	9.6	0.6	1	9.6	0.6	1

(*a*) The systematic errors ($\sim \pm 0.2$ MeV) have not been included.
(*b*) Reasons for separating 2-body and other decay modes are discussed in Sect. 3·1.

Some remarks are required concerning those 9 π-r events which are consistent with the decay scheme

$$(1) \qquad {}^7Li_\Lambda \to \pi^- + {}^7Be \,.$$

Because of the large relative uncertainty in determining the range of each recoil, it is not possible to infer the identity of individual recoils through a range-momentum relation. Both the pion and recoil show range spectra (see Fig. 1) which are not in consistent with the decay of a single hypernucleus. An average recoil range of (1.85 ± 0.2) μm was found while the average pion momentum is (107 ± 0.5) MeV/c. If all these events are to be attributed to the decay of a single species, then this would rule out an identification of the recoil as ^{6}Li (from the decay of $^6He_\Lambda$). These events could also be alternatively interpreted as the decays of certain hypernuclei with $Z > 3$, of which the lightest one is $^{10}Be_\Lambda$. Lacking reliable range momentum curves near this recoil range, one can not rule out this alternative. However, as the mesic decay mode should be greatly suppressed with increasing Z, and as there is no indication that $^{10}Be_\Lambda$ or any of the heavier hypernuclides be singularly abundant, we believe

that the more plausible interpretation is to attribute these events to the decay of $^7Li_\Lambda$.

Among the published events with the same decay characteristics as (1), one ([14]) was identified as $^7Li_\Lambda$ from an analysis of the kinematics both of production and decay.

One can, of course, nevertheless not exclude the possibility that among these events there may be some which represent the decay of $^6He_\Lambda$, $^{10}Be_\Lambda$ and possibly even heavier hypernuclides, nor is it possible to determine whether there is a mixture of two competing decays of $^7Li_\Lambda$. Thus the recoil ^{7}Be could *e.g.* be left in the first excited state (at 0.43 MeV above the ground state). For these reasons the $\bar{B}_\Lambda$ of $^7Li_\Lambda$ from these two-body decays is indicated separately in Table II, although it is not inconsistent with the value obtained from the other decay modes.

As indicated in Table I, the decay modes:

$$(2) \qquad {}^7He_\Lambda \to \pi^- + {}^3H + {}^4He\,,$$

$$(3) \qquad {}^{11}B_\Lambda \to \pi^- + {}^3He + 2\,{}^4He\,,$$

$$(4) \qquad {}^{12}B_\Lambda \to \pi^- + 3\,{}^4He\,,$$

have been identified for the first time. The limitations in establishing the existence of a given species or decay mode on the basis of one isolated event are self-evident. The reliability of these events may be judged with reference to Appendix III where the experimental details are presented. Appendix III also contains the data for one event representing the decay mode

$$(5) \qquad {}^7Li_\Lambda \to \pi^- + {}^3He + {}^4He$$

as well as three new examples of the decay mode.

$$(6) \qquad {}^9Li_\Lambda \to \pi^- + n + 2\,{}^4He$$

confirming previous observations ([15,16]).

3·2. *Non-uniquely identified events.* – For three body events in this class, the binding energies were calculated assuming π-p-r decay modes. The *charges* of the recoils could often be determined by extrapolation even where the range-

([14]) F. C. Gilbert, C. E. Violet and R. S. White: *Phys. Rev.*, **103**, 248 (1956).
([15]) P. H. Fowler: *Phil. Mag.*, **3**, 1460 (1958).
([16]) S. Limentani, J. H. Roberts, P. E. Schlein and P. H. Steinberg: *Nuovo Cimento*, **9**, 1046 (1958).

momentum curves do not enable one to discriminate between the isotopes, as can be seen from Fig. 2. An average of the mass, compatible with the inferred charge, was used in calculating B_Λ. In most events of this category the recoil energy is sufficiently small so that B_Λ was insensitive to the choice of recoil mass. The B_Λ's so obtained are included in Fig. 3, where it is seen that a large fraction of the events peak at B_Λ values corresponding to $A = 4$ and 5 hypernuclides. In addition, a few events with very low B_Λ suggest the presence of ${}^3H_\Lambda$, and events with higher binding energies imply a substantial contribution from hypernuclides of $Z > 2$. Neither in this group of non-unique events nor among the incomplete events is there any evidence for energy releases inconsistent with the mesic decay of a Λ-hypernucleus, namely larger than about 57 MeV.

3·3. *Identification bias.* – The criteria used in assigning a unique identity discriminate against events with very short recoils, as well as against those involving neutron emission. For example, decay modes such as

(7) *a*) $${}^2H_\Lambda \to \pi^- + {}^1H + {}^1H\,,$$

(8) *b*) $${}^6He_\Lambda \to \pi^- + n + {}^1H + {}^4He\,,$$

if they exist, are likely to remain unidentified.

a) There are 8 events without a visible recoil, in which the decay simulates the decay of a Λ at rest. In view of their very low B_Λ's, these events are attributed to the decay of ${}^3H_\Lambda$, although they could be due to ${}^2H_\Lambda$.

Two of these events had sufficiently long hyperfragment tracks to permit mass determinations from gap length measurements. These yielded values of $(3.1 \pm 0.37)m_p$ and $(3.25 \pm 0.64)m_p$, indicating very strongly that these are ${}^3H_\Lambda$ decays. Nevertheless, we do not use these two events for a B_Λ determination since one cannot decide which of the decay modes $\pi^- + {}^1H + {}^2H$ or $\pi^- + 2\,{}^1H + n$ is involved without recourse to the *a priori* knowledge of B_Λ for ${}^3H_\Lambda$.

b) No clear-cut examples of ${}^6He_\Lambda$ have been detected. However, the decay mode

(9) $${}^6He_\Lambda \to \pi^- + p + n + {}^4He + Q_6$$

may readily be confused with the abundant decay

(10) $${}^5He_\Lambda \to \pi^- + p + {}^4He + Q_5$$

if a slow neutron is emitted. Those decays in which the neutron carried off an appreciable momentum could be detected by a lack of coplanarity and large momentum unbalance.

A plot of the residual momentum ΔP from the unique $^5He_\Lambda$ events is shown in Fig. 5 along with a similar plot for the decays $^4H_\Lambda \to \pi^- + {}^4He$, in which the emission of neutrons can be ruled out. A comparison of the two indicates that it is very difficult to detect the emission of neutrons with momenta $\leqslant 40$ MeV/c against the existing « noise level » due to a combination of instrumental and measurement errors. It is clear that the ΔP distribution for $^5He_\Lambda$ decays may be well understood without recourse to the hypothesis of neutron emission.

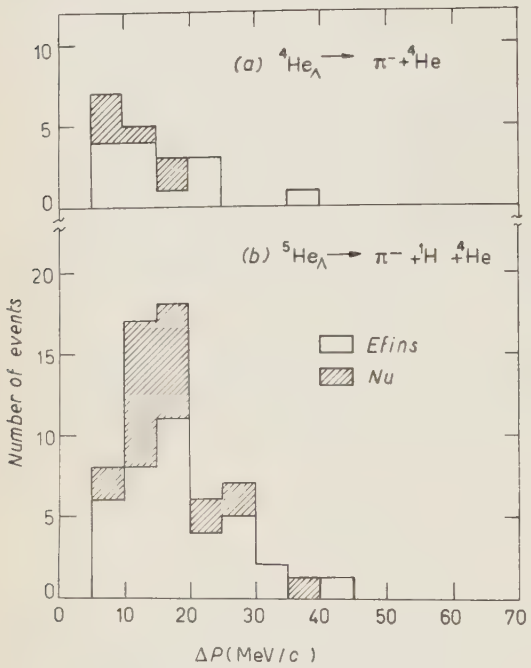

Fig. 5. – Histograms of the residual momentum, ΔP for:
(*a*) $^4H_\Lambda \to \pi^- + {}^4He$; (*b*) $^5He_\Lambda \to \pi^- + {}^1H + {}^4He$.

To determine whether slow neutrons (< 40 MeV/c) could indeed have been emitted, it is useful to set limits on the energy release in the hypothetic $^6He_\Lambda$ decay. The condition for the stability of $^6He_\Lambda$ against decay into $^5He_\Lambda + n$ is that Q_6 be less than Q_5. Similarly the stability of $^7He_\Lambda$ against decay into $^6He_\Lambda + n$, would impose a lower bound on Q_6. Using the data of Table II these conditions become:

$$(34.5 \pm 0.1) > Q_6 > (33.6 \pm 0.7) \text{ MeV} . \tag{11}$$

Since Q_6 includes the energy carried by the undetected neutron (< 0.8 MeV) the visible energy must satisfy the relation

$$(34.5 \pm 0.1) > Q_6 \text{ (visible)} > (32.8 \pm 0.7) \text{ MeV} . \tag{12}$$

Thus possible $^6He_\Lambda$ events may be included among those $^5He_\Lambda$ events having

$$(3.1 \pm 0.1) \leqslant B_\Lambda \leqslant (4.8 \pm 0.7) \text{ MeV} . \tag{13}$$

On the other hand, the binding energy of $^5He_\Lambda$ is 3.1 MeV, with an observed σ of 0.6 MeV. For a normal distribution about 5% of the events are expected

to yield a $B_\Lambda > 4.3$ MeV; only one of the 60 presumed $^5He_\Lambda$ events of this experiment has a binding in excess of this value ($B_\Lambda = 4.6$ MeV, $\Delta P = 12.5$ MeV/c).

Since neither the condition on Q_6 nor, as seen above, detection of neutrons through large $|\Delta P|$ alone gives a sensitive enough test for $^6He_\Lambda$, a search was made for a correlation between $|\Delta P|$ and B_Λ among $^5He_\Lambda$, with no positive results.

The same difficulties are encountered with non-uniquely identifiable events, and are here enhanced by the large uncertainties associated with the presence of very short recoils.

4. – Discussion and conclusions.

The variation of B_Λ with mass number A is shown in Fig. 6. As previously noted in the literature, there is a general tendency for B_Λ to increase with A, although there appear to be some departures from simple linear dependence. There are also indications for a structure due to the existence of several isotopic spin multiplets.

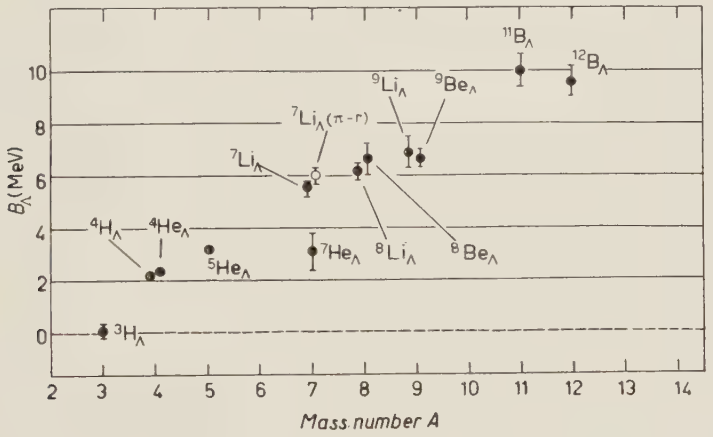

Fig. 6. – Plot of B_Λ *vs.* mass number, A.

Within the experimental errors, $^4H_\Lambda$ and $^4He_\Lambda$ are seen to have nearly equal binding energies. This suggests that they are members of an isotopic spin doublet, consistent with the assumption that the Λ has isotopic spin $T = 0$, and with the requirements of charge symmetry, as first pointed out by Dalitz ([17]). The appearance of only one hypernuclide each of mass 3 and 5 suggests accordingly that they are isotopic spin singlets.

([17]) R. H. Dalitz: *Phys. Rev.*, **99**, 1475 (1955).

The multiplets structure for $A = 7$ hypernuclides may be understood with the help of a level diagram (Fig. 7), in which the ordinate represents *total* binding energy.

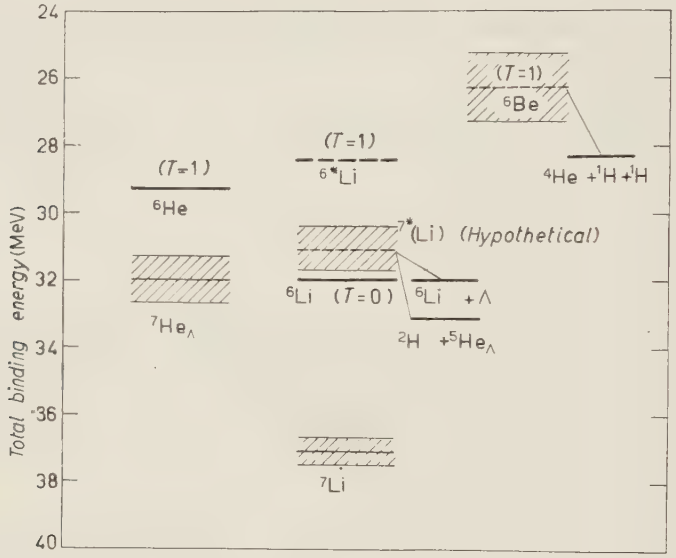

Fig. 7. – Isotopic spin multiplet structure of $A=7$ hypernuclei.

The ground states of the core nuclei ^{6}He and ^{6}Li ($T=1$ and $T=0$ respectively) are indicated by full lines. The first $T=1$ excited state of ^{6}Li, at 3.6 MeV above the ground state, is indicated by a dashed line. The $T=1$ state of ^{6}Be is unbound, decaying into ^{4}He+2p with an energy release of about 2 MeV ([18]). This $T=1$ state is indicated as a dashed line in Fig. 7, for comparison.

The levels corresponding to the observed $^7\mathrm{He}_\Lambda$ and $^7\mathrm{Li}_\Lambda$ binding energies are shown together with their experimental errors. The B_Λ for $^7\mathrm{He}_\Lambda$ is (2.5 ± 0.8) MeV less than that for $^7\mathrm{Li}_\Lambda$, where the latter is calculated excluding the two body decays. This suggests that they may not belong to the same isotopic spin multiplet. The ground state ^{6}He has $T=1$ while that of ^{6}Li has $T=0$. If the presence of the Λ does not greatly affect the structure of the core nuclei, it is reasonable to expect $^7\mathrm{He}_\Lambda$ and $^7\mathrm{Li}_\Lambda$ to have isotopic spins 1 and 0 respectively. This is consistent with the indications drawn from the binding energies. In fact, if the $T=1$ state of $^7\mathrm{Li}_\Lambda$, $(^{7*}\mathrm{Li})_\Lambda$ existed (*), it would decay rapidly by heavy particle emission, even though the available decay modes, shown in Fig. 7, violate isotopic spin conservation. The third

([18]) F. AJZENBERG and T. LAURITSEN: *Rev. Mod. Phys.*, **27**, 85 (1955).

(*) We propose the following notation: Λ bound to $A^* = (A^*)_\Lambda$; excited A_Λ: $(A_\Lambda)^*$.

member of the triplet, $^{7}Be_{\Lambda}$, corresponding to the unbound ^{6}Be core, has as yet not been detected.

The spin of $^{7}He_{\Lambda}$ (and hence of all members of the $T=1$ triplet) should be $J(^{7}He_{\Lambda})=\frac{1}{2}$, if one takes $J(\Lambda)=\frac{1}{2}$ and $J(^{6}He)=0$, and if one assumes that the Λ is in an s-state relative to the core. The $^{7}Li_{\Lambda}$ ground state would have a spin $J=\frac{1}{2}$ if the Λ-nucleon potential were stronger in the antiparallel spin orientation.

The $^{8}Li_{\Lambda}$ and $^{8}Be_{\Lambda}$ binding energies are quite compatible with an expected $T=\frac{1}{2}$ doublet for the mass 8 hypernuclei.

Fig. 8 shows a level diagram for the $A=9$ hypernuclides. To date, only $^{9}Li_{\Lambda}$ and $^{9}Be_{\Lambda}$ have been identified. As the ground state of ^{8}Li has $T=1$, $^{9}Li_{\Lambda}$ should have $T=1$, with $(^{9*}Be)_{\Lambda}$ and $^{9}B_{\Lambda}$ as the other members of the triplet. However, if $(^{9*}Be)_{\Lambda}$ were produced it would be unstable with respect to breakup into heavy particles, in analogy with the case of $(^{7*}Li)_{\Lambda}$ discussed above. All the observed $^{9}Be_{\Lambda}$ decays are of the form:

$$^{9}Be_{\Lambda} \rightarrow \pi^{-} + p + 2\,^{4}He\,.$$

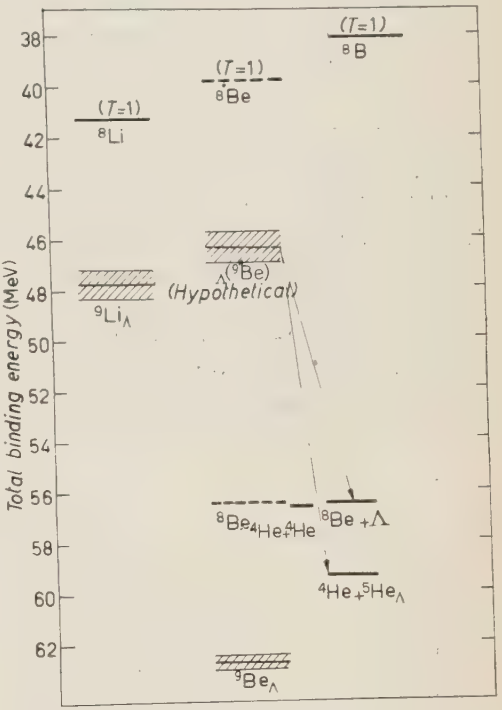

Fig. 8. – Isotopic spin multiplet structure of $A=9$ hypernuclei.

For all events observed the relative energy of the two ^{4}He in their barycentric system indicates that they come from the break-up of the ground state of ^{8}Be. This supports the assumption that in $^{9}Be_{\Lambda}$ the Λ-particle is bound to this latter system and consequently that $^{9}Be_{\Lambda}$ has $T=0$.

Taking as core nucleus two ^{4}He nuclei with relative energy 0.096 MeV, Suh [19] has calculated the Λ-nucleon interaction strength needed to give the observed B_{Λ} of $^{9}Be_{\Lambda}$; Suh's calculation gives results consistent with the Λ-nucleon interaction strength required for $^{5}He_{\Lambda}$ [20].

---

[19] K. S. Suh: *Phys. Rev.*, **111**, 941 (1958).
[20] R. H. Dalitz and B. W. Downs: *Phys. Rev.*, **111**, 967 (1958).

* * *

We are indebted to Professors V. L. TELEDGI and R. H. DALITZ for much helpful assistance and criticism. We wish in particular to thank Professor DALITZ for discussions concerning the theoretical aspects of our problems and Professor TELEGDI for help with the writing of the manuscript.

We wish to express our appreciation to Professors L. M. BROWN and J. H. ROBERTS for their valuable assistance and for helpful criticism and discussions.

We wish to thank Dr. F. INMAN for making available to us his IBM 650 program for hyperfragment analysis; this was adapted for some of our needs by Dr. E. SILVERSTEIN; we are deeply indebted to him for this.

At the Enrico Fermi Institute for Nuclear Studies, J. BAPTIST, T. BARTHA, M. MCCOY, P. KLIAUGA, E. MOORE, J. MOTT and P. SATERBLOM; at Northwestern University, D. ABELEDO, B. BUNKER, P. KAHN, S. LINFIELD, M. KAPLOW, L. WATSON, D. TROXEL and R. TREVINIA assisted in the scanning and measurements. We are grateful to all of them for their competent efforts.

We express our thanks to Dr. E. J. LOFGREN, Dr. H. HECKMAN, and the Bevatron staff whose co-operation made this experiment possible.

APPENDIX I

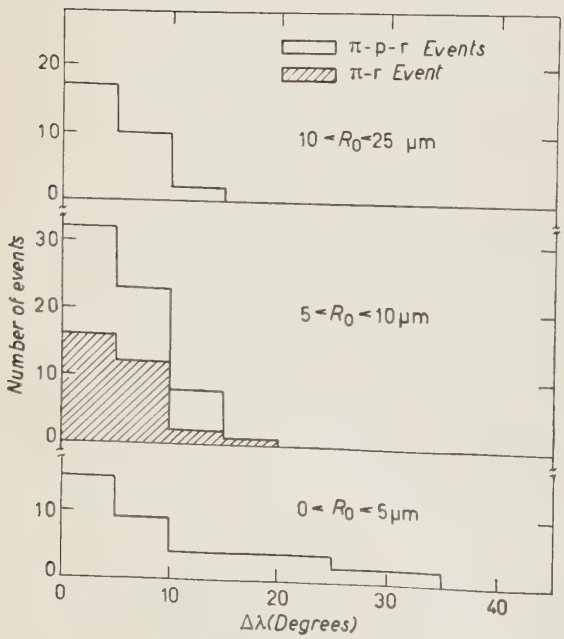

Fig. 9. – Histograms of difference between inferred and measured dip angles, $\Delta\lambda$, for various intervals of recoil range.

Range measurements of recoil tracks.

One of the limiting factors in obtaining precise measurements of short tracks not lying in the emulsion plane is the accuracy with which the vertical component (Δz) of the range can be determined. The measured value of Δz is therefore used only to establish that the event is colinear or coplanar within the experi-

mental errors. If this is the case, the dip of the recoil is inferred to be that value λ_i which makes the event colinear or coplanar ([2]). This value, together with the measured horizontal component is used to calculate the recoil range. The difference $\Delta\lambda$ between the observed and inferred dip angles is shown in Fig. 9 for different intervals of recoil ranges. As may be expected, the shorter recoils are likely to yield higher values of $\Delta\lambda$.

Appendix II

Charge discrimination from profile measurements.

For the NU stacks, consisting of 600 μm pellicles, the mean track thickness t measured over a projected distance of 9.1 μm centered at 31 μm of residual range was used as a parameter for charge discrimination. A cell length of 0.5 μm was used. The overall magnification was 6 500×. Fig. 10*a* shows t as a function of dip angle for the measured events.

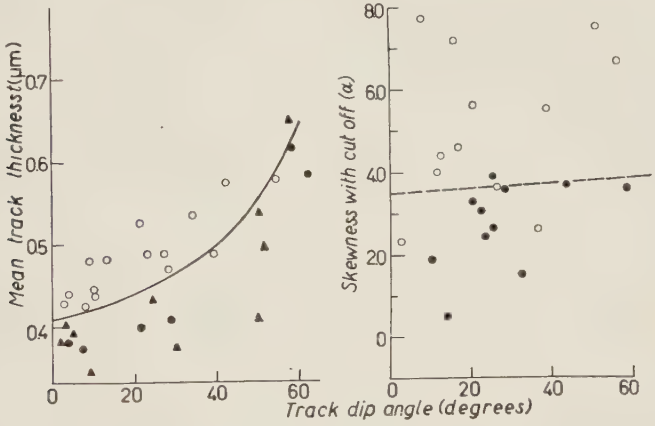

a) NU events *b*) EFINS events

Uniquely identified hyperfragments •: $Z=1$, ○: $Z=2$. Protons from uuique π-p-r decay: ▲.

Fig. 10. – Charge discrimination of hyperfragments and their decay products from profile measurements.

For the EFINS stack, consisting of 1200 μm pellicles, it was found more convenient to use another parameter. The thickness t_i was measured at intervals of 0.5 μm over the last 55 μm of track. The skewness of the distribution of t_i, found to be a charge sensitive parameter ([21]) was then used. Fig. 10*b* shows the results, plotted as a function of dip, for those events which could be measured.

([21]) R. Ammar: *Suppl. Nuovo Cimento*, **15**, 181 (1959).

Appendix III

Description of individual events.

One event was observed for each of the following hypernuclear decay modes:

a) $^{7}\mathrm{He}_{\Lambda} \rightarrow \pi^{-} + {}^{3}\mathrm{H} + {}^{4}\mathrm{He}$ $Q_0 = 45.12$ MeV (Event 2-55-2);

b) $^{11}\mathrm{B}_{\Lambda} \rightarrow \pi^{-} + {}^{3}\mathrm{He} + 2\,{}^{4}\mathrm{He}$ $Q_0 = 37.13$ MeV (Event 3-46-3);

c) $^{12}\mathrm{B}_{\Lambda} \rightarrow \pi^{-} + 3\,{}^{4}\mathrm{He}$ $Q_0 = 46.25$ MeV (Event 834).

Event 2-55-2. – Table III summarizes the range and angle measurements. This event cannot belong to the class π^{-}-p-r. In fact the minimum energy release involved [(39.8 ± 0.7) MeV, on the assumption that prongs 2 and 3 are protons] exceeds Q_{Λ} by a significant amount. Analysis of the event on the Silverstein's permutation code ([6]) yields only one acceptable interpretation, *i.e.* decay scheme *a*), with $B_{\Lambda} = (3.0 \pm 0.7)$ MeV and momentum unbalance $\Delta P = (24.3 \pm 23)$ MeV/c. Any other interpretation yields negative binding energies. Among these, those referring to known species are smaller than -2 MeV and involve incompatible kinematics. Interpretations in terms of other new species yield B_{Λ} smaller than -1 MeV, and ΔP in excess of 50 MeV/c. Decay scheme *a*) is therefore strongly preferred.

Table III. – *Event* 2-55-2. $^{7}\mathrm{He}_{\Lambda} \rightarrow \pi^{-} + {}^{3}\mathrm{H} + {}^{4}\mathrm{He}$.

Prong	Colatitude (degrees)	Azimuth (degrees)	Range (μm)
1 (π^{-})	25.4	64.2	21121
2 (^{3}H)	— 23.7	216.1	91.9
3 (^{4}He)	0	4.9	3.8
HF ($^{7}\mathrm{He}_{\Lambda}$)	21.6	249.4	45.6

Event 3-46-3. – The data for this event are contained in Table IV. The establishment $Z = 2$ for track 3 from thickness measurements ([21]) narrows

Table IV. – *Event* 3-46-3. $^{11}\mathrm{B}_{\Lambda} \rightarrow \pi^{-} + {}^{3}\mathrm{He} + 2\,{}^{4}\mathrm{He}$.

Prong	Colatitude (degrees)	Azimuth (degrees)	Range (μm)
1 (π^{-})	42.1	83.0	2040
2 (^{4}He)	— 16.4	3.0	7.1
3 (^{3}He)	33.6	248.6	79.8
4 (^{4}He)	— 35.7	107.5	21.5
HF ($^{11}\mathrm{B}_{\Lambda}$)	1.6	338.1	13.3

the possible interpretations to two

i) $^{11}B_\Lambda \rightarrow \pi^- + {}^3He + 2\,{}^4He$, $B_\Lambda = (9.93 \pm 0.6)$ MeV, $\Delta P = (23 \pm 19)$ MeV/c;

ii) $^{13}B_\Lambda \rightarrow \pi^- + n + 3\,{}^4He$, $B_\Lambda = (12.13 \pm 1.6)$ MeV, $P_n = (66 \pm 20)$ MeV/c;

i) is the only interpretation not involving neutron emission for which $\Delta P < 50$ MeV/c and ii) is the only one with neutron emission for which $B_\Lambda \geqslant 0$. On the basis of the low value of ΔP for i) we conclude that it is probably a more likely interpretation.

Event 834. – It is also a four body decay and is described in Table V. In this case the possible interpretations reduce to:

i) $^{12}B_\Lambda \rightarrow \pi^- + 3\,{}^4He$, $B_\Lambda = (9.55 \pm 0.5)$ MeV, $\Delta P = (26 \pm 33)$ MeV/c;

ii) $^{13}B_\Lambda \rightarrow \pi^- + n + 3\,{}^4He$, $B_\Lambda = (5.94 \pm 1.6)$ MeV, $P_n = (26 \pm 33)$ MeV/c.

Again, because of the low value of ΔP, it is concluded that i) is more probably correct.

TABLE V. – *Event* 834. $^{12}B_\Lambda \rightarrow \pi^- + 3\,{}^4He$.

Prong	Colatitude (degrees)	Azimuth (degrees)	Range (μm)
1 (π^-)	— 66.6	2.0	14 511
2 (^{4}He)	54	290.5	9.3
3 (^{4}He)	44	215.8	5.5
4 (^{4}He)	33.5	94.2	10.6
HF ($^{12}B_\Lambda$)	15.8	111	4.2

Finally, Table VI gives the original data for one event uniquely identified as $^7Li_\Lambda \rightarrow \pi^- + {}^3He + {}^4He$, ($Q_0 = 41.60$ MeV), while Table VII describes three examples of the decay $^9Li_\Lambda \rightarrow \pi^- + n + 2\,{}^4He$ ($Q_0 = 52.87$ MeV).

TABLE VI. – *Event* 3-35-2. $^7Li_\Lambda \rightarrow \pi^- + {}^3He + {}^4He$; $B_\Lambda = (5.47 \pm 0.6)$ MeV, $\Delta P = (27.4 \pm 11)$ MeV/c.

Prong	Colatitude (degrees)	Azimuth (degrees)	Range (μm)
1 (π^-)	— 16.4	172.0	10 300
2 (^{3}He)	12.7	163.4	23.0
3 (^{4}He)	— 9.3	347.8	40.1
HF ($^7Li_\Lambda$)	81.8	30.1	39.0

TABLE VII.

Prong	Colatitude (degrees)	Azimuth (degrees)	Range (μm)
Event 3-11-3. $^9Li_\Lambda \rightarrow \pi^- + n + 2\,^4He$; $B_\Lambda = (9.0 \pm 2.3)$ MeV, $P_n = (94.9 \pm 19)$ MeV/c.			
1 (π^-)	— 5.3	188.7	20 674
2 (^{4}He)	36.5	310.2	9.6
3 (^{4}He)	— 3.0	37.2	3.7
HF ($^9Li_\Lambda$)	— 30.0	356.4	30.2
Event 3-26-1. $^9Li_\Lambda \rightarrow \pi^- + n + 2\,^4He$; $B_\Lambda = (4.9 \pm 3.9)$ MeV, $P_n = (212 \pm 17)$ MeV/c.			
1 (π^-)	— 30.2	312.0	341.7
2 (^{4}He)	— 53.2	300.1	53.6
3 (^{4}He)	9.7	133.7	72.0
HF ($^9Li_\Lambda$)	58.4	70.8	28.7
Event 901. $^9Li_\Lambda \rightarrow \pi^- + n + 2\,^4He$; $B_\Lambda = (6.41 \pm 2.88)$ MeV, $P_n = (130.2 \pm 19.2)$ MeV/c.			
1 (π^-)	— 25.5	0.0	12 450
2 (^{4}He)	83.0	34.5	12.7
3 (^{4}He)	— 30.0	157.7	39.1
HF ($^9Li_\Lambda$)	49.0	22.0	5.0

RIASSUNTO

Dall'analisi di 134 decadimenti mesonici univocamente identificati si migliora la precisione con cui sono note le energie di legame degli ipernuclidi $^3H_\Lambda$, $^4H_\Lambda$, $^4He_\Lambda$, $^5He_\Lambda$, $^7Li_\Lambda$, $^8Li_\Lambda$, $^9Li_\Lambda$ e $^9Be_\Lambda$. Inoltre vengono descritti esempi individuali delle nuove specie $^7He_\Lambda$, $^{11}B_\Lambda$ e $^{12}B_\Lambda$. I dati presenti sono combinati con quelli raccolti nella rassegna EFINS. La struttura a multipletti di spin isotopico degli ipernuclei leggeri è discussa con riferimento alle informazioni dedotte dalle energie di legame.

IL NUOVO CIMENTO Vol. XV, N. 2 16 Gennaio 1960

Hyperfine Structure in Paramagnetic Free Radicals.

G. Cini-Castagnoli (*)

Istituto di Fisica dell'Università - Roma

(ricevuto il 17 Luglio 1959)

Summary. — Paramagnetic resonance of solutions in dioxane of the free radical $[(C_7H_7)_3\dot{N}]^+ClO_4^-$ has been investigated. Hyperfine structure has been found which can be interpreted in terms of the interaction of the unpaired electron with the Nitrogen nucleus and with some of the Hydrogens on the phenyl rings.

1. – Introduction.

Since the discovery of paramagnetic resonance absorption phenomena in free radicals (1), a large number of such resonances have been reported (2). Researches in this field have been concerned either with single peak resonances in solids (polycrystalline powders or single crystals) or with resonances in solutions which show hyperfine structure. The single peaks are often extremely narrow and are useful for precision magnetic field measurements in regions where proton resonance methods can not be used conveniently. The study of resonances exhibiting hyperfine splitting shows great promise as a tool for the analysis of the structure of molecules in which the unpaired electrons interact with a large number of atoms: for a number of molecules resonance experiments have provided valuable information on the distribution of electronic

(*) This work has been supported by the International Federation of University Women, Mary E. Woolley Fellowship and was carried out at the Physics Department, King's College in the University of Durham, Newcastle upon Tyne, England.

(1) A. N. Holden, C. Kittel, F. R. Merrit and W. A. Yager: *Phys. Rev.*, **77**, 147 (1950); C. H. Townes and J. Turkevich: *Phys. Rev.*, **77**, 148 (1950).

(2) See for instance *Discuss. Farad. Soc.*, **19** (1955), in particular the papers by: *a*) G. E. Pake, S. I. Weissmann and G. Townsend: p. 147; *b*) E. E. Schneider: p. 158.

wavefunctions over atoms having magnetic nuclei and hence on the positions of these atoms and on the nature of the bonding structure in the molecule.

In the present paper the results obtained on solutions in dioxane of the free radical $[(C_7H_7)_3\dot{N}]^+ClO_4^-$ are reported.

2. – Paramagnetic resonance absorption in solutions of free radicals.

The absorption of microwaves by free radicals arises from the fact that these compounds possess unpaired electrons When a molecule of a free radical is placed in a steady magnetic field B, its unpaired electron may assume either a parallel or an antiparallel orientation with respect to the applied magnetic field. If in the first instance the interaction of this unpaired electron with its surroundings is neglected, the energies of the electronic Zeeman levels are $E_+ = +\frac{1}{2}g\beta B$, $E_- = -\frac{1}{2}g\beta B$, $E_\pm$ are the eigenvalues of the « spin Hamiltonian »:

$$\mathscr{H} = g\beta \boldsymbol{B}\cdot\boldsymbol{S}\,, \tag{1}$$

where β is the Bohr magneton, g is the spectroscopic splitting factor, which has the value 2.002 3 for a free spin, and $\boldsymbol{S}$ the electron spin operator.

If now the magnetic interaction of the unpaired electron with n nuclei of spin 1 is taken into account, the Hamiltonian (1) becomes:

$$\mathscr{H} = g\beta \boldsymbol{B}\cdot\boldsymbol{S} + \sum_1^n \boldsymbol{A}_i \boldsymbol{I}_i\cdot\boldsymbol{S}\,, \tag{2}$$

where A_i describes the (isotropic) interaction with the i-th nucleus and is given essentially by the product of the magnetic moment of the nucleus and the magnetic field at the nucleus produced by the unpaired electron. This leads to a splitting of the electronic Zeeman levels into hyperfine components and consequently to a hyperfine structure of the resonance spectrum.

In a poly-atomic free radical in liquid solution the h.f.s. interaction of a given magnetic nucleus is determined exclusively by the density of the electronic spin magnetic moment at this nucleus *i. e.* by the value of the wave function of the unpaired electron at the position of the nucleus (2). This is a consequence of the molecular motions in the liquid which cause the magnetic field arising from the electron spin distribution outside the nucleus to be averaged out to zero and it implies that the interaction of the unpaired electron with its local nucleus, *i.e.* with the nucleus of the atom in the molecule on which the electron is localized, arises exclusively from that part of the electronic orbital which has *s*-character.

The resonance spectra of tri-phenyl-methyl

which consists of a complex pattern of a very large number of very closely spaced lines and of di-mesityl-methyl ([3])

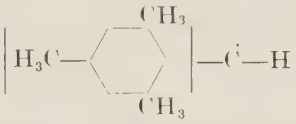

are assumed to arise from the h.f.s. interaction between the unpaired electron and the magnetic moments of some of the H-nuclei, since the magnetic moment of ^{12}C is zero. The same considerations can be applied to the structures observed by WEISSMAN *et al.* ([4]) and by VENKATARAMAN *et al.* ([5]) and also to the resonance spectra in X-irradiated plastics investigated by SCHNEIDER ([2]) which have been ascribed to radical end groups of the type

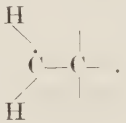

On the other hand, the hyperfine structures of free radicals containing besides protons other nuclei with non zero magnetic moments have been generally associated exclusively with the latter. Among such compounds we recall the sodium trimesitilboron ([6])

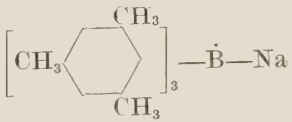

containing ^{11}B, the triarilaminium perchlorates ([7]) and various hydrazil compounds ([8]), containing ^{14}N.

([3]) H. S. JARRET and G. J. SLOAN: *Journ. Chem. Phys.*, **22**, 1783 (1954).

([4]) S. I. WEISSMANN: *Journ. Chem. Phys.*, **22**, 1135 (1954).

([5]) V. VENKATARAMAN and G. K. FRAENKEL: *Journ. Chem. Phys.*, **23**, 588 (1955).

([6]) S. I. WEISSMANN, J. TOWNSSEND, D. E PAUL and G. E. PAKE: *Journ. Chem. Phys.*, **21**, 222 (1953).

([7]) O. R. GILLIAM, R. I. WALKER and V. W. COHEN: *Journ. Chem. Phys.*, **23**, 1540 (1955).

([8]) H. S. JARRET: *Journ. Chem. Phys.*, **21**, 761 (1953).

The present investigation has been undertaken in order to determine whether the unpaired electron in the aminium ion

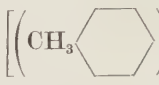

apart from interacting with the nitrogen nucleus, interacts also with protons on the phenyl rings which would indicate how far the wave function is extended over the molecule.

3. – Experimental procedure and results.

The main features of the sensitive paramagnetic resonance spectrometer which was available in the Newcastle Laboratories for the experiments on radicals, have been described by SCHNEIDER and ENGLAND (9); it consists of a microwave bridge and a super-heterodyne receiver for detecting the unbalanced signal caused by the magnetic absorption. The waveguide bridge is of the hybrid ring type and is designed to operate at frequencies near 9500 MHz. The signal power is obtained from a reflex klystron oscillator, type CV129 operated from HT batteries. A small amount of power is coupled into a calibrated absorption type cavity wavemeter, which enables the frequency to be determined to ± 1 MHz. The magnetic field is provided by an electromagnet having 5 in. pole faces with a Rose rim and a gap of 1.25 in.; at 3000 gauss the field is uniform to within less than 2 gauss over the volume of the liquid specimens used in the present work. Two additional coils on the magnet are supplied with alternating current from the 50 Hz main so that the field is periodically swept over the whole of the resonance region and the spectrum is displayed in the usual way on an oscilloscope by connecting the signal derived from the superheterodyne receiver on the y-plates and a voltage proportional to and in phase with the field modulation to the y- and x-deflection plates of the oscilloscope respectively.

The most important improvement which had been developed by Schneider (unpublished) since the earlier work, is a system for the frequency stabilisation of the signal klystron referring to the tuning frequency of the measuring cavity. It is based on a 465 kHz frequency modulation of the klystron (frequency deviation 100 kHz = .001%). The discriminating action of the measuring cavity leads to a small 465 kHz amplitude modulation if the mean klystron frequency deviates from the tuning frequency of the cavity. The consequent 465 kHz signal appearing at the output of the superhet receiver is converted

(9) E. E. SCHNEIDER and T. S. ENGLAND: *Physica*, **17**, 221 (1951).

in a phase sensitive detector into a d.c. frequency correcting voltage which is applied to the reflector of the klystron. The stabiliser reduces frequency noise, interference and tuning fluctuations arising from mechanical vibration, which are the factors limiting the sensitivity for the detection of weak resonances. At the time at which the work described here was carried out, it was possible to detect resonance signals on the oscilloscope (band width about 3 kHz) from less than 0.2 μg of crystalline DPPH which is equivalent to about 10^{17} electron spins (the signal is inversely proportional to the mean width which is about 4 gauss for DPPH).

For the study of the resonances of liquid solutions of radicals at room temperature a rectangular cavity having a tuning frequency of 9.526 MHz was constructed. It consists of a section of standard wave guide, one guide wave-length long, and is excited in the TE_{012} mode through a coupling hole in the end wall dividing it off from the main wave guide system.

The specimens were contained in small glass capillaries of 2.8 mm internal diameter which were introduced into the cavity through a hole in the centre of its narrow side. The specimens were thus in a position where the electric field is a minimum and the microwave magnetic field a maximum.

The solution of the aminium perchlorate was prepared by dissolving the weighed solid in a known volume of purified dioxane. The concentrations investigated ranged from about 0.01 to .32 molar. It is difficult to give the actual concentration of radical ions because, similar to some of the neutral radicals, the aromatic aminium radical ion tends to take up an extra electron from any reducing agent, so as to be converted into the electrically neutral and non-magnetic amine. But since this reducing reaction proceeds slowly with a reaction time of about 30 minutes while all operations including the actual measurements were performed within less than 10 minutes from the moment of dissolving the solid, it is reasonable to assume that during the resonance experiments a substantial fraction of the dissolved molecules was present in the form of free radical ions. A comparison with the resonance signal, from a small crystal of DPPH placed on the outside of the capillary produced simultaneously with that of the amine solution showed that, at the lower concentrations, about 10^{16} electron spins were present in the solution.

Table I summarizes the experimental results for different initial concen-

TABLE I.

Concentration	Full width at	Structure
pure solid powder	14.8 Gauss	unresolved
dioxane solution 0.32 molar	21 »	unresolved
dioxane solution 0.07 molar	25 »	partly resolved
dioxane solution 0.05 molar	25 »	8 peaks

trations. Some of the absorption spectra as displayed on the oscilloscope are shown in Fig. 1*a*, *b*, *c*. The horizontal scale is calibrated in terms of magnetic

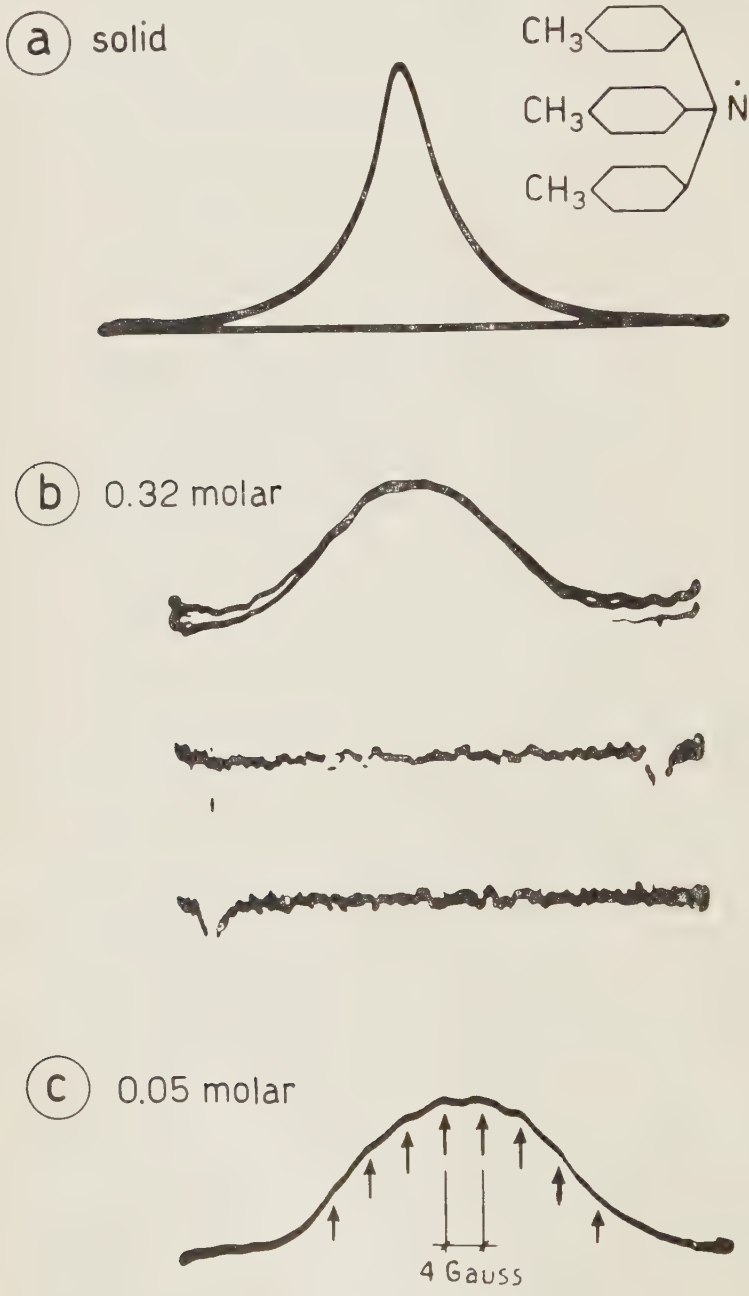

Fig. 1.

field strength by means of proton resonance signals displayed on the second trace of the double beam oscilloscope (see Fig. 1*b*). The coil with the water specimen of the radio frequency nuclear resonance spectrometer is placed close to the wave guide cavity in the field of the electromagnet (Fig. 1*b* is a double exposure at the same field with proton resonances at 14553 and 14346 MHz respectively). The variation of the overall width of the radical resonance in solution does not vary as much with concentration as in other free radicals (*e.g.* DPPH). At all concentrations the width of individual lines can be accounted for by spin-spin interaction.

The pure solid powder gives a single resonance line width a g-factor of 2.0033 (determined by comparison with the resonance positions of a single crystal of DPPH in different orientations and also by means of proton resonance). In dilute solution this line splits into 8 peaks the four central ones having about 4 gauss separation and those in the wings about 6 gauss (see Fig. 1*c*).

The spectrum can be analysed in many different ways. The unpaired electron apart from interacting with the nitrogen nucleus definitely interacts also with protons on the phenyl rings, but the spectrum is not resolved enough to give a full interpretation of the radicals' structure.

Two reasonable interpretations of the hyperfine structure are the following:

a) The electron interacts mainly with the protons in ortho and meta positions and, of course, with the nitrogen. If one assumes that the meta to ortho ratio is 2:3 and that the meta to nitrogen is 1:2 one gets 39 lines with the intensities 1 0 6 6 16 36 41 96 121 176 272 306 436 512 581 712 736 812 832.... The corresponding spectrum is in reasonable agreement with the experimental one if the width is ~ 2.6 gauss and the separation between individual peaks ~ 2 gauss. In formula (2)

$$A_{\text{ortho}} = 6 \text{ gauss}\,, \qquad A_{\text{meta}} = 4 \text{ gauss}\,, \qquad A_N = 8 \text{ gauss}\,.$$

b) One could assume that hyperconjugation is so effective that the interaction with the protons on the para methyl group is predominant; than one gets 14 lines with intensities

$$1,\ 9,\ 37,\ 93,\ 163,\ 219,\ 246\ \ldots$$

if it is assumed that the nitrogen splitting constant is twice that of the methyl protons. $A_N = 8$ gauss, methyl constant $A_P = 4$ gauss and width of individual lines ~ 8 gauss.

* * *

It is my pleasant duty to thank Dr. E. E. SCHNEIDER for his kind hospitality in his laboratory and for his continuous interest during the performance of this work. My best thanks to Dr. P. A. FORRESTER and to the Kings College Physics Department staff for their help.

RIASSUNTO

Si studia la risonanza paramagnetica di soluzioni in diossano di radicali liberi $[(C_7H_7)_3\dot{N}]\,ClO_4^-$. Si trova una struttura iperfine che può essere interpretata mediante l'interazione dell'elettrone spaziato con il nucleo di azoto e con alcuni dei nuclei di idrogeno dell'anello fenilico.

IL NUOVO CIMENTO Vol. XV, N. 2 16 Gennaio 1960

Internal Motions of Relativistic Fluid Masses.

F. Halbwachs, P. Hillion and J.-P. Vigier
Institut Henri Poincaré - Paris

(ricevuto il 4 Agosto 1959)

Summary. — On the basis of certain general results established by Weyssenhoff (1), Møller (2), Bohm and one of us (J.-P. V.) (3) on the behaviour of relativistic fluid masses enclosed within time-like tubes, we study internal motions corresponding to simple physical assumptions. We introduce a general new Lagrangian and Hamiltonian formalism in terms of Einstein-Kramer variables and relativistic Euler angles and apply it to some typical physical cases.

Introduction.

In a set of recent papers (3) the physical behaviour of relativistic fluid masses extended in ordinary space (that is enclosed within a time-like tube in Minkowski space) was studied in order to determine the laws of motion of certain global quantities. In the present paper we shall attempt a finer analysis of what goes on inside such tubes in order to reach a physical understanding of possible types of internal motion.

Such an attempt is necessarily limited. It is clear that the general motion of the fluid inside the tube can be as complex and violent as one pleases: since

(1) Weyssenhoff: *Acta Phys. Pol.*, **9**, 8 (1947).
(2) C. Møller: *Ann. Inst. H. Poincaré*, **11**, 251 (1949).
(3) A. Bohm and J.-P. Vigier: *Phys. Rev.*, **109**, 1882 (1958).

it varies with the internal tensions and initial conditions considered. Moreover, any departure from the point-like model implies that we dispose of an unlimited number of degrees of freedom and variables corresponding to the unlimited number of possible motions inside our time-like tube. As it is evidently hopeless to describe in detail such a motion, we must necessarily make some simplifying assumptions to reduce the number of variables needed. In order to do this let us remark that our present objective is to determine the behaviour of global quantities averaged over the total volume of the fluid mass. These correspond in a sense to collective variables describing overall properties of the motion. If we accept this point of view our first objective must be to introduce such typical variables associated in a clear way with some average properties of the fluid mass. After that, with the help of some physical restrictions, imposed on the internal motion, we can deduce in principle from a Lagrangian formalism the general laws of motion. Only then it will be possible to study simplified cases of stable internal motions which correspond to relativistic generalizations of Poincaré's classical theory of non relativistic fluid masses ([4]).

This brief analysis determines the plan of our paper. In Section **1**, we shall summarize known results of the general theory of relativistic fluid masses, and introduce new « global » variables. In Section **2** we shall study the Lagrangian and Hamiltonian formalism. In Section **3** we impose physically reasonable restrictions on the motion and determine the corresponding equations for the internal motion with the aid of a suitable Lagrangian and Hamiltonian. In Section **4**, we shall recall the usual procedure followed in the case of a non relativistic rotation, in order to put into evidence the constants of the motion by the introduction of Euler angles. In Section **5**, finally, we shall generalize the above procedure to the internal motion of a relativistic rotator in terms of relativistic Euler angles and determine the constants of the relativistic motion, which paves the way to its future quantization.

1. – As was stated in a former paper on the subject ([3]) no specific assumption on the exact nature of the internal fields constituting the fluid masses studied here is needed at this stage. They could be built for example by electromagnetic field concentration, combination of electromagnetic and gravitational fields (such as the « geons » proposed by WHEELER ([5])) or by still more complex combination of known and unknown fields. The only thing we shall suppose is that they are built out of an energy-momentum density $t_{\mu\nu}$ ($t_{\mu\nu} = t_{\nu\mu}$) and current density j_μ, strong within the particle and negligible out-

([4]) H. POINCARÉ: *Acta Math.*, **7**, 259 (1885).
([5]) J. A. WHEELER: *Phys. Rev.*, **97**, 511 (1955).

side [6], both satisfying the conservation relations:

$$\partial_\nu t_{\mu\nu} = 0 \tag{1a}$$

$$\partial_\mu j_\mu = 0 \tag{1b}$$

inside the tube which limits the particle.

As stated before, the theory of global variables has already been developped by various authors. If we assume that our particle is isolated with no external force, MOLLER has shown that it is possible to determine a physical point inside the fluid mass which corresponds to the classical picture [2] (when the tube is reduced to a line for example).

Let us resume his results. MOLLER first defines the total energy momentum of the particle by the relation:

$$G_\mu = \int_\Sigma t_{\mu 0} \mathrm{d}V ,$$

where $\mathrm{d}V$ denotes a volume element of a plane three dimensional section Σ of the tube and the $\int$ is taken over the whole section. He then shows that because of equations (1*a*) this G_μ is a four-vector independent of the chosen section. In the absence of an exterior force its components are constants of the motion:

$$\dot{G}_\mu = 0 . \tag{2}$$

Then with the help of this vector he defines a particularly remarkable frame Π_0 (which we shall hence forward call *Møller frame*) namely the one in which

$$G_i = 0 .$$

As we shall see, this frame will play an essential role in all that follows.

We have now the possibility of introducing a first physically remarkable point: the *center of gravity* (X_μ) defined in Π_0 by the relations:

$$X_i \int t_{c0} \mathrm{d}V = \int x_i t_{00} \mathrm{d}V , \quad X_0 = 0 .$$

This point moves with a four velocity u_μ ($u_\mu u_\mu = -c^2$) parallel to G_μ. In-

[6] F. HALBWACHS: *Théorie des fluides relativistes* (Paris, 1960), Chap. II and Appendix A.

troducing the scalar quantity M by

$$G_\mu G_\mu = - M^2 c^2 ,$$

we get

$$G_\mu = M u_\mu .$$

Next we can define an angular momentum $M^0_{\mu\nu}$ with respect to that center by the relations:

$$M^0_{\mu\nu} = \int [(x_\mu - X_\mu) t_{\nu 0} - (x_\nu - X_\nu) t_{\mu 0}] \, \mathrm{d}V .$$

This can be also shown to be a skew-tensor.

MØLLER then demonstrates that if we call τ the proper time taken along any arbitrary world line followed by the center of gravity we have (calling $\dot{A}$ the expression $\mathrm{d}A/\mathrm{d}\tau$):

$$\dot{M} = 0 ,$$

$$\dot{G}_\mu = 0 ,$$

$$\dot{M}^0_{\mu\nu} = 0 ,$$

$$\dot{u}_\mu = 0 .$$

The determination of Π^0 can now be made with the help of four unitary and orthogonal vectors, which we shall denote a^{ξ}_{μ}: (the index (ξ) labelling the vectors varies from one to four and is not a tensor index). We write:

$$a^{(4)}_\mu = \frac{u_\mu}{ic} = \frac{G_\mu}{iMc} \quad \text{with} \quad \dot{a}^{(4)}_\mu = 0 ,$$

The third space like axis $a^{(3)}_\mu$ (which can be called the Z axis) can be chosen parallel to the « spin vector » corresponding to the angular momentum $M^0_{\mu\nu}$ which is defined by the relation:

$$s^0_\mu = \frac{1}{c} \tilde{M}^0_{\mu\nu} u_\nu = i \tilde{M}^0_{\mu\nu} a^{(4)}_\nu , \qquad \left(\tilde{M}^0_{\mu\nu} \text{ is the dual } \frac{i}{2} \varepsilon_{\mu\nu\alpha\beta} M^0_{\alpha\beta} \right) .$$

This choice is justified by the fact that $M^0_{\mu\nu} a^{(4)}_\nu = 0$ and $\dot{M}^0_{\mu\nu} = 0$ so that

$$M^0_{\mu\nu} = \tfrac{1}{2} \varepsilon_{\mu\nu\alpha\beta} s^0_\alpha a^{(4)}_\beta \tag{3}$$

and

$$\dot{s}^0_\mu = 0 .$$

The last two remaining space-like axes must be taken orthogonal to $a_\mu^{(4)}$ and $a_\mu^{(3)}$. For example if we denote by R_μ the components of the four vector joining the center of gravity with another physically important point (such as the center of matter density which we shall define further) we can determine a vector

$$\Lambda_\mu = a_\mu^{(4)} - \frac{1}{P}(R_\mu - Q a_\mu^{(3)}),$$

which is evidently orthogonal to $a_\mu^{(4)}$ and $a_\mu^{(3)}$ if we write $P = R_\mu a_\mu^{(4)}$ and $Q = R_\mu a_\mu^{(3)}$. We can complete our orthogonal and unitary frame Π by the vectors

$$a_\mu^{(2)} = \frac{\Lambda_\mu}{\sqrt{\Lambda_\alpha \Lambda_\alpha}} \quad \text{and} \quad a_\mu^{(1)} = i\varepsilon_{\mu\nu\alpha\beta} a_\nu^{(2)} a_\alpha^{(3)} a_\beta^{(4)}.$$

As one knows, the orthogonality conditions on the a_μ^ξ system can be expressed by the equivalent relations

$$(4) \qquad \begin{cases} a_\mu^\xi a_\nu^\xi = \delta_{\mu\nu}, \\ a_\mu^\xi a_\mu^\eta = \delta^{\xi\eta}. \end{cases}$$

The essential point of the preceding discussion is that one can define a point X and a frame Π_0 centered on X independently of the detail behaviour of the internal structure of the particle. This implies:

a) that one can reduce the behaviour of the particle to the consideration of these quantities when we neglect this structure and approximate it as a rotating point;

b) that they provide a convenient frame of reference to study these internal motions. They play in a sense the well known role of the classical inertial frame in ordinary mechanics.

Now, if we want to study the internal motions let us first remark that they depend on so many factors (internal stresses, tensions, etc.) that a detailed study is *a priori* hopeless except in simplified cases. This is also true in classical mechanics, where studies of detailed fluid motions inside fluid masses have only been carried out in particular cases with special geometrical symmetries (4).

In general, the kinematical behaviour of the matter inside our tube is represented by a bundle of world lines tangent at each point to j_μ and comparable to a world-rope. Its complete description could be attempted in two steps;

a) determination of an average world-line l considered as the path of the ropes' central geometrical point;

b) average motion of the bundle around that line.

Evidently, if the dimensions of the tube are small and if we assume that the lines of this bundle are twisted in a continuous way around l, we can avoid step *b*, and restrict ourselves to the determination of l considered as describing the average twist of the global motion around the path of the center of gravity. Now as was shown before ([3]) the determination of l is very easy if we assume it to be the world-line followed by the center of matter density.

Such a center, as we know, can be defined in Π^0 by the relation.

$$Y_\mu \int j_4 \, \mathrm{d}V = \int x_\mu j_4 \, \mathrm{d}V .$$

This point moves with the velocity

$$\frac{\mathrm{d}Y_\mu}{\mathrm{d}\tau} = \dot{Y}_\mu \qquad (\dot{Y}_\mu \dot{Y}_\mu = -c^2)$$

and we know ([5]) that if we call τ the corresponding proper time along the world line followed by Y_μ, R_μ the vector $Y_\mu - X_\mu$, we can write the angular momentum with respect to it in the form:

$$\begin{aligned} M_{\mu\nu} &= \int \dot{[}(x_\mu - Y_\mu) t_{\nu 4} - (x_\nu - Y_\nu) t_{\mu 4}] \, \mathrm{d}V = \\ &= \int [(x_\mu - X_\mu) t_{\nu 4} - (x_\nu - X_\nu) t_{\mu 4}] \, \mathrm{d}V + \int [(X_\mu - Y_\mu) t_{\nu 4} - (X_\nu - Y_\nu) t_{\mu 4})] \, \mathrm{d}V = \\ &= \dot{M}_{\mu\nu} + R_\nu G_\mu - R_\mu G_\nu . \end{aligned}$$

Then, if we take the derivative of both sides with respect to τ we get:

$$\dot{M}_{\mu\nu} = G_\mu \dot{Y}_\nu - G_\nu \dot{Y}_\mu \tag{5}$$

So we have for Y_μ the set of classical equations ([6])

$$\begin{cases} \dot{G}_\mu = 0 , & M^2 c^2 R_\mu = - M_{\mu\nu} G_\nu , \\ \dot{M}_{\mu\nu} = G_\mu \dot{Y}_\nu - G_\nu \dot{Y}_\mu , & R_\mu G_\mu = 0 . \end{cases} \tag{6}$$

Now the motion of this center of matter density and the corresponding global quantities $M_{\mu\nu}$ and $\dot{Y}_\mu$ can be determined by various sets of kinema-

tical parameters. Following a well-known method we shall first attempt to describe them with the help of the Einstein-Kramer variables, that is we shall parametrize l with the help of a second orthogonal tetrad b_μ^ξ reflecting global properties of the whole droplet, referred this time to the center of matter density.

We first write:

$$b_\mu^{(4)} = \frac{\dot{Y}_\mu}{ic},$$

$$b_\mu^{(3)} = \frac{s_\mu}{\sqrt{s_\alpha s_\alpha}} \qquad \text{with } s_\mu = \tilde{M}_{\mu\nu}\dot{Y}_\nu$$

and determine a vector B_μ by the relation:

$$B_\mu = b_\mu^{(4)} - \frac{1}{P'}(R_\mu - Q' b_\mu^{(3)}),$$

with $P' = R_\mu b_\mu^{(4)}$ and $Q' = R_\mu b_\mu^{(3)}$. Then denoting by $b_\mu^{(2)}$ the normalized vector $B_\mu/\sqrt{B_\alpha B^\alpha}$ we have defined four orthogonal and unitary vectors $b_\mu^{(2)}$, $b_\mu^{(3)}$, $b_\mu^{(4)}$ and $b_\mu^{(1)}$ with

$$b_\mu^{(1)} = \frac{i}{2}\varepsilon_{\mu\nu\alpha\beta} b_\nu^{(2)} b_\alpha^{(3)} b_\beta^{(4)}.$$

We have also evidently:

$$\begin{cases} b_\mu^\xi b_\nu^\xi = \delta_{\mu\nu} \\ b_\mu^\xi b_\mu^\eta = \delta^{\xi\eta} \end{cases} \tag{7}$$

and will denote by Σ^0 the corresponding frame. As is well known [7] the instantaneous rotation of this frame is given by the expression $\omega_{\mu\nu}$ such that:

$$\dot{b}_\mu^\xi = \omega_{\mu\nu} b_\nu,$$

with

$$\omega_{\mu\nu} = \tfrac{1}{2}(\dot{b}_\mu^\xi b_\nu^\xi - \dot{b}_\nu^\xi b_\mu^\xi) = \dot{b}_\mu^\xi b_\nu^\xi. \tag{8}$$

Physically, the $\omega_{\mu\nu}$ can also be interpreted as the projection of $\dot{b}_\mu^\xi$ on the b_μ direction since $\dot{b}_\mu^\xi b_\nu^\xi = \omega_{\mu\nu}$.

The $\omega_{\mu\nu}$ tensor evidently describes the instantaneous rotation in a close neighbourhood of Y_μ.

Following TAKABAYASI [8] we then define the instantaneous rotation vector

[7] F. GÜRSEY: *Nuovo Cimento*, **5**, 784 (1957).
[8] T. TAKABAYASI: *Nuovo Cimento*, **13**, 532 (1959).

and acceleration by the set of relations:

$$\begin{cases} D_\mu = \tilde{\omega}_{\mu\nu} b_\nu^{(4)} \\ \dot{b}_\mu^{(4)} = \omega_{\mu\nu} b_\nu^{(4)} \end{cases}$$

where

$$\tilde{\omega}_{\mu\nu} = \tfrac{1}{2} \varepsilon_{\mu\nu\alpha\beta} \omega_{\alpha\beta} .$$

If we now move along l and denote by τ the proper time along this line, the frame Σ_0 will undergo a Lorentz transformation with coefficients depending on τ. As we said before, it is very natural to study the relative motion of (Y_μ) and Σ_0 with respect to (X_μ) and Π_0 and write

$$(9) \qquad \begin{cases} Y_\mu = X_\mu + R_\mu , \\ b_\mu^\xi = A^{\xi\eta} a_\mu^\eta . \end{cases}$$

In a sense this discussion shows that within the frame of the preceding physical assumptions (when we neglect step b), the internal motions of a relativistic fluid droplet can be described by the relative behaviour of two frames centered on two points namely.

$$-\Sigma^0 \ (b_\mu^\xi) \quad \text{with its origin on} \quad (Y_\mu) ,$$

$$-\Pi^0 \ (a_\mu^\xi) \qquad » \quad » \quad » \quad » \quad (X_\mu) .$$

As we have shown, in the case where no external force is acting, Π_0 and (X_μ) move in a straight line, while Σ_0 and (Y_μ) spiral around it according to the laws of motion. Our model can thus be compared to a relativistic hydrogen atom where the proton and a fixed frame centered on it play the part of (X_μ) and Π_0, Σ_0 and (Y_μ) representing the motion of the planetary electron (with its classical « spin »). It can be considered as a realistic representation within usual space-time, of the bilocal theories introduced by YUKAWA [9], RAYSKI [10] and other authors [11]. However, such theories which rest on the double point model (without the two frames) can be considered as a degenerate case of the proposed model of relativistic rotator.

Our next step is evidently to express a Lagrangian formalism in Π^0 in terms of R_μ and the b_μ^ξ's. But before we do that we would like to remark that our hydrogen-like model already indicates qualitatively how these motions

[9] H. YUKAWA: *Phys. Rev.*, **91**, 415 (1953).

[10] J. RAYSKI: *Proc. Phis. Soc.*, A **64**, 957 (1951).

[11] O. HARA, T. MARUMORI, Y. OHNUKI, and H. SHIMODAIRA: *Prog. Theor. Phys.*, **12**, 117 (1954).

could be quantized, if we recall de Broglie's [12] early interpretation of Bohr's model for such an atom. Indeed, we shall show in a later paper in collaboration with Professor Bohm that stable or metastable types of internal motions correspond to periodic motions of (Y_μ) on quantized orbits (corresponding in a sense to Bohr's original orbits) while Σ_0 comes back periodically to the same relative orientation (with respect to Π_0) after an entire number of circuits.

2. – According to our program, let us pass now to the Lagrange formulation of the laws of motion.

This can be done easily if we follow Gürsey [7] and choose as variables the co-ordinates of the center of matter density Y_μ and the components b_μ^ξ which determine Σ_0, all these variables depending on the proper time τ along the world line l followev by Y_μ. But before we give any explicit form for l let us recall briefly two general results.

A) If we suppose that the internal structure of a relativistic body is expressed by a set of vectors q_μ^r expressing certain global properties (instantaneous rotation, etc.) of this structure and localized at a definite « center » of the body, we can assume the free motion will be described by a Lagrangian function [13]:

$$L(\dot{Y}_\mu, q_\mu^r, \dot{q}_\mu^r) ,$$

with

$$\delta \int_{M_2}^{M_1} L(\dot{Y}_\mu, q_\mu^r, \dot{q}_\mu^r)\, \mathrm{d}\tau = 0 , \tag{9}$$

where $\dot{A}$ denotes as usual the expression $\mathrm{d}A/\mathrm{d}\tau$, τ is the proper time associated to the world line followed by the « center ». The summation is taken along this world line from a fixed point M_1 up to a fixed point M_2.

As a consequence of (9) we get Euler's equations

$$\frac{\mathrm{d}}{\mathrm{d}\tau}\frac{\partial L}{\partial \dot{q}_\mu^r} = \frac{\partial L}{\partial q_\mu^r} , \tag{10a}$$

$$\frac{\mathrm{d}}{\mathrm{d}\tau}\frac{\partial L}{\partial \dot{Y}_\mu} = 0 . \tag{10b}$$

Note that (10*b*) can also be written in the form

$$\dot{K}_\mu = 0 \qquad \text{with} \qquad K_\mu = \frac{\partial L}{\partial \dot{Y}_\mu} . \tag{11}$$

[12] L. de Broglie: *Thèse*, Paris (1927).
[13] F. Halbwachs and J.-P. Vigier: *Compt. Rend. Acad. Sci.*, 248, 490, 1124 (1959).

If we now apply an idea of E. NOETHER [14] and consider variations δY_μ, δq_μ^r *resulting from an arbitrary Lorentz transform* $A_{\mu\nu}$, they will no longer be independent, and on another hand, they will no longer vanish at the limits of integrations. However, the variation $\delta \int_{M_1}^{M_2} L \, d\tau$ will still be zero since the Lagrangian is a scalar. We thus get:

$$\delta \int_{M_1}^{M_2} L \, d\tau = \int_{M_1}^{M_2} \left(\frac{\partial L}{\partial \dot{Y}_\mu} \delta \dot{Y}_\mu + \frac{\partial L}{\partial q_\mu^r} \delta q_\mu^r + \frac{\partial L}{\partial \dot{q}_\mu^r} \delta \dot{q}_\mu^r \right) d\tau = 0 ,$$

which gives, when we integrate by parts:

$$\int \left(-\frac{d}{d\tau} \frac{\partial L}{\partial \dot{Y}_\mu} \delta Y_\mu \right) d\tau + \int \left(\frac{\partial L}{\partial q_\mu^r} - \frac{d}{d\tau} \frac{\partial L}{\partial \dot{q}_\mu^r} \right) \delta q_\mu^r \, d\tau +$$

$$+ \int \frac{d}{d\tau} \left(\frac{\partial L}{\partial \dot{Y}_\mu} \delta Y_\mu \right) d\tau + \int \frac{d}{d\tau} \left(\frac{\partial L}{\partial \dot{q}_\mu^r} \delta q_\mu^r \right) d\tau = 0 .$$

The first two terms vanish as a consequence of Euler's equations so we have:

$$\frac{d}{d\tau} \left(\frac{\partial L}{\partial \dot{Y}_\mu} \delta Y_\mu + \frac{\partial L}{\partial \dot{q}_\mu^r} \delta q_\mu^r \right) \equiv \frac{d}{d\tau} \left(\frac{\partial L}{\partial \dot{q}_\mu^r} \delta q_\mu^r + K_\mu \delta Y_\mu \right) = 0$$

If we write down explicitely the variations $\delta Y_\mu \, dq_\mu^r$ resulting from an arbitrary infinitesimal Lorentz transform, and set:

$$S_{\alpha\beta} = q_\alpha^r \frac{\partial L}{\partial \dot{q}_\beta^r} - q_\beta^r \frac{\partial L}{\partial \dot{q}_\alpha^r} ,$$

we get finally, taking (11) into account

$$\dot{S}_{\alpha\beta} = K_\alpha \dot{Y}_\beta - K_\beta \dot{Y}_\alpha . \tag{12}$$

Then if we identify the « canonical conjugated momenta » K_μ and $S_{\mu\nu}$ with the integrated global quantities G_μ and $M_{\mu\nu}$ of the droplet theory in Section **1**, equations (11) and (12) are just the two Weyssenhoff's equations of motion (2) and (5).

B) If we have a Lagrangian of the considered type which depends on various vector variables q_α^r and is a quadratic form of the $\dot{q}_\alpha^r$ we can write the equation of motion in a relativistic Hamiltonian form. Introducing the conju-

[14] E. NOETHER: *Götting. Nachr.*, 235 (1918).

gate variables by the relations:

$$p^r_\alpha = \frac{\partial L}{\partial \dot{q}^r_\alpha}(q^r_\alpha, \dot{q}^r_\alpha), \tag{13}$$

we can introduce the scalar Hamiltonian $H = p^r_\alpha \dot{q}^r_\alpha - L(q^r_\alpha p^r_\alpha)$ and find, taking into account Euler's equations:

$$\frac{\mathrm{d}}{\mathrm{d}\tau}\left(\frac{\partial L}{\partial \dot{q}^r_\alpha}\right) \equiv \dot{p}^r_\alpha = \frac{\partial L}{\partial q^r_\alpha}$$

the usual relations

$$\dot{p}^r_\alpha = -\frac{\partial H}{\partial q^r_\alpha} \qquad \text{and} \qquad \dot{q}^r_\alpha = \frac{\partial H}{\partial p^r_\alpha}. \tag{14}$$

Note that $H(p^r_\alpha q^r_\alpha)$ is a constant of the motion, since

$$\frac{\partial H}{\partial \tau} = \frac{\partial H}{\partial p^r_\alpha}\dot{p}^r_\alpha + \frac{\partial H}{\partial q^r_\alpha}\dot{q}^r_\alpha = 0,$$

because of (14) when we replace in $L(q^r_\lambda, \dot{q}^r_\lambda)$ the $\dot{q}^r_\lambda$'s by their values in terms of the p^r_α deduced from (13). As we shall see in the usual relativistic theory, H is just proportional to the rest mass term and we have $H = -\frac{1}{2}m_0c^2$. Moreover, introducing the usual Poisson brackets

$$[f(q, p), g(q, p)] = \frac{\partial f}{\partial q}\frac{\partial g}{\partial p} - \frac{\partial f}{\partial p}\frac{\partial g}{\partial q},$$

we see that the equations of motion (14) imply that the variation of any function $A(p, q)$ along l will be described by the usual relation

$$\dot{A} \equiv \frac{\mathrm{d}A}{\mathrm{d}\tau} = [A, H],$$

each quantity A whose Poisson bracket vanishes being a constant of the motion.

The preceding formalism can evidently be applied to a Newtonian point particle. If we denote by $X_\lambda(\tau)$ the mechanical variables characterizing its position we can choose the Lagrangian

$$L = \tfrac{1}{2}\, m_0 \dot{X}_\mu \dot{X}_\mu$$

which gives as Euler equation

$$\frac{\mathrm{d}}{\mathrm{d}\tau}(m_0\dot{X}_\mu) = 0 .$$

The corresponding Hamiltonian equations follow easily. We have:

$$G_\mu = \frac{\partial L}{\partial \dot{X}_\mu} = m_0 \dot{X}_\mu ,$$

which imply

$$L = \tfrac{1}{2} G_\mu \dot{X}_\mu .$$

So

$$H = G_\mu \dot{X}_\mu - L = \tfrac{1}{2} G_\mu \dot{X}_\mu ,$$

or in terms of canonical variables:

$$H = \frac{1}{2m_0} G_\mu G_\mu .$$

The canonical equations of the motion are:

$$\dot{G}_\mu = 0 \quad \text{and} \quad G_\mu = m_0 \dot{X}_\mu$$

and according to the latter, we get

$$\dot{H} = -\tfrac{1}{2} m_0 c^2 .$$

If we now come back to our problem of determining a Lagrange formalism for the extended particle the most natural assumption is to add to the point particle Lagrangian some terms which will globally take into account the internal behaviour of the particle. However, we must keep in mind the essential fact that any specific form of L represents only certain possible simple particular behaviour of the extended body among the unlimited number of possibilities (related to the detailed internal behaviour) so that no form chosen can correspond to a general theory. Any specific choice must therefore be guided by physical reasons and justified by its experimental consequences.

3. – Our specific proposal is to add to the point particle Lagrangian the relativistic generalization of the classical term representing the rotation energy described by the motion of the fram Σ_0 with respect to Π_0.

In three dimensions where Σ_0 is represented by three vectors b_k^r ($b_k^r b_j^r = \delta_{kj}$) and the angular velocity is the antisymetrical expression $\omega_{ij} = \dot{b}_i^r b_j^r$, we know

that such a term can be written in the form

$$\tfrac{1}{2} I^{ij} \omega_i \omega_j \, .$$

I^{ij} being the symetrical tensor of inertia with

$$\omega_i = \varepsilon_{ijk} \omega_{jk} \, .$$

As we have shown elsewhere ([15]), the relativistic generalization takes the form:

$$\frac{1}{8} I_{\mu\nu\alpha\beta} \omega_{\mu\nu} \omega_{\alpha\beta} \qquad (\omega_{\mu\nu} \quad \dot{b}^{\xi}_{\mu} b^{\xi}_{\nu})$$

the relativistic inertial tensor $I_{\mu\nu\alpha\beta}$ being symetric with respect to the change of μ, ν to α, β and antisymetric in both pairs $\alpha\beta$ and $\mu\nu$.

Naturally, this term can be simplified in many physical cases and we can assume various simple forms corresponding to typical cases. For example NAKANO has proposed ([16]) to use the form $\frac{1}{4} I \omega_{\mu\nu} \omega_{\mu\nu}$ which represents a natural relativistic generalization of the non-relativistic spherical rigid body, I being taken constant. Introducing the EK variables and taking into account relation (7), T takes the very simple form:

$$T = \tfrac{1}{4} I \dot{b}^{\xi}_{\mu} \dot{b}^{\xi}_{\mu} \, .$$

We shall treat this simple case completely with the help of two sets of variables in order to illustrate the preceding Hamiltonian formalism.

The complete Lagrangian will contain the ordinary mass term $\frac{1}{2} m_0 \dot{Y}_{\mu} \dot{Y}_{\mu}$ and a set of terms entailing the orthonormality condition (7), which can be written

$$\lambda_{\mu\nu} (b^{\xi}_{\mu} b^{\xi}_{\nu} - \delta_{\mu\nu})$$

with the symetrical set of Lagrange multipliers $\lambda_{\mu\nu}$. But we must not forget that we have chosen the fourth EK vector $b^{(4)}_{\mu}$ colinear to $\dot{Y}_{\mu}$, that is tangent to the world line followed by the center of matter density. This can be expressed in two equivalent ways:

1) We write simply, with the index (r) running from 1 to 3 only:

$$(15) \qquad L = \frac{1}{2} m_0 \dot{Y}_{\mu} \dot{Y}_{\mu} - \frac{1}{4} I \left(\dot{b}^{r}_{\mu} \dot{b}^{r}_{\mu} - \frac{1}{c^2} \ddot{Y}_{\mu} \ddot{Y}_{\mu} \right) + \lambda_{\mu\nu} \left(b^{r}_{\mu} b^{r}_{\nu} - \frac{1}{c^2} \dot{Y}_{\mu} \dot{Y}_{\nu} - \delta_{\mu\nu} \right) .$$

([15]) F. HALBWACHS, B. HILLION and J.-P. VIGIER: *Nuovo Cimento*, Letter to the Editor, **11**, 882, (1959).

([16]) T. NAKANO: *Prog. Theor. Phys.*, **15**, 333 (1956).

This Lagrangian can be treated by a well known generalization ([17]) of the Lagrange formalism with second derivatives and gives suitable Euler equations. But certain difficulties arise if one will pass to the Hamiltonian formalism. To do this we can use a well known formal device.

2) We keep independently both variables $ic b_\mu^{(4)}$ and $\dot{Y}_\mu$ and introduce a subsidiary Lagrange condition which makes them to be equal, with a new Lagrange multiplier k_μ:

$$L = \tfrac{1}{2} m \dot{Y}_\mu \dot{Y}_\mu - \tfrac{1}{4} I \dot{b}_\mu^\xi \dot{b}_\mu^\xi + \lambda_{\mu\nu}(b_\mu^\xi b_\nu^\xi - \delta_{\mu\nu}) + k_\mu(ic b_\mu^{(4)} - \dot{Y}_\mu) \,. \tag{16}$$

This form can be treated in Hamiltonian formalism without any difficulty.

The canonical angular momentum derived from expression (16) is just, as we recalled in Section **2**,

$$M_{\mu\nu} = b_\mu^\xi \frac{\partial L}{\partial \dot{b}_\mu^\xi} - b_\nu^\xi \frac{\partial L}{\partial \dot{b}_\mu^\xi} = \frac{1}{2} I(\dot{b}_\mu^\xi b_\nu^\xi - \dot{b}_\nu^\xi b_\mu^\xi) = I\omega_{\mu\nu} \tag{17}$$

so that $M_{\mu\nu}$ is parallel to $\omega_{\mu\nu}$, which corresponds to the well known classical behaviour of the spherical rotator.

Then introducing the canonical variables:

$$G_\mu = \frac{\partial L}{\partial \dot{Y}_\mu} = m_0 \dot{Y} - k_\mu,$$

$$\beta_\mu^\xi = \frac{\partial L}{\partial \dot{b}_\mu^\xi} = -\frac{1}{2} I \dot{b}_\mu^\xi \,,$$

we get the Hamiltonian

$$H = G_\mu \dot{Y}_\mu - \beta_\mu^\xi \dot{b}_\mu^\xi - L$$

that is, by elimination of the time derivatives:

$$H = \frac{1}{2m_0}(G_\mu + k_\mu)^2 - \frac{1}{I}\beta_\mu^\xi \beta_\mu^\xi - ic k_\mu b_\mu^{(4)} - \lambda_{\mu\nu}(b_\mu^\xi b_\nu^\xi - \delta_{\mu\nu}) \,.$$

The corresponding canonical equations are:

$$\frac{\partial H}{\partial Y_\mu} \equiv 0 = -\dot{G}_\mu \,, \qquad \frac{\partial H}{\partial G_\mu} \equiv \frac{1}{m_0}(G_\mu + k_\mu) = \dot{Y}_\mu \,,$$

$$\frac{\partial H}{\partial b_\mu^r} \equiv -2\lambda_{\mu\nu} b_\nu^r = -\dot{\beta}_\mu^r \,, \qquad \frac{\partial H}{\partial \beta_\mu^r} \equiv -\frac{2}{I}\beta_\mu^r = \dot{b}_\mu^r \,,$$

([17]) M. VON LAUE: *La Relativité* (Paris, 1924).

$$\frac{\partial H}{\partial b_\mu^{(4)}} \equiv -2\lambda_{\mu\nu} b_\nu^{(4)} - ick_\mu \equiv -\dot{\beta}_\mu^{(4)}\,, \qquad \frac{\partial H}{\partial \beta_\mu^{(4)}} \equiv -\frac{2}{I}\beta_\mu^{(4)} \equiv \dot{b}_\mu^{(4)}\,,$$

$$\frac{\partial H}{\partial k_\mu} \equiv \frac{1}{m_0}(G_\mu + k_\mu) - icb_\mu^{(4)} = 0\,, \qquad \rightarrow \text{that is} \quad icb_\mu^{(4)} \equiv \dot{Y}_\mu\,,$$

$$\frac{\partial H}{\partial \lambda_{\mu\nu}} \equiv b_\mu^\xi b_\nu^\xi - \delta_{\mu\nu} = 0\,.$$

Naturally, this Lagrangian could be complicated in many ways be adding various Lagrange conditions and taking various forms for the inertial tensor. We could also add to the Lagrangian some terms depending on our two centers of the form $V(R_\mu)$, this potential between the two points corresponding to the global effect of the internal stresses of the droplet. Of course, it is not necessary to use the b_μ^ξ variables; any equivalent set would do. For example, if we study the motion in the frame Π_0 we can introduce the relativistic generalization of the Euler angles which transform Π_0 into Σ_0. This will be done in the next Section. In fact, we shall see that this new set of variables allows a clear physical understanding of the relativistic behaviour of the two frames and facilitates the comparison with the non-relativistic behaviour of the classical body in three dimensions.

4. – In order to clarify the exact behaviour of our spherical four dimensional rotator, let us first summarize briefly certain results concerning the three dimensional rigid spherical rotator. As one knows such a rotator is described by three orthogonal unitary vectors b_k^r attached to the body and satisfying the conditions:

$$b_j^r b_k^r = \delta_{jk}\,, \qquad b_k^r b_k^s = \delta^{rs}\,. \tag{18}$$

The instantaneous rotation of this frame with respect to a fixed laboratory frame a_k^r is described by the pseudo-vector ω_i defined by the well known relation:

$$\omega_i = \varepsilon_{ijk}\,\dot{b}_j^r\, b_k^r \qquad \text{(the } \textit{dot} \text{ means the derivation d/d}t\text{)}. \tag{19}$$

The rotation energy in the spherical case takes the well known form:

$$T = \tfrac{1}{2} I\omega_i\omega_i = \tfrac{1}{2} s_i\omega_i\,, \tag{20}$$

where I represents the classical moment of inertia and s_i the angular momentum which is just $I\omega_i$; taking into account relation (19) this becomes:

$$T = \tfrac{1}{2} I\varepsilon_{ijk}\varepsilon_{ilm}\,\dot{b}_j^r b_k^r b_l^s \dot{b}_m^s = \tfrac{1}{2} I\dot{b}_j^r \dot{b}_j^r\,,$$

which is just the non-relativistic limit of the internal energy taken into account in the Nakamo Lagrangian.

The total Lagrangian can be written:

$$L = \tfrac{1}{2} I \dot{b}_j^r \dot{b}_j^r + \lambda_{ij}(b_i^r b_j^r - \delta_{ij}) ,$$

the λ_{ij} being a symetrical set of Lagrange's multipliers implying condition (18).

We pass to the Hamiltonian formalism with the help of the conjugated momenta:

$$\beta_j^r = \frac{\partial L}{\partial \dot{b}_j^r} = I \dot{b}_j^r$$

and form the Hamiltonian

$$H = \beta_j^r \dot{b}_j^r - L$$

which becomes in our case

$$H = \frac{1}{I} \beta_j^r \beta_j^r - \lambda_{ij}(b_i^r b_j^r - \delta_{ij}) .$$

The canonical equations can then be written:

$$\frac{\partial H}{\partial \beta_j^r} = \frac{1}{I} \beta_j^r = \dot{b}_j^r ,$$

$$\frac{\partial H}{\partial b_j^r} = - \lambda_{ij} b_i^r = - \dot{\beta}_j^r .$$

The total angular momentum $s_i s_i = I^2 \omega_i \omega_i = \beta_j^r \beta_j^r$ is evidently a constant of the motion since $[H, s_i s_i] = 0$.

As one knows this formulation can be greatly simplified by the use of the Euler angles, which transform a_k^r into b_k^r.

Writing this transformation in the classical matrix form:

$$\begin{pmatrix} b_k^{(1)} \\ b_k^{(2)} \\ b_k^{(3)} \end{pmatrix} = \begin{vmatrix} \cos\varphi & \sin\varphi & 0 \\ -\sin\varphi & \cos\varphi & 0 \\ 0 & 0 & 1 \end{vmatrix} \begin{vmatrix} \cos\theta & 0 & -\sin\theta \\ 0 & 1 & 0 \\ \sin\theta & 0 & \cos\theta \end{vmatrix} \begin{vmatrix} \cos\psi & \sin\psi & 0 \\ -\sin\psi & \cos\psi & 0 \\ 0 & 0 & 1 \end{vmatrix} \cdot \begin{pmatrix} a_k^{(1)} \\ a_k^{(2)} \\ a_k^{(3)} \end{pmatrix}$$

we obtain after calculation the well known table of the direction cosines:

r \ s	$b_k^r = A^{rs} a_k^s$		
	$\cos\varphi\cos\theta\cos\psi - \sin\varphi\sin\psi$	$\cos\varphi\cos\theta\sin\psi + \sin\varphi\cos\psi$	$-\cos\varphi\sin\theta$
	$-\sin\varphi\cos\theta\cos\psi - \cos\varphi\sin\psi$	$-\sin\varphi\cos\theta\sin\psi + \cos\varphi\cos\psi$	$\sin\varphi\sin\theta$
	$\sin\theta\cos\psi$	$\sin\theta\sin\psi$	$\cos\theta$

With the help of these new variables and the definition (19) we get the usual expression for the projections of ω_i on the moving frame b_k^r:

$$(21)\qquad \begin{cases} \omega'^1 = -\cos\varphi\,\sin\theta\,\dot{\psi} + \sin\varphi\,\dot{\theta}\,, \\ \omega'^2 = \sin\varphi\,\sin\theta\,\dot{\psi} + \cos\varphi\,\dot{\theta}\,, \\ \omega'^3 = \dot{\varphi} + \cos\theta\,\dot{\psi}\,. \end{cases}$$

The detail of this calculation in a simplified matrix form can be found in a paper from one of us (F. H.) [18]. As a consequence, the Lagrangian expressed in Euler angles takes the well known form:

$$L = \tfrac{1}{2} I(\dot{\varphi}^2 + \dot{\theta}^2 + \dot{\psi}^2 + 2\dot{\varphi}\,\dot{\psi}\cos\theta)\,,$$

condition (18) being satisfied automatically. This gives, with the help of the canonical momentum

$$p_\varphi = \frac{\partial L}{\partial \dot{\varphi}} = I(\dot{\varphi} + \dot{\psi}\cos\theta)\,,$$

$$p_\psi = \frac{\partial L}{\partial \dot{\psi}} = I(\dot{\psi} + \dot{\varphi}\cos\theta)\,,$$

$$p_\theta = \frac{\partial L}{\partial \dot{\theta}} = I\dot{\theta}\,,$$

the usual Hamiltonian in canonical form:

$$H = \frac{1}{2I}\left[\frac{p_\varphi^2 + p_\psi^2 - 2p_\varphi p_\psi\cos\theta}{\sin^2\theta} + p_\theta^2\right].$$

On the other hand, we can compare the usual expression

$$H = \tfrac{1}{2}(p_\varphi\,\dot{\varphi} + p_\psi\,\dot{\psi} + p_\theta\dot{\theta})\,,$$

with the form resulting from the formula (20)

$$H = \tfrac{1}{2} s'^i \omega'_i\,.$$

So we get, with the help of relation (21):

$$p_\varphi = s'_3\,,$$

$$p_\theta = s'_1\sin\varphi + s'_2\cos\varphi,$$

$$p_\psi = -s'_1\sin\theta\cos\varphi + s'_2\sin\theta\sin\varphi + s'_3\cos\theta\,,$$

---

[18] F. Halbwachs: to be published in *Ann. Inst. H. Poincaré.*

or conversely

$$s'_1 = p_\theta \sin\varphi + p_\varphi \operatorname{ctg}\theta \cos\varphi - p_\psi \frac{\cos\varphi}{\sin\theta},$$

$$s'_2 = p_\theta \cos\varphi - p_\psi \operatorname{ctg}\theta \sin\varphi + p_\psi \frac{\sin\varphi}{\sin\theta},$$

$$s'_3 = p_\varphi,$$

as the projection of the angular momentum $\boldsymbol{s}$ on the axes of the moving frame b_k^r.

The components on the fixed frame a_k^r are ([18]):

$$s_1 = -p_\theta \sin\psi - p_\psi \operatorname{ctg}\theta \cos\psi + p_\varphi \frac{\cos\psi}{\sin\theta},$$

$$s_2 = \quad p_\theta \cos\psi - p_\psi \operatorname{ctg}\theta \sin\psi + p_\varphi \frac{\sin\psi}{\sin\theta},$$

$$s_3 = \quad p_\psi .$$

These expressions of s_k and likewise those of s'_k allow us to express the total angular momenta

$$s^2 = s_k s_k = s'_k s'_k = \frac{1}{\sin^2\theta}(p_\varphi^2 + p_\psi^2 - 2p_\varphi p_\psi \cos\theta) + p_\theta^2 = 2IH .$$

These results, compared to the above canonical form of the Hamiltonian shows immediately that we have:

$$[H, p_\varphi] = 0 , \qquad [H, p_\psi] = 0 , \qquad [H, s^2] = 0 .$$

That is, we have, as it is well known, three evident constants of the motion, namely the projections s_3 of the angular momentum vector on the fixed $a_\mu^{(3)}$ axe, its projection s'_3 on the moving $b_\mu^{(3)}$ axe and its magnitude s.

Finally, a short calculation yields the following form for the rotation energy in Euler angles:

$$T = I(\dot\psi^2 + \dot\varphi^2 + \dot\theta^2 + 2\dot\varphi\dot\psi\cos\theta) .$$

5. Our next and last step is to pass to the four dimensional theory. In order to do that, let us summarize the relativistic generalization of Euler angles. This generalization which we have developed in a recent paper ([19]) expands a result obtained theoretically by EINSTEIN and MAYER ([20]) and further and

([19]) F. HALBWACHS, P. HILLION and J.-P. VIGIER: to be published in *Ann. Inst. H. Poincaré*.

([20]) A. EINSTEIN and R. MAYER: *Sitzber. Akad. Berlin* (1932).

more precisely by CASIMIR ([21]) and VAN WINTER ([22]). One can show that the Lorentz transform which transforms the a_μ^ξ into the b_μ^ξ can be written into the matrix form:

$$(22)\quad \begin{pmatrix} b_\mu^{(1)} \\ b_\mu^{(2)} \\ b_\mu^{(3)} \\ b_\mu^{(4)} \end{pmatrix} = \begin{pmatrix} \cos\frac{\varphi^+}{2} & \sin\frac{\varphi^+}{2} & 0 & 0 \\ -\sin\frac{\varphi^+}{2} & \cos\frac{\varphi^+}{2} & 0 & 0 \\ 0 & 0 & \cos\frac{\varphi^+}{2} & \sin\frac{\varphi^+}{2} \\ 0 & 0 & -\sin\frac{\varphi^+}{2} & \cos\frac{\varphi^+}{2} \end{pmatrix} \begin{pmatrix} \cos\frac{\varphi^-}{2} & \sin\frac{\varphi^-}{2} & 0 & 0 \\ -\sin\frac{\varphi^-}{2} & \cos\frac{\varphi^-}{2} & 0 & 0 \\ 0 & 0 & \cos\frac{\varphi^-}{2} & -\sin\frac{\varphi^-}{2} \\ 0 & 0 & \sin\frac{\varphi^-}{2} & \cos\frac{\varphi^-}{2} \end{pmatrix} \cdot$$

$$\cdot \begin{pmatrix} \cos\frac{\theta^+}{2} & 0 & -\sin\frac{\theta^+}{2} & 0 \\ 0 & \cos\frac{\theta^+}{2} & 0 & \sin\frac{\theta^+}{2} \\ \sin\frac{\theta^+}{2} & 0 & \cos\frac{\theta^+}{2} & 0 \\ 0 & -\sin\frac{\theta^+}{2} & 0 & \cos\frac{\theta^+}{2} \end{pmatrix} \begin{pmatrix} \cos\frac{\theta^-}{2} & 0 & -\sin\frac{\theta^-}{2} & 0 \\ 0 & \cos\frac{\theta^-}{2} & 0 & -\sin\frac{\theta^-}{2} \\ \sin\frac{\theta^-}{2} & 0 & \cos\frac{\theta^-}{2} & 0 \\ 0 & \sin\frac{\theta^-}{2} & 0 & \cos\frac{\theta^-}{2} \end{pmatrix} \cdot$$

$$\cdot \begin{pmatrix} \cos\frac{\psi^+}{2} & \sin\frac{\psi^+}{2} & 0 & 0 \\ -\sin\frac{\psi^+}{2} & \cos\frac{\psi^+}{2} & 0 & 0 \\ 0 & 0 & \cos\frac{\psi^+}{2} & \sin\frac{\psi^+}{2} \\ 0 & 0 & -\sin\frac{\psi^+}{2} & \cos\frac{\psi^+}{2} \end{pmatrix} \begin{pmatrix} \cos\frac{\psi^-}{2} & \sin\frac{\psi^-}{2} & 0 & 0 \\ -\sin\frac{\psi^-}{2} & \cos\frac{\psi^-}{2} & 0 & 0 \\ 0 & 0 & \cos\frac{\psi^-}{2} & -\sin\frac{\psi^-}{2} \\ 0 & 0 & \sin\frac{\psi^-}{2} & \cos\frac{\psi^-}{2} \end{pmatrix} \begin{pmatrix} a_\mu^{(1)} \\ a_\mu^{(2)} \\ a_\mu^{(3)} \\ a_\mu^{(4)} \end{pmatrix}$$

It can be shown ([19]) that this formulation constitutes a natural generalization of the three dimensional theory with the help of complex conjugated angles:

$$\varphi^\pm = \varphi_1 \pm i\varphi_2\,, \qquad \theta^\pm = \theta_1 \pm i\theta_2\,, \qquad \psi^\pm = \psi_1 \pm i\psi_2\,.$$

([21]) CASIMIR: *Thesis*, Leiden (1931).
([22]) C. VAN WINTER: *Thèse*, Groningen (1957).

The real quantities φ_1, θ_1 ψ_1 correspond to the usual space Euler angles, while φ_2, θ_2, ψ_2 represent hyperbolic angles (varying from $-\infty$ to $+\infty$) expressing pure Lorentz transforms.

Following a procedure initiated by EINSTEIN and MAYER ([20]) we have shown in a preceding paper ([19]) that, if one introduces two sets of complex conjugated self dual tensors:

$$I^{r\pm}_{\mu\nu} = \varepsilon^{rst} b^s_\mu b^t_\nu \pm (b^r_\mu b^{(4)}_\nu - b^r_\nu b^{(4)}_\mu)$$

and the corresponding tensors associated to the a^ξ_μ

$$A^{r\pm}_{\mu\nu} = \varepsilon^{rst} a^s_\mu a^t_\nu \pm (a^r_\mu a^{(4)}_\nu - a^r_\nu a^{(4)}_\mu),$$

transformation (22) transforms the $A^{r+}_{\mu\nu}$ into the $I^{r+}_{\mu\nu}$ in terms of φ^+, θ^+ and ψ^+ only.

In the same way the $A^{r-}_{\mu\nu}$ transform into the $I^{r-}_{\mu\nu}$ in terms of φ^-, θ^- and ψ^- only.

Now with the help of these $I^{r\pm}_{\mu\nu}$ we can build ([19]) two sets of three dimensional complex vectors $B^{r\pm}_k$ belonging to a complex three dimensional Euclidian space.

We have

$$B^{r\pm}_k = b^r_4 b^{(4)}_k - b^r_k b^{(4)}_4 \pm \varepsilon_{ijk} b^r_i b^{(4)}_j .$$

If we form the corresponding fixed vectors

$$A^{r\pm}_k = a^r_4 a^{(4)}_k - a^r_k a^{(4)}_4 \pm \varepsilon_{ijk} a^r_i a^{(4)}_j ,$$

one finds, after some calculation, that transformation (22) induces a simple complex Euler rotation from the A^{r-}_k to the B^{r+}_k with Euler angles φ^+, θ^+, ψ^+ and from the A^- to the B^- with Euler angles φ^-, θ^-, ψ^-.

We have for example:

$$\begin{pmatrix} B^{(1)+}_k \\ B^{(2)+}_k \\ B^{(3)+}_k \end{pmatrix} = \begin{vmatrix} \cos\varphi^+ & \sin\varphi^+ & 0 \\ -\sin\varphi^+ & \cos\varphi^+ & 0 \\ 0 & 0 & 1 \end{vmatrix} \begin{vmatrix} \cos\theta^+ & 0 & -\sin\theta^+ \\ 0 & 1 & 0 \\ -\sin\theta^+ & 0 & \cos\theta^+ \end{vmatrix} \begin{vmatrix} \cos\psi^+ & \sin\psi^+ & 0 \\ -\sin\psi^+ & \cos\psi^+ & 0 \\ 0 & 0 & 1 \end{vmatrix} \begin{pmatrix} A^{(1)+}_k \\ A^{(2)+}_k \\ A^{(3)+}_k \end{pmatrix}$$

and the corresponding expression for $B^{r\pm}_k$ and $A^{r\pm}_k$.

Of course, the $B_k^{r\pm}$ and $A_k^{r\pm}$ both satisfy the usual three dimensional orthogonality conditions:

$$B_k^{r\pm}B_j^{r\pm} = \delta_{jk}\,, \qquad B_k^{r\pm}B_k^{s\pm} = \delta^{rs}\,,$$
$$A_k^{r\pm}A_j^{r\pm} = \delta_{kj}\,, \qquad A_k^{r\pm}A_k^{s\pm} = \delta^{rs}\,.$$

This procedure corresponds to the well known isomorphism between the Lorentz transform and complex Euclidian rotations established by CARTAN [23].

It is therefore tempting to utilize, instead of the b_μ^ξ the new sets of complex variables $B_k^{r\pm}$ (and express their variations in terms of the complex Euler angles) in order to bring into light any analogy with the well known three dimensional theory.

The best way to write the Hamiltonian formulation of the Nakano motion in terms of the generalized Euler angles is now evidently to start from the form (15) of the Lagrangian. Then in this case no matter if we put $b_\mu^{(4)}$ or $(1/ic)\dot{Y}_\mu$ in the matrix formula (22), the expressions in the Lagrangian will be finally expressed in terms of the complex angles so that the Lagrangian will depend only on the first derivatives of the new angular variables.

The correspondence between the old and new variables will be expressed in the form:

$$(23)\qquad \begin{pmatrix} b_\mu^{(1)} \\ b_\mu^{(2)} \\ b_\mu^{(3)} \\ \frac{1}{ic}\dot{Y}_\mu \end{pmatrix} =$$

$$= \begin{pmatrix} \cos\frac{\varphi^+}{2} & \sin\frac{\varphi^+}{2} & 0 & 0 \\ -\sin\frac{\varphi^+}{2} & \cos\frac{\varphi^+}{2} & 0 & 0 \\ 0 & 0 & \cos\frac{\varphi^+}{2} & \sin\frac{\varphi^+}{2} \\ 0 & 0 & -\sin\frac{\varphi^+}{2} & \cos\frac{\varphi^+}{2} \end{pmatrix} \begin{pmatrix} \cos\frac{\varphi^-}{2} & \sin\frac{\varphi^-}{2} & 0 & 0 \\ -\sin\frac{\varphi^-}{2} & \cos\frac{\varphi^-}{2} & 0 & 0 \\ 0 & 0 & \cos\frac{\varphi^-}{2} & -\sin\frac{\varphi^-}{2} \\ 0 & 0 & \sin\frac{\varphi^-}{2} & \cos\frac{\varphi^-}{2} \end{pmatrix}.$$

[23] E. CARTAN: *Leçons sur la Théorie des Spineurs* (Paris, 1938), T. 1.

$$\cdot\begin{pmatrix} \cos\frac{\theta^+}{2} & 0 & -\sin\frac{\theta^+}{2} & 0 \\ 0 & \cos\frac{\theta^+}{2} & 0 & \sin\frac{\theta^+}{2} \\ \sin\frac{\theta^+}{2} & 0 & \cos\frac{\theta^+}{2} & 0 \\ 0 & -\sin\frac{\theta^+}{2} & 0 & \cos\frac{\theta^+}{2} \end{pmatrix}\begin{pmatrix} \cos\frac{\theta^-}{2} & 0 & -\sin\frac{\theta^-}{2} & 0 \\ 0 & \cos\frac{\theta^-}{2} & 0 & -\sin\frac{\theta^-}{2} \\ \sin\frac{\theta^-}{2} & 0 & \cos\frac{\theta^-}{2} & 0 \\ 0 & \sin\frac{b^-}{2} & 0 & \cos\frac{\theta^-}{2} \end{pmatrix}\cdot$$

$$\cdot\begin{pmatrix} \cos\frac{\psi^+}{2} & \sin\frac{\psi^+}{2} & 0 & 0 \\ -\sin\frac{\psi^+}{2} & \cos\frac{\psi^+}{2} & 0 & 0 \\ 0 & 0 & \cos\frac{\psi^+}{2} & \sin\frac{\psi^+}{2} \\ 0 & 0 & -\sin\frac{\psi^+}{2} & \cos\frac{\psi^+}{2} \end{pmatrix}\begin{pmatrix} \cos\frac{\psi^-}{2} & \sin\frac{\psi^-}{2} & 0 & 0 \\ -\sin\frac{\psi^-}{2} & \cos\frac{\psi^-}{2} & 0 & 0 \\ 0 & 0 & \cos\frac{\psi^-}{2} & -\sin\frac{\psi^-}{2} \\ 0 & 0 & \sin\frac{\psi^-}{2} & \cos\frac{\psi^-}{2} \end{pmatrix}\begin{pmatrix} a_\mu^{(1)} \\ a_\mu^{(2)} \\ a_\mu^{(3)} \\ a_\mu^{(4)} \end{pmatrix}$$

If we introduce these new variables in the Lagrangian (15) we see immediately that the orthonormality conditions taken in the form

$$b_\mu^r b_\nu^r - \frac{1}{c^2}\dot{Y}_\mu \dot{Y}_\nu = \delta_{\mu\nu}\,, \tag{24}$$

are identically satisfied so that the third term in the Lagrangian identically vanishes. Further, because relations (24) are equivalent to

$$b_\mu^\xi b_\mu^\eta = \delta^{\xi\eta}$$

the rest mass term in the Lagrangian put in terms of the Euler angles, reduces identically to the constant $-\frac{1}{2}m_0c^2$.

We are thus left with the bare rotation term:

$$T = -\frac{1}{4}I\left(\dot{b}_\mu^r \dot{b}_\mu^r - \frac{1}{c^2}\ddot{Y}_\mu \ddot{Y}_\mu\right)$$

With the aid of the matrix form (23) we can express [18] the components of the angular velocity $\omega_{\mu\nu} = \dot{b}_\mu^r b_\nu^r - (1/c^2)\ddot{Y}_\mu \dot{Y}_\nu$ and finally the rotation energy T.

In terms of the $B_k^{r\pm}$ variable we get:

$$T = \frac{I}{2}(\dot{B}_k^{r+}\dot{B}_k^{r+} + \dot{B}_k^{r-}\dot{B}_k^{r-})$$

and in terms of the Euler angles:

$$T = \frac{I}{2}[(\dot{\psi}^+)^2 + (\dot{\varphi}^+)^2 + (\dot{\theta}^+)^2 + 2\dot{\varphi}^+\dot{\psi}^+\cos\theta^+ + (\dot{\psi}^-)^2 + (\dot{\varphi}^-)^2 + (\dot{\theta}^-)^2 + 2\dot{\varphi}^-\dot{\psi}^-\cos\dot{\theta}^-].$$

This is the eventual form we should take for our Hamiltonian.

This is a very interesting result, since it shows that the Hamiltonian of the four dimensional spherical rotation splits into those of two three dimensional complex conjugated Euclidian rigid rotators. We can therefore apply to each of these rotators the preceding three dimensional theory (since the presence of the symbol i does not modify qualitatively the Hamiltonian formalism).

Although the two complex rotators are not independent, their Hamiltonians are expressed respectively in terms of the two sets φ^+, θ^+, ψ^+ and φ^-, θ^-, ψ^-, together with their conjugated momenta p_{φ^+}, p_{θ^+}, p_{ψ^+} and p_{φ^-}, p_{θ^-}, p_{ψ^-} which are considered as usually as independent canonical variables. Thus the Poisson brackets with the Hamiltonian of each quantity made up with the variables of one of these sets are independent from those of the other, so that the constants of the motion for the whole Hamiltonian are simply those of each separate three dimensional top. We may thus simply transfer to the relativistic rotator the results we have recalled in Section **4**.

Thus we can say that the constant of motion $M_{\mu\nu} + Y_\mu G_\nu - Y_\nu G_\mu$ put into evidence in the four dimensional formulation [relations (5) and (17)] splits into six separate ones which are the same as for the non-relativistic top, that is

$$(s^+)^2 = s_i^+ s_i^+ , \quad (s^-)^2 = s_i^- s_i^- , \quad s_3^+ , \quad s_3^- , \quad s_3'^+ , \quad s_3'^- .$$

This essential result relates our physical classical theory to the mathematical work of VAN WINTER ([22]) and prepares the wanted quantization.

5. – Conclusion.

As we said before, the preceding theory does not pretend to give any detailed description of what goes on inside our relativistic fluid masses; its main result is to show:

a) that such masses can be roughly compared to relativistic rotators built of two points and two frames spiraling around each other;

b) that the relative motion of such rotators can be described in terms of those of two three dimensional complex rotators.

This paves the way to establish a quantum theory for these internal motions. It appears already that the usual quantum procedure will introduce a set of quantum numbers corresponding to the preceding constants of the motion. Indeed we shall see in a further paper that they lead to a classification of internal states which reproduces the well known Nishijima-Gell Mann scheme for elementary particles.

* * *

In conclusion, we wish to express our deepest thanks to Professors L. DE BROGLIE, J. L. SYNGE and DAVID BOHM for many helpful discussions and suggestions.

In fact, this work is part of a common program of research established on the basis of common ideas with Professor BOHM, program that will be developed in a series of further papers.

Note added in proof:

The choice proposed on pages 213 and 215 for the $a_\mu^{(1)}$ $a_\mu^{(2)}$ and $b_\mu^{(1)}$ $b_\mu^{(2)}$ is here given for the sake of a simple example. In a series of further papers (in *CR Acad Sc.*) it was shown that we can use the corresponding gauge arbitraryness in view of satisfying some important and meaningful conditions. The directions chosen are fixed in space for $a_\mu^{(1)}$ and $a_\mu^{(2)}$, and rotate with a definite constant velocity for $b_\mu^{(1)}$ and $b_\mu^{(2)}$. Thus the choice is very different from the one here proposed.

RIASSUNTO (*)

Sulla base di alcuni risultati generali ottenuti da WEISSENHOFF (1), MOLLER (2), BOHM, e da uno di noi (J.-P. V.) (4) sul comportamento di masse fluide relativistiche rinchiuse in tubi-tempo, studiamo i moti interni corrispondenti a semplici presupposti fisici. Introduciamo un nuovo formalismo generale Lagrangiano ed Hamiltoniano in funzione delle variabili di Einstein-Kramer e degli angoli relativistici di Eulero e li applichiamo ad alcuni casi fisici.

(*) *Traduzione a cura della Redazione.*

Temporary Capture of Cosmic Ray Particles and Their Contribution to the High Intensity Belts.

R. Gall

Instituto de Geofisica de la Universidad de México
Instituto Nacional de la Investigación Científica - México

J. Lifshitz † (*)

Instituto Nacional de la Investigación Científica - México

(ricevuto il 17 Agosto 1959)

Summary. — The theory of the temporary permanence of charged particles in the vicinity of unstable principal periodic orbits in the earth's magnetic field is discussed in relation to the high intensity belts surrounding the earth. The intervals of energies of protons temporarily trapped by this mechanism are calculated for various latitudes and distances. Several possible sources of charged particles and their contribution to the high intensity belts are discussed. The intensity due to the temporary capture of *primary cosmic ray protons* is calculated. The theoretical intensity curves are compared with the experimental curves taken aboard Pioneer III. The secondary albedo protons spectrum is deduced. Theoretical isointensity curves for captured primary and secondary protons are plotted for the distances from 2 to 8 earth's radii.

1. – Introduction.

One of the important results of measurements made aboard American and Russian satellites and space probes is the discovery of belts of high intensity corpuscular radiation surrounding the earth [1-3]. This paper is concerned

(*) J. Lifshitz died on May 20th, 1959. The other author takes full responsability for the text.

(1) J. A. Van Allen and L. A. Frank: *Nature*, **183**, 430 (1959).

(2) J. A. Van Allen, C. E. McIlwain and G. H. Ludwig: *Journ. Geophys. Res.*, **64**, 271 (1959).

(3) S. N. Vernov, A. E. Čudakov, P. V. Vakulov and Yu. I. Pogačev: *Dokl. Akad. Nauk SSSR*, **125**, 304 (1959).

with the temporary trapping of charged particles in the vicinity of unstable periodic orbits and their possible contribution to the radiations belts. The contribution of both primary and secondary cosmic ray particles is considered.

The principal periodic orbits in the field of the geomagnetic dipole have been studied extensively in connection with the geomagnetic theory of cosmic radiation ([1-10]). Their stability has been investigated by several authors and the characteristic exponents have been computed ([10-12]). For each value of Störmer's parameter ([5]) $\gamma_1 > \gamma_1^*$ ($\gamma_1^* = 0.788\,524$), a pair of principal periodic orbits exists. These are called the internal and external periodic orbits according to their relative positions with respect to the geomagnetic dipole (Figs. 1*b* and 2). For $1 < \gamma_1 < 1.313$ only one solution exists. The two orbits coincide when the constant γ_1 equals 0.788 524 and become equatorial for values of γ_1 greater than 1.313. The stability of the latter has been studied ([12a]).

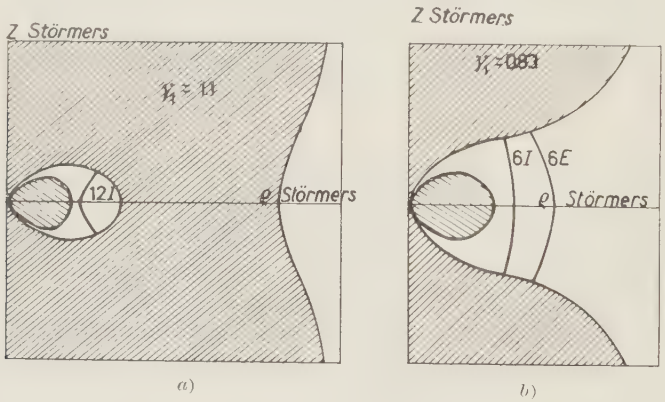

a) *b*)

Fig. 1. – Unstable periodic orbits in the meridian plane. Forbidden (shaded) and allowed Störmer zones for $\gamma_1 > 1$ and $\gamma_1 < 1$. (*a*) Internal orbit $12I$; $\gamma_1 = 1.1$. (*b*) External and internal orbits $6E$ and $6I$; $= 0.83$.

([4]) G. STÖRMER: *Zeits. Astrophys.*, **1**, 237 (1930).
([5]) G. LEMAITRE and M. S. VALLARTA: *Phys. Rev.*, **50**, 493 (1936).
([6]) M. S. VALLARTA: *An outline of the theory of allowed cones of cosmic radiation*, University of Toronto Press, Applied Mathematical Series, no. 3, p. 21 (1938).
([6a]) M. S. VALLARTA: *Theory of Geomagnetic Effects of Cosmic Radiation, Handb. d. Phys.*, **46**, (in press).
([7]) H. POINCARÉ: *Les Méthodes Nouvelles de la Mécanique Céleste*, vol. **1** chap. IV (Paris, 1892).
([8]) G. LEMAITRE and M. S. VALLARTA: *Ann. Soc. Scient. de Bruxelles*, **56**, 115 (1936).
([9]) G. LEMAITRE: *Ann. Soc. Scient. de Bruxelles*, A **54**, 194 (1934).
([10]) O. GODART: *Ann. Soc. Scient. de Bruxelles*, **58**, 27 (1938).
([11]) A. BAÑOS, H. URIBE and J. LIFSHITZ: *Rev. Mod. Phys.*, **11**, 137 (1939).
([12]) J. LIFSHITZ: *Journ. Math. and Phys.*, **21**, no. 4, 284 (1942).
([12a]) R. DE VAGELAERE: *Canadian J. of Math.*, **2**, 440 (1950).

According to a theorem of Poincaré, the perturbation of the periodic orbit (7) is given by

$$\delta r = \exp[\Omega t] F_1(t) + \exp[-\Omega t] F_2(t) , \tag{1}$$

where F_1 and F_2 are Fourier series and Ω is the characteristic exponent.

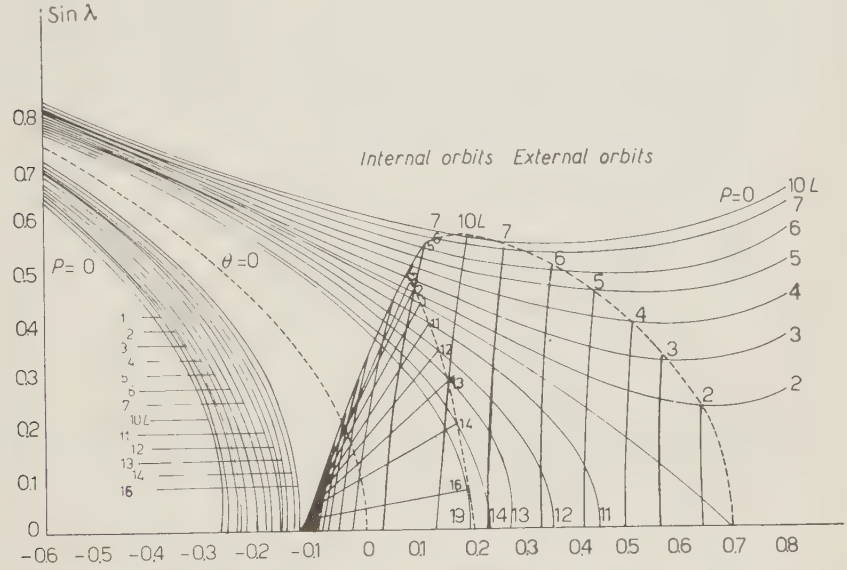

Fig. 2. - Principal periodic orbits. Some of the continua of external and internal orbits, both stable and unstable, for various values of Störmer's parameters γ_1 in the x, $\sin\lambda$ plane (12). $P(x,\lambda) = (2\gamma_1)^{-4} \exp[2x] - (\exp[-x]\cos\lambda - 1/\cos\lambda)^2$.

A periodic orbit is stable if its Ω is imaginary. Such a characteristic exponent yields periodic solutions in the neighborhood of the orbit. Any particle that remains in the neighborhood of a stable periodic orbit would have to originate there; this would be the case with decay protons and electrons of albedo neutrons. These orbits will be considered in a future paper.

If Ω is real, the orbit is unstable and admits two families of asymptotic orbits, one initially towards the orbit and the other initially away from the orbit (11).

A charged particle coming from either infinity or the earth, approaching an unstable periodic orbit either along an asymptotic or a nearly asymptotic orbit, will remain in the neighborhood of the periodic orbit for a time inversely proportional to Ω; it will then proceed either towards the earth or towards

infinity, depending on its original direction. In this paper we shall refer to the temporary trapping of the charged particle in the vicinity of an unstable periodic orbit as the *temporary capture of the particle by the orbit* [13].

2. – Capture of principal periodic orbits.

A few of the members of the continuum of principal periodic orbits, both stable and unstable, are shown in the x, $\sin\lambda$ plane in Fig. 2. In addition to these, we also have considered the following orbits:

Orbit	γ_1
$6I^*$	0.812
$6I'$	0.815
$11I'$	1.070
$12I'$	1.140
$12I^*$	1.150

The characteristic exponents of the orbits are shown in Fig. 3, where $(\Omega/\omega)^2$ in plotted versus γ_1. Here ω is the fundamental frequency of the periodic

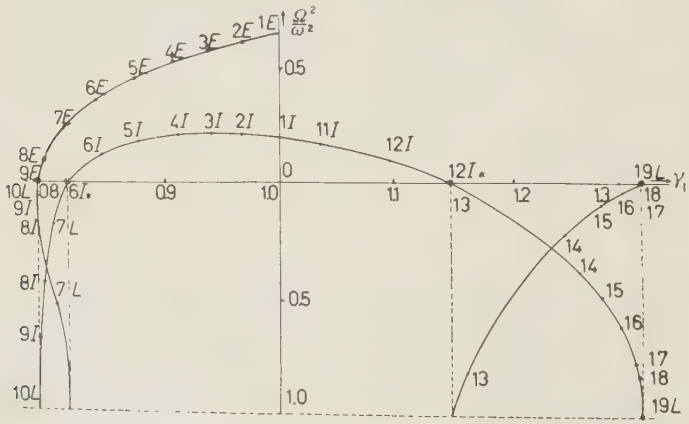

Fig. 3. Characteristic exponents (Ω) and fundamental frequencies (ω) of the principal periodic orbits. The unstable orbits lie above the γ_1 axis, the stable below. The orbits for $\gamma_1<1$ capture both primary and secondary particles, those for $\gamma_1>1$ only secondaries [12].

---

[13] R. GALL and F. LIFSHITZ: *Memoria 2a Asamblea Regional*, Soc. Mex. de Fisica (1959), p. 68.

SOCIETÀ ITALIANA DI FISICA

SCUOLA INTERNAZIONALE DI FISICA

SOTTO GLI AUSPICI DEL

MINISTERO DELLA PUBBLICA ISTRUZIONE

E DEL

CONSIGLIO NAZIONALE DELLE RICERCHE

CORSI ESTIVI 1960

VILLA MONASTERO

VARENNA SUL LAGO DI COMO

NORME GENERALI

A) - Oltre alle lezioni tenute dagli insegnanti ufficiali, seminari e conferenze verranno svolti da specialisti su argomenti connessi ai vari Corsi.

B) - Le lezioni, i seminari, le conferenze, le discussioni saranno normalmente tenuti in inglese o in francese.

C) - L'organizzazione e la direzione dei Corsi sono affidate ai Direttori.

D) - Chi desiderà partecipare a un Corso dovrà inviare la domanda di ammissione non più tardi di 25 giorni prima dell'inizio del Corso (cioè rispettivamente, a seconda del Corso: entro il 28 Aprile, il 26 Maggio, il 16 Giugno, il 7 Luglio), corredandola, in modo chiaro e leggibile, delle seguenti informazioni: 1) Nome e Cognome; 2) Data e luogo di nascita; 3) Nazionalità; 4) Indirizzo attuale; 5) Titoli di studio universitari ottenuti e indicazione dell'Università che li ha conferiti; 6) Professione attuale; 7) Elenco delle pubblicazioni di Fisica (e per il 3° Corso 1960 anche di quelle di Biofisica e Biologia); 8) Quale conoscenza orale e scritta ha dell'inglese e del francese; 9) Se verrà a Varenna solo o accompagnato da familiari, e, nel caso che venga solo, se è disposto a prendere alloggio in camera in comune con altro allievo. Inoltre il richiedente deve allegare alla domanda una lettera di presentazione, rilasciata da un professore universitario di Fisica o, eventualmente, nel caso del 3° Corso 1960, da un professore universitario di Biofisica o Biologia, il quale assicuri che il richiedente ha interesse per i suoi studi a frequentare il Corso indicato e che già possiede adeguata preparazione.

E) - L'accettazione delle domande è decisa dal Presidente della Società unitamente al Direttore del Corso, tenendo conto dei documenti presentati dai vari richiedenti e di un'equa ripartizione dei posti tra le varie nazioni cui i richiedenti stessi appartengono. - La comunicazione delle deliberazioni prese è inviata agli interessati entro 12 giorni dalla scadenza di presentazione delle domande (cioè, rispettivamente: entro il 10 Maggio, il 7 Giugno, il 28 Giugno, il 19 Luglio).

F) - Gli allievi sono vivamente pregati di giungere a Varenna il pomeriggio del giorno precedente l'inizio del Corso (cioè, rispettivamente, il pomeriggio del 22 Maggio, del 19 Giugno, del 10 Luglio, del 31 Luglio), e, giunti a Varenna, di presentarsi al nostro incaricato presso il Bar dell'« Albergo Stazione », di fronte alla Stazione stessa, per l'assegnazione dell'alloggio, per informazioni circa il Corso, ecc.

G) - Gli allievi saranno alloggiati o nella foresteria della Villa Monastero o in alberghi di Varenna, vicino alla Villa, in camere ad 1 o 2 letti. - Nella stessa Villa o negli alberghi sarà organizzata la mensa della Scuola.

H) - Le somme di cui al n. 10) sono da versarsi, non più tardi di 5 giorni dopo l'inizio del Corso (cioè, rispettivamente, entro il 28 Maggio, il 25 Giugno, il 16 Luglio, il 6 Agosto) all'Amministrazione della Scuola, a Varenna, in valuta italiana. Borse di studio, in numero molto limitato, potranno essere accordate a quegli allievi che ne giustifichino il bisogno.

I) - La Scuola cercherà, nei limiti delle possibilità locali (che sono però assai limitate causa la stagione balneare), di trovare una sistemazione adeguata in alberghi di Varenna per i familiari che intendessero accompagnare gli allievi. I familiari possono essere accolti, insieme all'allievo, alla mensa della Scuola. - Tutte le spese per alloggio, vitto, ecc., relative ai familiari sono da computarsi a parte e totalmente a carico dell'allievo: esse, per trattamento uguale a quello fatto all'allievo, si aggirano dalle 2.600 alle 3.600 Lire per giorno e per persona adulta, e dovranno essere regolate direttamente dall'allievo con l'albergatore.

J) - Il 1° Corso 1960 sulle Teorie ergodiche precede un altro Corso dello stesso titolo che si terrà dal 2 all'11 Giugno a Varenna nella Villa Monastero e sarà organizzato dall'Unione Matematica Italiana. Sebbene siano indipendenti l'uno dall'altro, questi due Corsi trattano il medesimo argomento, il primo sotto l'aspetto fisico e il secondo sotto quello matematico. Chi desidera partecipare a entrambi i Corsi, può rivolgersi per informazioni al prof. P. Caldirola (vedi 4) e 5)).

Milano, 10 Febbraio 1960

Il Segretario della S.I.F.
G. C. Dalla Noce

Il Presidente della S.I.F.
G. Polvani

I Direttori dei Corsi
P. Caldirola, G. Racah, N. Rashevsky, A. Gozzini

orbits. All the unstable orbits lie above the γ_1 axis, all the stable ones below it. For $6I^*$, $12I^*$, and $10L$, $(\Omega/\omega)^2 = 0$.

As mentioned above, the trapping time in the vicinity of an orbit is inversely proportional to Ω; as seen in Fig. 3, the internal orbits are more effective in capturing particles than the external ones and contribute more to the high intensity belt.

For the values of the integral of motion $\gamma_1 > 1$ (Fig. 1*a*), the permitted zone of motion consists of two parts, one of which is finite ([13a]). The particles in the vicinity of orbits of this finite region ($11I$, $11I'$, $12I$, $12I'$) are secondary. For $\gamma_1 < 1$ (Fig. 1*b*), there exists only one connected allowed region in which both the internal and external orbits can capture particles coming from infinity as well as secondary particles.

The *principal* periodic orbits exist between the geomagnetic latitudes $\pm 35°$. Consequently, the trapping of charged particles by these orbits can only explain the contribution to the high intensity belts lying within these latitude limits. The contribution of other families of periodic orbits will be discussed in a future paper.

Secondary particles of lower energies that are fed into the high intensity belt must originate at higher latitudes. This fact is deduced from the calculations of the present authors on albedo cones ([14,15]). The calculations show that particles which originate at low latitudes follow trajectories close to the earth, while particles originating at higher latitudes can move away in such directions as to be asymptotic or nearly asymptotic to a periodic orbit.

The possible contributions of the albedo particles ([13a]) originating at low latitudes to the lower layers of the high intensity belt will be studied further and discussed in a separate paper.

3. – Energies of captured protons.

For each periodic orbit corresponding to a fixed value of γ_1 a continuum of orbits exists (Fig. 4), each of which corresponds to a particular energy. The greater the energy, the shorter will be the orbit and the closer it will be to the earth's center (*). An upper limit is thus set to the energy of particles that can remain in the vicinity of these orbits, since a periodic orbit of sufficiently high energy would be tangent to the earth's atmosphere and, therefore,

([13a]) M. S. Vallarta: *Memoria 2a Asamblea Regional*, p. 67 Soc. Mex. de Fisica.
([14]) R. Gall and J. Lifshitz: *Phys. Rev.*, **101**, 1821 (1956).
([15]) R. Gall and J. Lifshitz: *Nuovo Cimento*, **7**, 601 (1958).
(*) The earth's center is defined by the central geomagnetic dipole.

would have no physical meaning. In this paper, only those periodic orbits were considered, lying wholly within distances from the earth's center equal to or greater than $1\frac{1}{8}$ of the earth's radius.

For particles of low energy, no such limit exists. However, because of the smaller velocity of the particle and its longer trajectory, it is found that, given the same number of particles of two different energies, the intensity of the lower energy particles will be smaller. Due to this effect, the contribution of such particles to the high intensity belt becomes vanishingly small for sufficiently small energies.

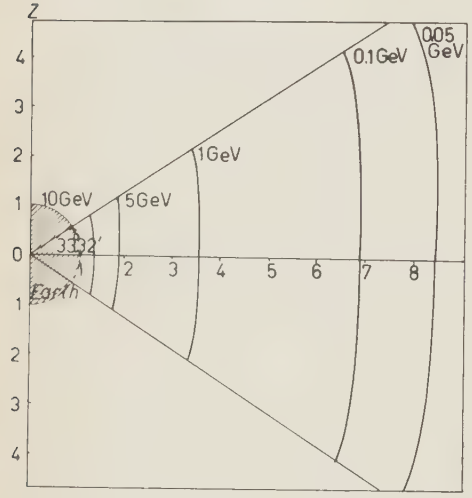

Fig. 4. – Some members of the continuum of the 6*I* orbit in the meridian plane. Each orbit corresponds to a different proton energy which determines its distance from the earth's center. (All distances are in units of earth's radii).

If we consider any fixed latitude λ, the distance R in störmers of each of the unstable periodic orbits from the dipole can be obtained by reading off the values of x (Fig. 2) and applying the transformation

$$R = \frac{1}{2\gamma_1} e^x .$$

As one moves towards higher latitudes, the number of orbits for a given λ decreases.

If we now consider the k-th periodic unstable orbit at latitude λ and at distance r (in cm) from the dipole, then the energy ε_K of a particle of rest mass m_0c^2 and charge q captured by this orbit is given by

$$\varepsilon_K = \sqrt{C_r(R)^4 + m_0^2c^4} - m_0c^2 , \tag{2}$$

where

$$C_r = \frac{q^2M^2}{r^4} , \tag{3}$$

M is the earth's dipole moment.

For protons and electrons $C_r = 5.896\,72 \cdot 10^{28} r^{-4}$.

The energies of protons and electrons captured by the family of unstable periodic orbits were computed for latitudes of 0, 5, 10, 20 and 30° at each of the following 19 distances from the dipole: $1\frac{1}{8}$, $1\frac{1}{4}$, $1\frac{1}{2}$, $1\frac{3}{4}$, 2, $2\frac{1}{2}$, 3, $3\frac{1}{2}$, ...,

$8\frac{1}{2}$, and 9 earth's radii. At each λ and r, two energy intervals exist, one for the internal and the other for the external orbits. Figs. 5*a* and 5*b* show these intervals for 5° and 30° at all distances.

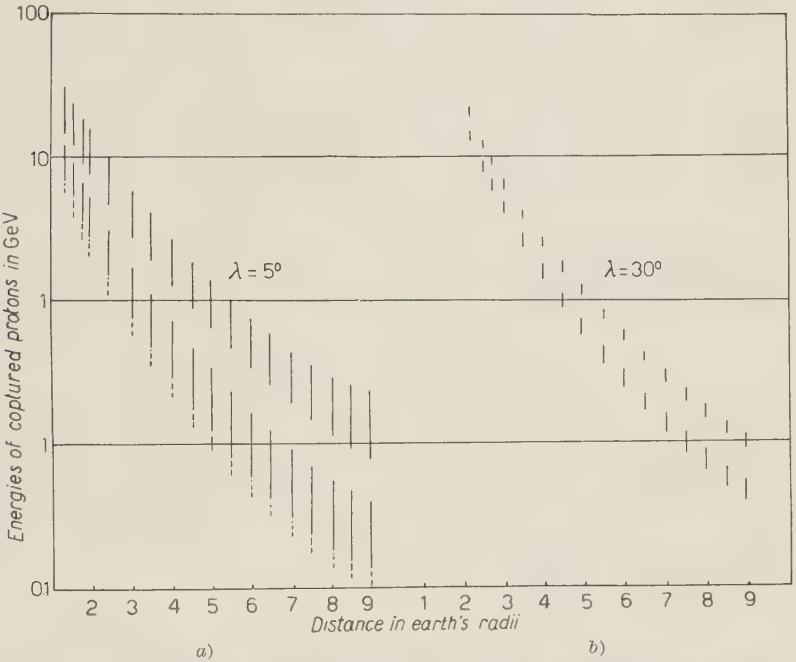

Fig. 5. – Energies of protons captured at various distances from the earth's center by the continua of external (upper segment) and internal (lower segment) periodic orbits. The energies of the captured secondary protons are indicated by broken lines. (*a*) $\lambda = 5°$. (*b*) $\lambda = 30°$.

4. – The intensity of captured particles from an arbitrary source.

Particles from an arbitrary source with a differential energy spectrum $D(\varepsilon)$ that enter the geomagnetic field along certain directions will be temporarily captured by the unstable periodic orbits and contribute to the high intensity belts.

In order to evaluate the total intensity I at a distance r and latitude λ due to the source $D(\varepsilon)$, the intensity per unit energy, i_k, of particles of energy ε_k, captured by the k-th orbit for these values of λ and r, must first be computed.

The intensity i_k depends on the following factors.

a) The number of oscillations the particle makes in the vicinity of the orbit. This number is proportional to ω/Ω. We shall refer to it as the *weight*

of the orbit and define a relative weight, p_k, as the ratio of the weight of the k-th orbit to that of the $1E$ orbit (Fig. 3)

$$p_k = \frac{(\omega/\Omega)_k}{(\omega/\Omega)_{1E}} . \tag{4}$$

b) The volume defined as the vicinity of the orbit. As a first approximation we shall assume that this vicinity is a portion of a spherical shell. If the k-th orbit is at a distance r, the intensity of i_k is then inversely proportional to $(r/r_t)^2$, where r_t is the earth's radius.

c) The intensity of particles of energy ε_k at the source.

For particles of any given energy ε_k, the value of i_k at a distance r and latitude λ is therefore given by

$$i_k = C_0 \cdot p_k \cdot \frac{1}{(r/r_t)^2} \cdot D(\varepsilon_k) , \tag{5}$$

where C_0 is a proportionality constant.

The total intensity I at a given latitude λ and distance r of particles of energy spectrum $D(\varepsilon)$, captured by internal and external unstable periodic orbits existing at this latitude, is evaluated by integrating the areas under the respective i_k *vs.* ε_k curves.

The intensity I was actually computed for primary and secondary cosmic rays by an IBM Model 650 calculating machine. The computations were carried out for 5 latitudes and 19 distances, and the areas corrected for the asymptotic behavior of the i_k *vs.* ε_k curves at the ends, (6^*I, 12^*I, and $10L$ orbits).

5. – Sources contributing to the high intensity belt.

Sources that might contribute to the high intensity belts have been discussed by various authors ([1,16-18]). Solar plasma and secondary cosmic rays, including albedo protons and neutrons, as well as their decay products, have been suggested as possible sources. It has also been suggested that the first maximum in the intensity curve is caused by the cosmic ray albedo and the second (more distant from the earth) by solar plasma.

([16]) S. N. VERNOV *et al.*: *Special Lecture, 5th Gen. Assembly of CSAGI* (Moscow, July 30 - August 9, 1958).

([17]) S. F. SINGER: *Phys. Rev. Lett.*, **1**, 171, 181 (1958).

([17a]) S. F. SINGER: *2nd Symposium on Space Physics and Medicine*, San Antonio, Texas, November 1958.

([18]) P. J. KELLOGG: *Nuovo Cimento*, **11**, 48 (1959).

Particles sent by any source into the geomagnetic field will be temporarily captured and cause an increase in the intensity of the radiation belts. According to our theory, the distance at which this increase can be detected depends upon the spectrum of the source. If capture by unstable periodic orbits were the only operating mechanism, then, for example, a source of protons of energies less than 50 MeV could only be detected at distances greater than six earth's radii (Fig. 5).

The capture mechanism discussed here is just as effective in capturing primary as secondary particles. The fact that the higher energy particles are captured closer to the earth suggests that the first maximum of the intensity of the radiation belt is caused by primary cosmic ray particles, while the second maximum is due to all secondary cosmic ray particles.

In this paper, we have only considered two sources, namely, primary protons and albedo protons of cosmic rays.

The intensity i_k of the primary protons captured by the k'th orbit at a given λ, r, was computed at all latitudes and distances previously mentioned. Equation (5) was used, in which $D(\varepsilon)$ was replaced by the primary differential spectrum ([19]) $N(\varepsilon)$, where

$$(6)\quad N(\varepsilon)\mathrm{d}\varepsilon = 0.048\varepsilon^{-\frac{2}{3}}[(1+0.09\varepsilon^{\frac{4}{3}})]^{-\frac{2}{3}}\mathrm{d}\varepsilon \qquad \text{for } \varepsilon \geqslant 0.500 \text{ GeV}$$

$$= 0 \qquad \text{for } \varepsilon < 0.500 \text{ GeV}.$$

0.500 GeV was chosen as a reasonable cut-off for periods when the solar activity is not too high ([20-21]). The total intensity I of the captured primary protons was then calculated for all latitudes and distances by the

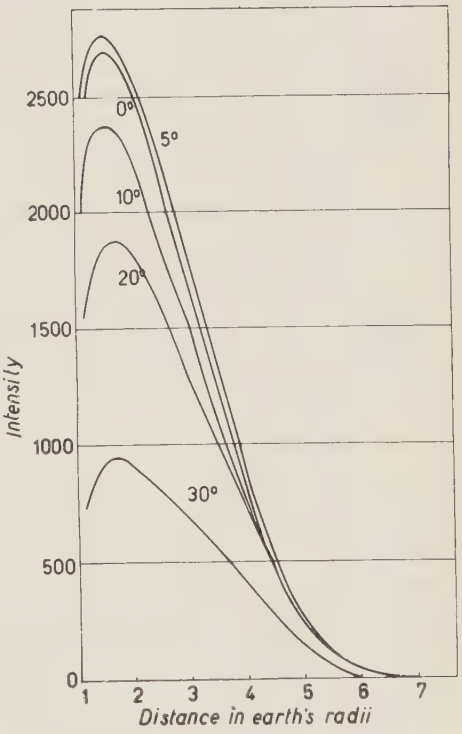

Fig. 6. – The intensity curves of captured primary protons. Intensity *vs.* distance at various latitudes.

([19]) H. V. Neher, in J. G. Wilson ed.: *Progress in Cosmic Ray Physics*, p. 300 (New York-London, 1952).

([20]) H. V. Neher: *Phys. Rev.*, **103**, 228 (1956).

([21]) P. Meyer and F. A. Simpson: *Suppl. Nuovo Cimento*, **8**, 233 (1958).

method described in the previous section. Fig. 6 shows intensity decreases with the distance but passes through a maximum at approximately 1.7 r_t, the position and intensity of this maximum being a function of the latitude. As the atlitude increases, the intensity first increases slightly and then decreases considerably.

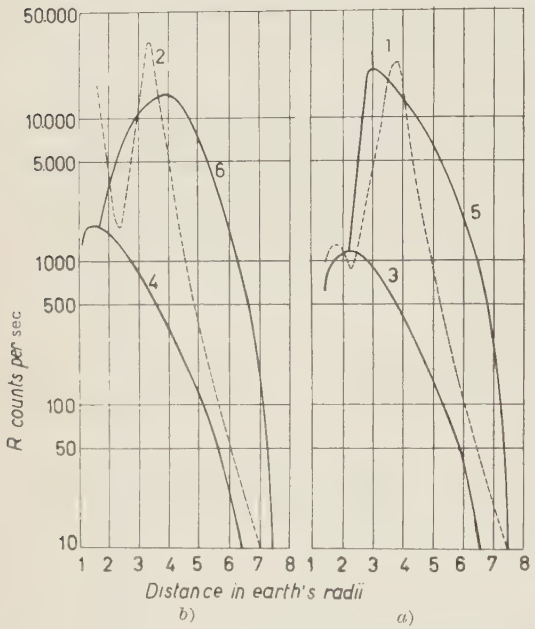

Fig. 7. – Experimental and theoretical intensity curves for the (*a*) out-bound and (*b*) in-bound leg of Pioneer III's trajectory. Curves 1 and 2 show R measured aboard Pioneer III; curves 3 and 4 show the calculated value of R for captured primary protons, and curves 5 and 6 for captured primary and secondary protons.

A study of the energies (Fig. 5) of the protons, captured at distances between 2.5 and 4.5 r_t suggested the idea that the second maximum of the experimental intensity curves is due to albedo particles. The experimental curves could then be reproduced by the additive capture of primary and secondary cosmic rays. An attempt was made to deduce a distribution of captured secondary protons by comparing the theoretical intensity curves for captured *primary* protons (Figs. 7*a*,*b*, curve 3 and 4) with the experimental Intensity (*) curves (1) obtained aboard Pioneer III (Figs. 7*a*,*b*, curves 1 and 2).

Curves 3 and 4 were obtained by plotting the intensity of captured primary protons at the geomagnetic latitudes λ and distances r of the outgoing and incoming trajectories of Pioneer III. Differences ΔI between the experimental and the theoretical curves were taken and set equal to the total intensity of protons of the secondary source whose distribution was to be found. However, no distribution seems to exist which would reproduce both curves obtained by space probes, if capture by periodic orbits were the only mechanism operating. This negative result indicates that other mechanisms must also contribute to the high intensity belts.

(*) In actual fact not the Intensity I, but the counting rate R, was plotted versus distance where $R = I/1.6$.

A distribution function of the form $59(1+\varepsilon)^{-6}$ was tested and seems to give satisfactory results when limited to the range $0.45 \leq \varepsilon \leq 2.20$ GeV. If the cut-off is not applied at the lower limit, the intensity becomes too high at large distances from the earth's center. The higher energy cut-off brings the intensity at shorter distances down to the observed level. The energy spectrum finally used for the secondary protons was the above function modified at the two ends so that it has a sharp peak at 0.52 GeV which tends to zero towards the lower cut-off value and has a tail extending to 2.20 GeV. The intensity due to this calculated source was computed for 0, 5, 10, 20 and 30° of geomagnetic latitude at all 19 distances.

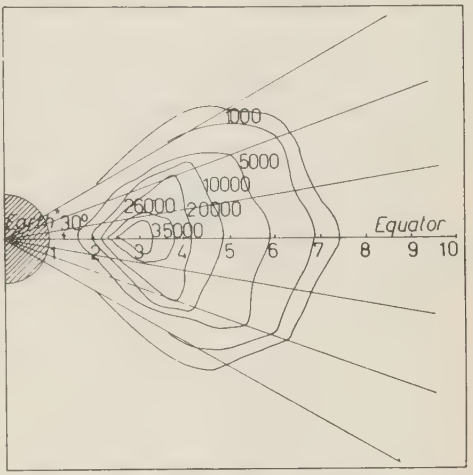

Fig. 8. – Iso-intensity curves in the geomagnetic meridian plane. The intensity is due to both primary and secondary protons temporarily trapped by unstable periodic orbits. Only curves for distances larger than $2r_t$ were drawn. (All distances are in units of earth's radii).

The intensities due to this distribution of secondary protons were evaluated for λ and r corresponding to the outgoing and incoming legs of Pioneer III's trajectory and added to the intensities of captured primary protons at these λ, r values. The resulting curves are plotted in Figs. 7*a*,*b* (curves 5 and 6).

Isointensity curves in the geomagnetic meridian plane were also plotted and are shown in Fig. 8.

6. – Discussion.

Principal periodic orbits and the capture mechanism suggested here are only valid if the dipole approximation to the geomagnetic field is also valid.

The capture mechanism discussed here can only partly account for the existence of the radiation belts. We believe that several mechanisms are responsible for the radiation belts ([12a]). The mirror points mechanism ([17,18]) could probably explain the capture of lower energy particles, for which the approximation of the constancy of the magnetic moment holds.

Solar plasma was not considered among the sources discussed in this paper.

The injection of solar plasma is accompanied by a perturbation of the geomagnetic field which, especially at large distances, causes a deviation from the dipole field. When a small enough perturbation exists, capture of the solar plasma particles by unstable periodic orbits would occur. Depending on the energy spectrum of the plasma, an increase in the intensity of the radiation belt would occur at corresponding distances, and for high enough energy of plasma particles the second maximum would be affected. The characteristics of the second maximum would be expected to vary more with time than those of the first maximum.

There are discrepancies between the experimental curves and those calculated on the basis of the temporary capture by unstable periodic orbits, which may be partially corrected by using a more adequate energy spectrum of secondary protons. An explanation of the remaining basic discrepancies will have to be postponed until some idea of the relative importance of other mechanisms becomes available.

The isointensity curves shown in Fig. 8 depend strongly on the distribution chosen for secondary protons and are drawn for distances larger than $2r_t$. They will be extended to the region below $2r_t$ when the contribution of albedo trajectories to the lower layers of the intensity belts will be studied.

The proportionality constant C_0 is the only free parameter in the present theory and was chosen to be 10^5 in order to bring the calculated value of the intensity within the range of measured values. This constant is associated with the influx and efflux of particles into and out of the radiation belts. A full discussion of this constant must also be postponed until quantitative data are available for other trapping mechanisms.

A more detailed discussion also requires a knowledge of any variations in the characteristics of the high intensity belts with time.

The soundness of the theory of temporary capture by unstable periodic orbits could be checked experimentally by determining the energy distribution of the particles composing the first and second radiation belts.

* * *

The authors wish to thank Professor MANUEL SANDOVAL VALLARTA for valuable discussions on the subject. We would also like to thank Mrs. LUCILA SÁNCHEZ DE CAMACHO for help with the calculations, Mr. LUIS OTTALENGO of the Centro Electrónico de Cálculo of the National University, for computations on the IBM calculating machine, and Mrs. JOAN KRUGER DE HAUFF for careful reading of the English text.

RIASSUNTO (*)

Si discute la teoria della permanenza temporanea di particelle cariche in prossimità di orbite periodiche principali instabili nel campo magnetico terrestre in relazione alle fasce di alta intensità che circondano la terra. Si calcolano per varie latitudini e distanze gli intervalli di energia di protoni temporaneamente catturati da tale meccanismo. Si esaminano numerose sorgenti possibili di particelle cariche ed il loro contributo alle fasce di alta intensità. Si calcola l'intensità dovuta alla temporanea cattura di protoni della radiazione cosmica primaria. Si confrontano le curve teoriche dell'intensità con le curve sperimentali rilevate dal Pioneer III. Si deduce lo spettro dei protoni secondari d'albedo. Si tracciano le curve teoriche passanti per i punti di uguale intensità a distanze comprese fra 2 e 8 raggi terrestri.

(*) *Traduzione a cura della Redazione.*

Particle Production in 6.2 GeV p-p Collisions Treated by a Statistical Model.

R. HAGEDORN

CERN - Geneva

(ricevuto il 26 Settembre 1959)

Summary. — The Fermi theory of particle production is used in a rigorous and refined form in order to calculate spectra and mean particle numbers for all produced particles (*i.e.* $\mathcal{N}$, π, $\bar{\mathcal{N}}$ and strange particles) in 6.2 GeV (kin. lab.) p-p collisions.

1. – The Fermi model.

The probability for a certain final state b is in the Fermi model [1]:

$$P_b = W^{(b)}_{\alpha\beta\gamma}(T) \left\{ \frac{\prod (2S_j+1)^{\sigma_j}}{\prod N_i!} \right\}_b \Omega^{n-1} \varrho^*_b(E, m_1 \dots m_n, \boldsymbol{p}=0) , \tag{1}$$

here $W_{\alpha\beta\gamma}(T)$ is the number of linearly independent isospin eigenfunctions of total isospin T and fixed but arbitrary T_3, which can be built up with α particles of isospin $\frac{1}{2}$, β particles of isospin 1 and γ particles of isospin $\frac{3}{2}$ [2].

The next factor counts the multiplicities of ordinary spin where σ_j is the number of particles of spin S_j, the product $\prod N_j!$ stays for the indistinguishability of the particles. $\Omega^{n-1} \cdot (2\pi)^{3n-3}$ is the so called interaction volume and $\varrho^*(E, m_1 \dots m_n)$ is essentially the phase space density of the final state:

$$\varrho^*(E, m_1 \dots m_n, \boldsymbol{p}) = \int \mathrm{d}\boldsymbol{p}_1 \dots \mathrm{d}\boldsymbol{p}_n \delta(E - \sum_i \sqrt{p_i^2 + m_i^2}) \, \delta(\sum_i \boldsymbol{p}_i - \boldsymbol{p}) . \tag{2}$$

[1] F. CERULUS and R. HAGEDORN: CERN Report 59-3.

[2] Y. YEIVIN and A. DE-SHALIT: *Nuovo Cimento*, **1**, 1147 (1955); V. S. BARAŠENKOV and B. M. BARBAŠEV: *Suppl. Nuovo Cimento*, **7**, 19 (1957).

Also the momentum spectrum of a particle in the C.M.S. of the collision (CMS) is given essentially by ϱ^*, *e.g.* for the particle m_n:

$$w_n(p)\,\mathrm{d}p \sim 4\pi p^2\,\mathrm{d}p \cdot \varrho^*(E - \sqrt{m_n^2 + p^2},\, m_1 \ldots m_{n-1},\, \boldsymbol{p} = -\boldsymbol{p}_n)\,. \tag{3}$$

We have a Monte Carlo method [3] which allows us to calculate such integrals with any prescribed accuracy and we choose the accuracy such that the results given below are

exact within less than $\pm 1\%$ for the particle numbers,

» » » » $\pm 3\%$ for the spectra.

In particular, the influence of small differences in the masses, between *e.g.* Σ and Λ, shows up clearly far outside the statistical error.

We have considered all reactions at this energy, which contribute to the observable final states and give a list of them below (Table I, Appendix I).

For all these reactions P_b has been calculated with the formula (1) and then the kinetic energy spectra $w(\varepsilon)$, of the different kinds of particles which come out from the Monte Carlo calculation in normalized form

$$\int w(\varepsilon)\,\mathrm{d}\varepsilon = 1\,, \tag{4}$$

are multiplied by P_b and by the number of particles $n_i^{(b)}$ which are represented by $w(\varepsilon)$ in the reaction considered:

$$W_i^{(b)}(\varepsilon) = P_b \cdot n_i^{(b)} \cdot w_i^{(b)}(\varepsilon) \qquad \begin{cases} i \text{ labels the kind of particle} \\ b \quad \text{» \quad » \quad » \quad » reaction.} \end{cases} \tag{5}$$

Finally, they are added up for each kind of particle:

$$W_i(\varepsilon) = \sum_b P_b\, n_i^{(b)}\, w_i^{(b)}(\varepsilon)\,, \tag{6}$$

which is the not-normalized total spectrum of particle i. We have then, since $w_i^{(b)}(\varepsilon)$ is normalized to unity:

$$\int W_i(\varepsilon)\,\mathrm{d}\varepsilon = \sum_b P_b n_i^{(b)} = \langle n_i \rangle \cdot \sum_b P_b\,.$$

---

[3] F. CERULUS and R. HAGEDORN: *Suppl. Nuovo Cimento*, **9**, 646 (1958).

Here $\langle n_i \rangle$ is the mean absolute particle number per collision, averaged over all reactions with proper weight factors.

Finally, the normalized total spectrum and the mean kinetic energy are calculated for each kind of particle.

2. – Refinements to the simple Fermi model.

We have, however, made a few refinements which seem to be essential:

1) We include the formation of the isobar $\mathcal{N}^*$ ($T=\frac{3}{2}$, $S=\frac{3}{2}$ mass 1.316) which afterwards decays into $\mathcal{N}+\pi$ ([4]).

2) We include final state annihilation of $\mathcal{N}$-$\mathcal{N}$-pairs by saying that they will annihilate, if they come out with a small momentum relative to each other and thus stay for some time near to each other. We assumed that the probability for annihilation is given by

[probability for a certain relative momentum, p] times [probability for annihilation when the relative momentum is p_r].

The first factor is calculated by means of the phase-space by simulating a $\mathcal{N}$-$\mathcal{N}$-pair with relative momentum $\boldsymbol{p}_r$ by one particle of mass

$$m^* = 2M_{\mathcal{N}} + \frac{p_r^2}{4M_{\mathcal{N}}} ;$$

the second factor is taken to be

$$\frac{\sigma_{\text{annihil}}(p_r)}{\sigma_{\text{total}}(p_r)} ,$$

calculated with the help of a simple model with complex potential, which represents fairly well the data for $\text{p}\bar{\text{p}}$-scattering up to 300 MeV (*).

The number of annihilating pairs at a given reaction b turns then out to be approximately (see Appendix II)

$$\Delta\bar{N} \simeq \bar{N}\left[1-\left(1-\frac{\Delta\varrho^*}{\varrho^*}\right)^2\right],$$

with

$$\Delta\varrho^* = \text{const}\int_0^{p_0} \frac{\sigma_{\text{annihil}}}{\sigma_{\text{total}}} \cdot p_r^2 \cdot \varrho^*(E, m_1 \ldots m_{n-1}, m^*(p_r))\, \mathrm{d}p_r .$$

([4]) S. Z. Belenki *et al.*: *Usp. Fiz. Nauk*, **62** (2), 1 (1957).
(*) Private communication by F. Cerulus (not published).

This has then to be subtracted from the number of pairs which the primary interaction yields. In a similar way the $\mathcal{N}$-spectrum is changed, in particular the low energy part of it is reduced as it is to be expected from this model of final state annihilation. We give below the original $\mathcal{N}$-spectrum, the $\Delta\mathcal{N}$-spectrum (that is: the spectrum of the annihilating $\mathcal{N}$) and the observable spectrum $\overline{\mathcal{N}} - \Delta\overline{\mathcal{N}}$.

In the yield of $\mathcal{N}$ this final state annihilation gives a reduction by a factor 0.26, which is quite important.

3) We consider a third rather trivial final state interaction by calculating the spectra of γ and Λ^0 from the decays:

$$\pi^0 \to 2\gamma$$

$$\Sigma^0 \to \Lambda^0 + \gamma$$

and by adding up all such γ-spectra and by adding this Λ^0 to those produced directly.

4) The interaction volume is split into three factors:

$$\Omega^{n-1} \to \Omega_1^{n_1} \cdot \Omega_2^{n_2} \cdot \Omega_3^{n_3} ,$$

where now $n_1 =$ number of $\pi + \mathcal{N} + \mathcal{N} + \mathcal{N}^*$,

$n_2 =$ number of $\Sigma + \Lambda + \Xi$,

$n_3 =$ number of $\mathrm{K} + \overline{\mathrm{K}}$.

We calculated now everything in several versions, namely (*)

(i) $\Omega_\pi = \Omega_\mathrm{Y} = \dfrac{4\pi}{3}\,\lambda\!\!\!^{-3}_\pi$, Ω_K variable,

(ii) $\Omega_\pi = \dfrac{4\pi}{3}\,\lambda\!\!\!^{-3}_\pi$, $\Omega_\mathrm{Y} = \Omega_\mathrm{K}$ variable .

Assumption (i) seems to be related to global symmetry whereas assumption (ii) treats the hyperons and K-mesons the same way.

If one considers Ω as an expression of the coupling strength, then one should expect Ω_K to be $10 \div 15$ times smaller than Ω_π.

(*) We use simultaneously the notation

$$\Omega_1 \equiv \Omega_\pi , \qquad \Omega_2 \equiv \Omega_\mathrm{Y} \text{ (hyperons)} , \qquad \Omega_3 \equiv \Omega_\mathrm{K} .$$

If, on the other hand, one interprets it as expressing ranges of interactions, then Ω_K should be the same expression as Ω_π but with $\hat{\lambda}_K$ replacing $\hat{\lambda}_\pi$. Then it should be about 40 times smaller than Ω_π.

The meaning of Ω being obscure, we varied Ω_K from $\Omega_K = \Omega_\pi$ down to $\Omega_K \cong \frac{1}{50}\Omega_\pi$ and that in both versions (i) and (ii).

The curves given below show then the effect of this variation.

It is interesting to see that there are certain quantities which depend strongly neither on Ω_K nor on the choice of (i) or (ii), *e.g.* the total γ, $\overline{\pi}$, π-production, whereas others depend very strongly, changing by orders of magnitude.

The normalized spectra are hardly influenced and can be said to be independent of the version taken.

Further explanations will be found in the figure captions.

3. – Angular distribution.

In this kind of model nothing is known concerning angular distribution: in fact, one calculates only an average spectrum over all angles.

4. – Inelasticity.

In the Fermi model, as used here, it is assumed that the entire available energy is distributed statistically between all possible end products. This can of course only be true if the two nucleons suffer a « central » collision. The present calculations should therefore strictly speaking be compared only with inelastic events with high inelasticity.

5. – Concluding remarks.

The present calculation shows that the Fermi model, taken seriously, is everything else but a simple model. It was possible to perform this calculation only with the help of an electronic computer (CERN's Ferranti Mercury) [5].

We got the impression that the model may very well be able to reproduce many experimental facts—except angular distribution—and that the discre-

[5] Cfr. R. HAGEDORN: Report CERN 59-25.

pancies encountered so far (up to ≈ 50 GeV) lie not in the model but in the fact that it has not been used correctly; may that concern very bad approximations for the phase space or the omission of the other factors, which easily become of the order of 1/100 or may it come from considering only a small subset of all possible and contributing reactions at a given energy.

Certainly the final state interactions play an important role also.

Recently π-π-interactions with a resonant state (which would appear in the present work as a particle of about 4 pion masses, isospin 1 and angular momentum 1) have been discussed [6]. In fact, the inclusion of such an interaction in the treatment of nucleon pair annihilation with the statistical model [7] leads to surprisingly good agreement with experiments.

Consequently, it seems that this interaction should be included also here. We have done such calculations, with the definite result that it leads to disagreement with experiments. The total pion number comes out to be approximately 4, instead of 2.8 as here and in the experiment. Other authors [8] come to similar conclusions in the case of π-p inelastic collisions.

It is very hard to see how one could find a reason, which rules out π-π-interactions in nucleon-nucleon collisions, but makes it important in annihilation. A possible way out would be to relate the π-π isobar to the nucleon isobar. Then one has to include either the nucleon isobar or the pion isobar, but not both of them and obviously the nucleon isobar should be taken in nucleon-nucleon or pion-nucleon collisions and the pion isobar in annihilation processes.

There might be another explanation, which is much less ambitious: the experimental results include non-central collisions and these, for purely geometrical reasons are the most frequent ones. The present theory, however, applies to central collisions only. One could imagine, that for large impact parameters, the number of pions produced goes down, since only part of the primary kinetic energy is available for particle production. If we now would include the pion isobar (which gives 4 pions per collision) and simultaneously could include the effect of non-central collisions, then these two might somehow compensate and the 2.8 pions might result again.

To test this explanation, further considerations on the mechanism of non-central collisions are required, together with a large amount of additional calculations. All one can say at the moment is that if the impact parameter is not larger than $\approx 1/2\mu$, equilibrium could be established in the whole interaction region, within the collision time (for the energy considered here). Col-

(6) W. Fraser and J. Fulco: *Phys. Rev. Lett.*, **2**, 365 (1959).
(7) F. Cerulus: *Nuovo Cimento*, **14**, 827 (1959).
(8) V. S. Barašenkov and V. M. Maltsev: Dubno Report R-350 (May 1959).

lisions with an impact parameter $\geq 1/2\mu$ should be considered as peripheral (*). They might lead to lower multiplicities (and also be mainly responsible for angular anisotropy). At the present moment the influence of the π-π isobar is therefore still an open question.

The results, together with further explanations, are given in Appendix I.

* * *

The author is very grateful to Dr. CERULUS (CERN) for many discussions covering almost every part of the present work, in particular the effect of final state annihilation and the π-π isobar. In the spirit of our collaboration in earlier publications Dr. CERULUS even took over the tedious job of preparing some of the data tapes and watching the runs of some Monte Carlo calculations on the computer. Finally he read critically the manuscript.

APPENDIX I

The initial state is always p+p, the final states are listed below together with their probabilities in percent of the total cross-section (which cannot be calculated by this theory). We give two versions:

$$(\alpha) \quad \Omega_Y = \Omega_\pi; \qquad \Omega_K = \frac{1}{8.5}\,\Omega_\pi\,, \qquad (\text{« global symmetry »}),$$

$$(\beta) \quad \Omega_Y = \Omega_K = \frac{1}{8.5}\,\Omega_\pi\,.$$

(The value 1/8.5 is purely accidental — it just happened that this was one of the values for which everything was calculated in order to draw the curves of Figs. 13-21. This value, however, is the nearest to 1/10, which we would consider reasonable. Anyway, the difference is unimportant).

We neglected all those reactions which, within a group of similar reactions, are very improbable, with respect to the others of the same group, with some exceptions. These exceptions have no influence at all, we list them for curiosity only.

Notation. – 1.09 ± 5 means $1.09\cdot10^{\pm5}$ etc.

(*) See a forthcoming paper on results at 25 GeV by the author, to be published in *Nuovo Cimento*, Vol. **15**, n. 3.

SOCIETÀ ITALIANA FISICA

INTERNATIONAL SCHOOL OF PHYSICS

UNDER THE AUSPICES OF THE

MINISTERO DELLA PUBBLICA ISTRUZIONE

AND THE

CONSIGLIO NAZIONALE DELLE RICERCHE

SUMMER COURSES 1960

VILLA MONASTERO

VARENNA SUL LAGO DI COMO

During the year 1960, thanks to contributions from the Ministero della Pubblica Istruzione, the Consiglio Nazionale delle Ricerche, the Comitato Nazionale per le Ricerche Nucleari, and other italian and foreign Authorities, Companies and Organizations, the following *Summer Courses* will be held at Varenna in the Villa Monastero, the use of which has been kindly granted by the Ente Villa Monastero.

	1st COURSE 1960 (XIV since the beginning of the School) 23rd May - 31st May (See J) in the General Information)	2nd COURSE 1960 (XV since the beginning of the School) 20th June - 9th July	3rd COURSE 1960 (XVI since the beginning of the School) 11th July - 30th July	4th COURSE 1960 (XVII since the beginning of the School) 1st August - 17th August
1) *Title*	**Ergodic Theories**	**Nuclear Spectroscopy.**	**Physicomathematical Aspects of Biology**	**Topics on Radiofrequency Spectroscopy**
2) *Subjects treated*	The problem of « master equations »; Ergodic theory in quantum statistical Mechanics; Ergodic theory in classical statistical Mechanics.	Mathematical techniques: Systematics of light and heavy nuclei; β - decay; Electromagnetic properties of nuclei; Theory of nuclear matter.	Diffusion phenomena and permeabilities; The Physics of the respiratory tract; Dynamics of the cardiovascular system (tentative); Nervous system, peripheric and central; Sensory phenomena; The Physics of the gene (tentative); Reaction rates: General mathematical principles in Biology.	Gaseous maser; Radiofrequency spectroscopy of excited atoms; Multiple resonances in solid and liquid state.
	A. Loinger, Università di Pavia - *Pavia* (Italy)	G. Alaga, University of Zagreb - *Zagreb* (Yugoslavia)	A. F. Bartholomay, Harvard Medical School - *Boston*, Mass. (U.S.A.)	A. Abragam, Centre d'Etudes Nucléaires de Saclay - *Gif-sur-Yvette* (Seine et Oise) (France)
	G. Ludwig, Freie Universität Berlin, Institut für Theoretische Physik - *Berlin* (Germany)	J. Goldstone, Gavendish Laboratory - *Cambridge* (Great Britain)	E. Boeri, Università di Ferrara - *Ferrara* (Italy)	B. Elschner, Physikalisches Institut der Universität - *Jena* (Germany)
	L. Rosenfeld, Nordisk Institut for Teoretisk Atomfysik - *Copenhagen* (Denmark)	B. Mottelson, Nordisk Institut for Teoretisk Atomfysik - *Copenhagen* (Denmark)	J. B. Defares, Universiteit van Leyden - *Leyden* (Netherlands)	A. Kastler, Ecole Normale Supérieure - *Paris* (France)
	C. Truesdell, Indiana Univer-		H. de Vries, Rijksuniversi-	A. Nieremberg, University of

	Rijksuniversiteit - *Utrecht* (Netherlands)	(Israel)	N. Rashevsky, University of Chicago - *Chicago*, Ill. (U.S.A.) T. Teorell, Uppsala Universitet - *Uppsala* (Sweden) M. E. Wise, Radiological Protection Service - *Belmont-Sutton* (Great Britain)	C. H. Townes, Columbia University - *New York*, N. Y. (U.S.A.)
4) *Organizer and Director of the Course*	Prof. Piero Caldirola, Professor of Theoretical Physics at the University of Milan	Prof. Giulio Racah, Professor of Theoretical Physics at the University of Jerusalem	Prof. Nicolas Rashevsky, Chairman of the Committee on Mathematical Biology at the Chicago University	Prof. Adriano Gozzini, Professor of Optics at the University of Pisa
5) *All correspondence should be sent to*	Prof. Piero Caldirola Istituto di Fisica dell'Università Via Saldini, 50 MILANO (Italy)	Prof. Giulio Racah Department of Theoretical Physics Hebrew University JERUSALEM (Israel)	Prof. Nicolas Rashevsky Commit. Mathem. Biology University of Chicago 5741, Drexel Avenue CHICAGO, Ill. (U.S.A.)	Prof. Adriano Gozzini Istituto di Fisica dell'Università Piazza Torricelli, 2 PISA (Italy)
6) *Duration of the Course*	9 days.	20 days.	20 days.	17 days.
7) *Opening of the Course*	Monday, 23rd May, 9.30 a.m.	Monday, 20th June, 9.30 a.m.	Monday, 11th July, 9.30 a.m.	Monday, 1st August, 9.30a.m.
8) *Closing of the Course*	Tuesday, 31st May, in the afternoon.	Saturday, 9th July, in the afternoon.	Saturday, 30th July, in the afternoon.	Wednesday, 17th August, in the afternoon.
9) *Number of students*	40.	40.	40.	40.
10) *Total fee to be paid by students to the management of the School for attendance, room accomodation and full board*	L. 18.000, if the student has single room accomodation; L. 15.750, if the student shares room accomodation with another student.	L. 40.000, if the student has single room accomodation; L. 35.000, if the student shares room accomodation with another student.	L. 40.000, if the student has single room accomodation; L. 35.000, if the student shares room accomodation with another student.	L. 34.000, if the student has single room accomodation; L. 29.750, if the student shares room accomodation with another student.

GENERAL INFORMATION

A) - In addition to the Courses which are listed above, seminars on questions related to the basic subjects of the different Courses will be held by visiting scientists.

B) - The lectures, seminars, conferences and discussions will generally be held in English or French.

C) - The organization and direction of the Courses is entrusted to the Directors.

D) - An application should arrive not later than 25 days before the beginning of the Course (*i.e.* resp., not later than April 28th, May 26th, June 16th, July 7th) displaying the following information, which should be set out clearly and legibly: 1) Christian name and surname; 2) Date and place of birth; 3) Nationality; 4) Present address; 5) Degrees and other qualifications obtained, with name of University in each case; 6) Present professional activity; 7) List of publications in Physics (and for the 3rd Course 1960 also in Biophysics and Biology); 8) Standard of knowledge of English and French - written and spoken; 9) Whether intending to stay at Varenna unaccompanied or with members of family and, in the former case, whether willing to share a room with another student. The applicant should send, together with his application, a note of reference from a University Professor of Physics or, eventually, in the case of the 3rd Course 1960, from a University Professor of Biophysics or Biology, testifying the applicant's interest and preparation for the activities of the School.

E) - Each application will be considered by the President of the Italian Physical Society and by the Director of the School on the basis of the information submitted, with regard also to a fair distribution of the places available among students of various nations. The decisions on the admittance to the School will be made known to the applicants within 12 days from the date fixed for the arrival of applications (*i.e.* resp., May 10th, June 7th, June 28th, July 19th).

F) - Students will oblige in arriving at Varenna in the afternoon of the day preceding the opening of the Course (*i.e.* resp., in the afternoon of May 22nd, June 19th, July 10th, July 31st) and calling at our delegate at the Bar of the « Albergo Stazione », in front of the Station itself, for lodgings, and to receive information and papers concerning the Course.

G) - Accomodation for the students will be provided in rooms with 1 or 2 beds either in the guest quarters of the Villa Monastero or in hotels at Varenna. Meals will be had at the Villa itself or at a hotel in Varenna.

H) - Fees as per 10) should be paid not later than 5 days after the beginning of the Course (*i.e.* before May 28th, June 25th, July 16th, August 6th respectively) to the management of the School, at Varenna, in Italian currency. A very limited number of scholarships may be granted to students whose economic conditions might otherwise prevent them from attending the School.

I) - The School will do everything possible to find suitable accomodation in local hotels for members of families accompanying the students. It should be noted, however, that, in view of the holiday season, local possibilities are limited. Members of students' families may avail themselves of the catering arrangements being organized for the School. All expenditure involved in the hotel accomodation, board etc. for students' relatives will be payable separately. These expenses will be, according to the hotel, from 2.600 to 3.600 Lire per person pér day and are to be settled directly with the hotel management.

J) - The 1st Course 1960 on Ergodic Theories precedes the other one which, under the same title, is to be held from 2nd to 11th June in Varenna at the Villa Monastero, and is organized by the Unione Matematica Italiana. Though independent one from the other, the two Courses deal in the same subject, the former under the physical aspect, the latter under the mathematical one. People who want to attend both these Courses should ask for information prof. P. Caldirola (see 4) and 5)).

Milan, 10th February 1960

The Secretary of the S.I.F.
G. C. Dalla Noce

The President of the S.I.F.
G. Polvani

The Directors of the Courses
P. Caldirola, G. Racah, N. Rashevsky, A. Gozzini

TABLE I. – *Reactions considered.*

Reactions	Prob. in % (α)		Prob. in % (β)	
$2\mathcal{N}$ (elastic, incoherent)	1.32,	− 1	1.41,	− 1
$2\mathcal{N}+\pi$	4.59,	+ 0	4.88,	+ 0
$2\mathcal{N}+2\pi$	1.09,	+ 1	1.16,	+ 1
$2\mathcal{N}+3\pi$	5.51,	+ 0	5.80,	+ 0
$2\mathcal{N}+4\pi$	8.23,	− 1	8.74,	− 1
$2\mathcal{N}+5\pi$	3.70,	− 2	3.93,	− 2
$\mathcal{N}^*+\mathcal{N} \rightarrow 2\mathcal{N}+\pi$	5.01,	− 1	5.32,	− 1
$\mathcal{N}^*+\mathcal{N}+\pi \rightarrow 2\mathcal{N}+2\pi$	1.08,	+ 1	1.15,	+ 1
$\mathcal{N}^*+\mathcal{N}+2\pi \rightarrow 2\mathcal{N}+3\pi$	2.43,	+ 1	2.58,	+ 1
$\mathcal{N}^*+\mathcal{N}+3\pi \rightarrow 2\mathcal{N}+4\pi$	8.70,	+ 0	9.24,	+ 0
$\mathcal{N}^*+\mathcal{N}+4\pi \rightarrow 2\mathcal{N}+5\pi$	6.92,	− 1	7.35,	− 1
$\mathcal{N}^*+\mathcal{N}+5\pi \rightarrow 2\mathcal{N}+6\pi$	1.91,	− 2	2.03,	− 2
$2\mathcal{N}^* \rightarrow 2\mathcal{N}+2\pi$	4.70,	− 1	5.00,	− 1
$2\mathcal{N}^*+\pi \rightarrow 2\mathcal{N}+3\pi$	1.06,	+ 1	1.13,	+ 1
$2\mathcal{N}^*+2\pi \rightarrow 2\mathcal{N}+4\pi$	1.21,	+ 1	1.29,	+ 1
$2\mathcal{N}^*+3\pi \rightarrow 2\mathcal{N}+5\pi$	2.55,	+ 0	2.71,	+ 0
$2\mathcal{N}^*+4\pi \rightarrow 2\mathcal{N}+6\pi$	1.05,	− 1	1.12,	− 1
$2\mathcal{N}^*+5\pi \rightarrow 2\mathcal{N}+7\pi$	1.13,	− 3	1.20,	− 3
$3\mathcal{N}+\overline{\mathcal{N}}$ (without final state annihil.)	9.46,	− 3	1.00,	− 2
$\Lambda+\mathcal{N}+\mathrm{K}$	3.43,	− 1	4.28,	− 2
$\Lambda+\mathcal{N}+\mathrm{K}+\pi$	8.21,	− 1	1.08,	− 1
$\Lambda+\mathcal{N}+\mathrm{K}+2\pi$	2.81,	− 1	3.50,	− 2
$\Lambda+\mathcal{N}+\mathrm{K}+3\pi$	1.77,	− 2	2.21,	− 3
$\Lambda+\mathcal{N}^*+\mathrm{K} \rightarrow \Lambda+\mathcal{N}+\mathrm{K}+\pi$	4.23,	− 1	5.26,	− 2
$\Lambda+\mathcal{N}^*+\mathrm{K}+\pi \rightarrow \Lambda+\mathcal{N}+\mathrm{K}+2\pi$	5.68,	− 1	7.06,	− 2
$\Lambda+\mathcal{N}^*+\mathrm{K}+2\pi \rightarrow \Lambda+\mathcal{N}+\mathrm{K}+3\pi$	1.04,	− 1	1.20,	− 2
$\Lambda+\mathcal{N}^*+\mathrm{K}+3\pi \rightarrow \Lambda+\mathcal{N}+\mathrm{K}+4\pi$	2.38,	− 3	2.96,	− 4

TABLE I (*continued*).

Reactions	Prob. in %	
	(α)	(β)
$\Sigma+\mathcal{N}+K$	5.49, — 1	6.83, — 2
$\Sigma+\mathcal{N}+K+\pi$	1.30, + 0	1.61, — 1
$\Sigma+\mathcal{N}+K+2\pi$	3.45, — 1	4.29, — 2
$\Sigma+\mathcal{N}+K+3\pi$	2.14, — 2	2.67, — 3
$\Sigma+\mathcal{N}^*+K \rightarrow \Sigma+\mathcal{N}+K+\pi$	6.62, — 1	8.24, — 2
$\Sigma+\mathcal{N}^*+K+\pi \rightarrow \Sigma+\mathcal{N}+K+2\pi$	9.98, — 1	1.24, — 1
$\Sigma+\mathcal{N}^*+K+2\pi \rightarrow \Sigma+\mathcal{N}+K+3\pi$	1.16. — 1	1.44, 2
$\Sigma+\mathcal{N}^*+K+3\pi \rightarrow \Sigma+\mathcal{N}+K+4\pi$	2.47, — 3	3.08, — 4
$\Xi+\mathcal{N}+2K$	1.30, — 2	1.61, — 3
$\Xi+\mathcal{N}+2K+\pi$	1.39, — 3	1.73, — 4
$\Xi+\mathcal{N}+2K+2\pi$	1.09, — 5	1.36, — 6
$\Xi+\mathcal{N}+2K+3\pi$	3.64, — 9	4.54, —10
$\Xi+\mathcal{N}^*+2K \rightarrow \Xi+\mathcal{N}+2K+\pi$	2.76, — 3	3.43, — 4
$\Xi+\mathcal{N}^*+2K+\pi \rightarrow \Xi+\mathcal{N}+2K+2\pi$	3.04, — 5	3.79, — 6
$\Xi+\mathcal{N}^*+2K+2\pi \rightarrow \Xi+\mathcal{N}+2K+3\pi$	7.06, —10	8.78, —11
$2\mathcal{N}+K+\bar{K}$	6.60, — 2	7.01, — 2
$2\mathcal{N}+K+\bar{K}+\pi$	3.45, — 2	3.66, — 2
$2\mathcal{N}+K+\bar{K}+2\pi$	2.11, — 3	2.24, — 3
$2\mathcal{N}+K+K+3\pi$	2.48, — 5	2.64, — 5
$\mathcal{N}^*+\mathcal{N}+K+\bar{K} \rightarrow 2\mathcal{N}+K+\bar{K}+\pi$	8.15, — 2	8.65, — 2
$\mathcal{N}^*+\mathcal{N}+K+\bar{K}+\pi \rightarrow 2\mathcal{N}+K+\bar{K}+2\pi$	1.66, — 2	1.77, — 2
$\mathcal{N}^*+\mathcal{N}+K+\bar{K}+2\pi \rightarrow 2\mathcal{N}+K+\bar{K}+3\pi$	2.98, — 4	3.16, — 4
$\mathcal{N}^*+\mathcal{N}+K+\bar{K}+3\pi \rightarrow 2\mathcal{N}+K+\bar{K}+4\pi$	3.71, — 7	3.94, — 7
$2\mathcal{N}^*+K+\bar{K} \rightarrow 2\mathcal{N}+K+\bar{K}+2\pi$	1.65, — 2	1.75, — 2
$2\mathcal{N}^*+K+\bar{K}+\pi \rightarrow 2\mathcal{N}+K+\bar{K}+3\pi$	6.42, — 4	6.82, — 4
$2\mathcal{N}^*+K+\bar{K}+2\pi \rightarrow 2\mathcal{N}+K+\bar{K}+4\pi$	3.43, — 7	3.65, — 7

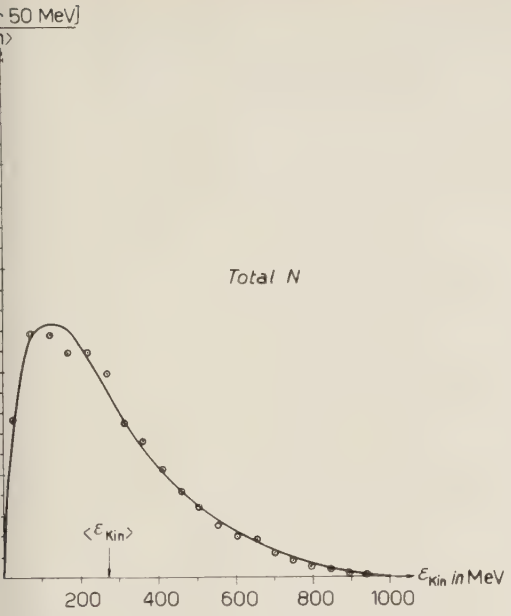

Fig. 1. – Total nucleon spectrum.

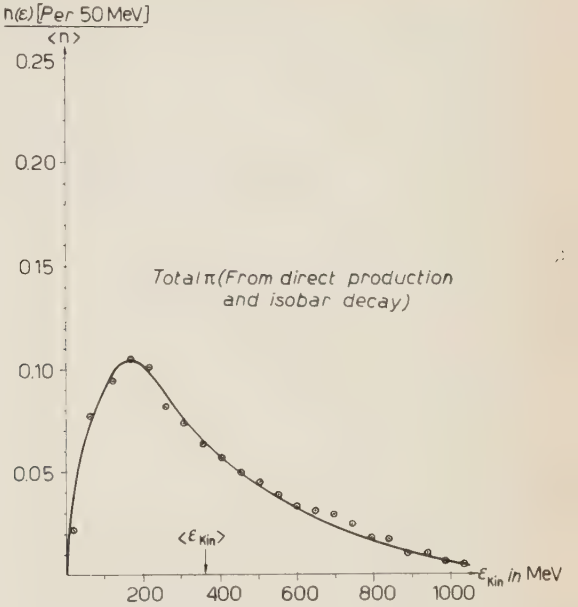

Fig. 2. – Total π-spectrum. The peak at low energy is mainly due to the decaying $\mathcal{N}^*$ (compare Fig. 3). The π^+ and π^- spectrum will look similar except for the high-energy tail, where the charge-state probabilities are different for π^+, π^0 and π^-.

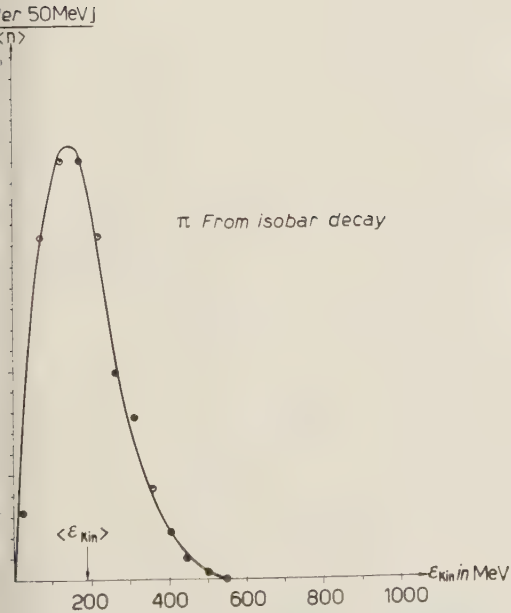

. – The π-mesons coming from the decaying isobar.

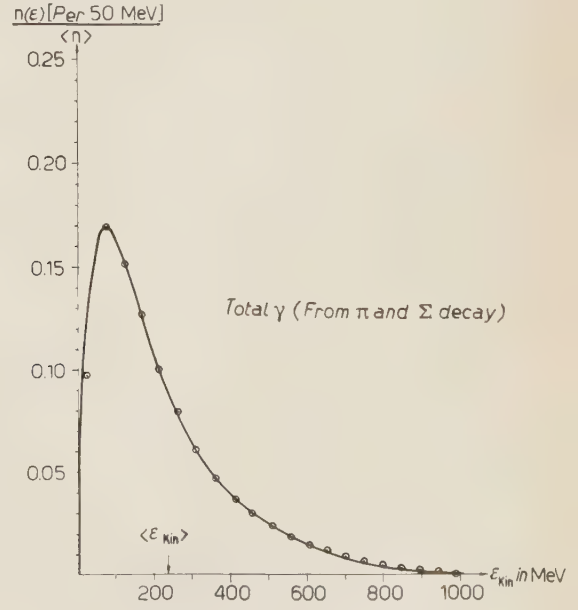

Fig. 4. – The total γ-spectrum coming from $\pi^0 \to 2\gamma$ and $\Sigma^0 \to \Lambda + \gamma$. Other γ-processes are not contained herein.

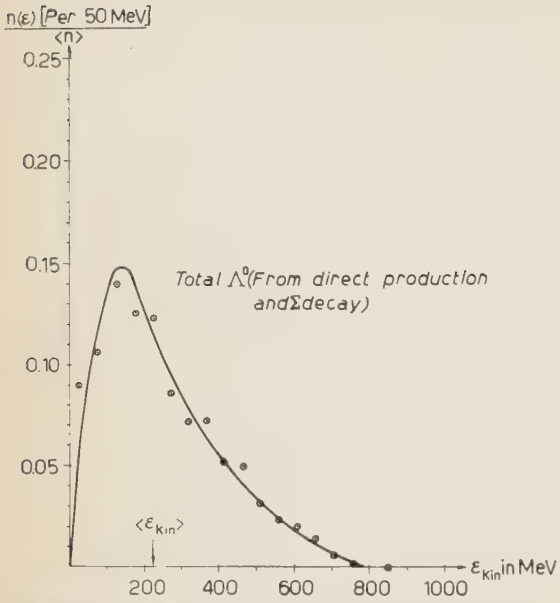

Fig. 5. Total Λ-spectrum, including the decay of $\frac{1}{3}$ of the produced Σ.

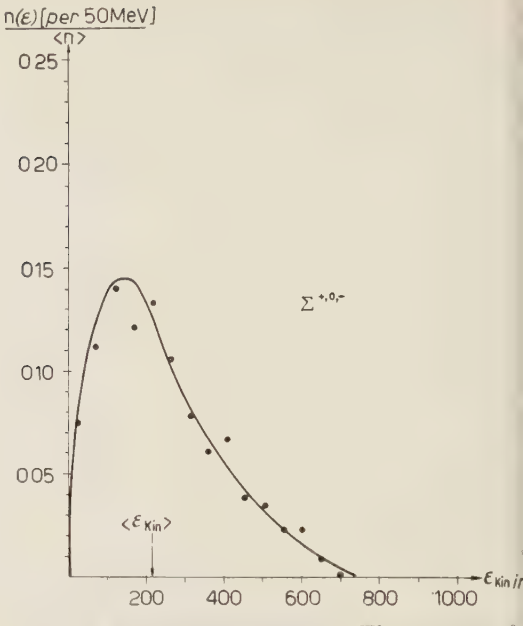

Fig. 6. Total Σ-spectrum. The spectra fo and Σ^- may be somewhat different, in parti for the higher energies.

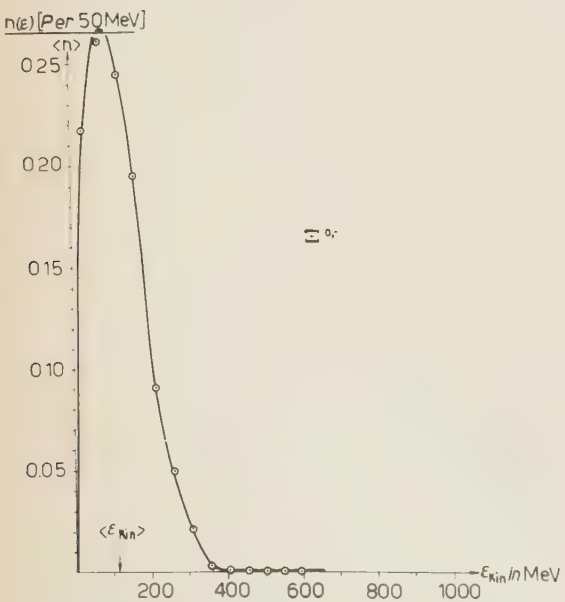

Fig. 7. – The total Ξ-spectrum.

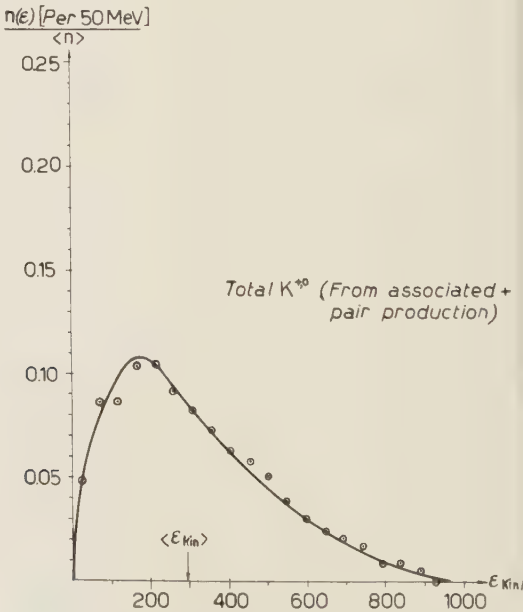

Fig. 8. – Total K-spectrum. To this cont the K-mesons from associated production those from pair production.

Explanations for Figs. 1-12 (*spectra*). – All spectra represent kinetic energies in the C.M. system of the colliding protons. They are normalized to unity. The quantity represented is the ratio:

$$\frac{\text{number of particles } n(\varepsilon) \text{ per energy interval}}{\text{mean total number } \langle n \rangle \text{ of particles of that kind}}$$

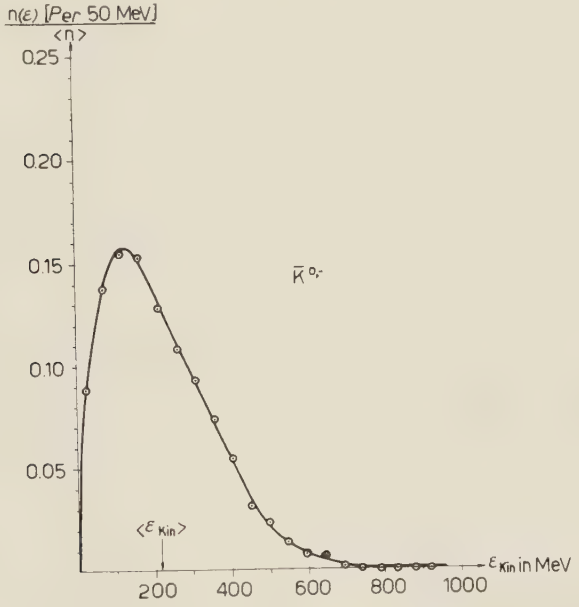

Fig. 9. - $\overline{K}$-spectrum. Only KK-pair production contributes. Note the different shape as compared with Fig. 8.

The energy interval was chosen to be 50 MeV except for the antinucleons, where it is 1 MeV.

The points are the resulting values from the above described weighted

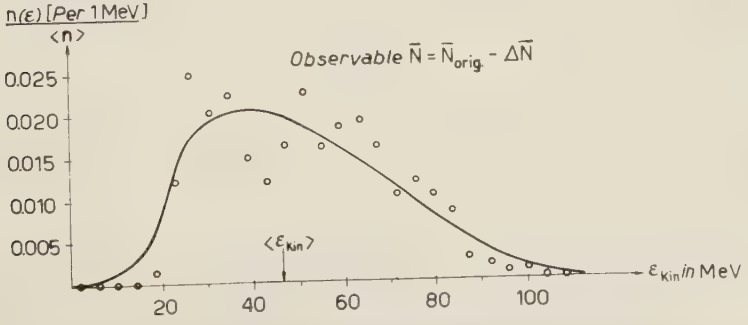

Fig. 10. – Observable anti-nucleon spectrum, assuming final state annihilation.

superposition of the Monte Carlo spectra. Some spectra are represented very smoothly, namely those to which many of the reactions listed in Table I contribute (*e.g.* π-spectra). Some others show still large fluctuations (*e.g.* $\mathcal{N}$).

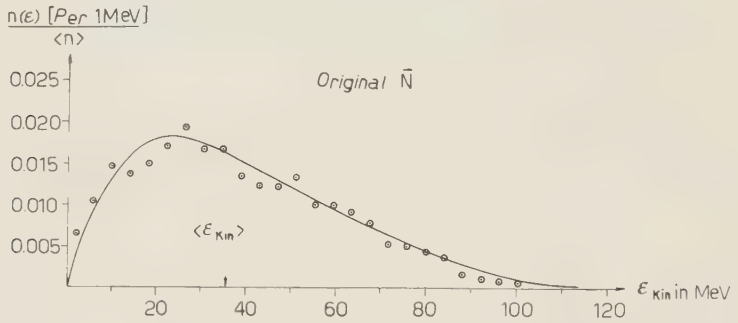

Fig. 11. – Original anti-nucleon spectrum, without final state annihilation.

The solid curves are partly drawn by hand and partly found by a least square fit by a Fourier series of $\sin \nu\varepsilon$, $\nu = 1 \ldots 5$. The curves are statistically more accurate than the points and their error is probably of the order of — or less

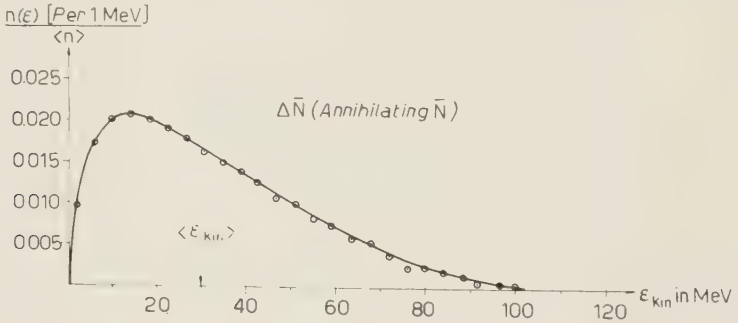

Fig. 12. – Spectrum of those anti-nucleons, which have a chance to annihilate in final state. This spectrum, with a proper weight factor is subtracted from the original $\mathcal{N}$-spectrum, giving that of Fig. 10. Note that all three spectra are normalized to unity.

than — about 3%, for some curves much better. The amount of scattering of the drawn in points gives a qualitative feeling for the goodness of fit of the curve.

Explanations for Figs. 13-21. – Here the mean values of absolute particle numbers per collision and some ratios of such numbers are shown for each kind of particle. We made no attempt to divide them up for the different charges. Roughly, but not exactly, the numbers of $\pi^+ : \pi^0 : \pi^-$ will be 1 : 1 : 1

and analogously for $\Sigma, \mathcal{N}$. But for cases in which very few particles are produced, this is certainly wrong. If in experimental analysis one classifies events according to the number of prongs, then one has to be very careful.

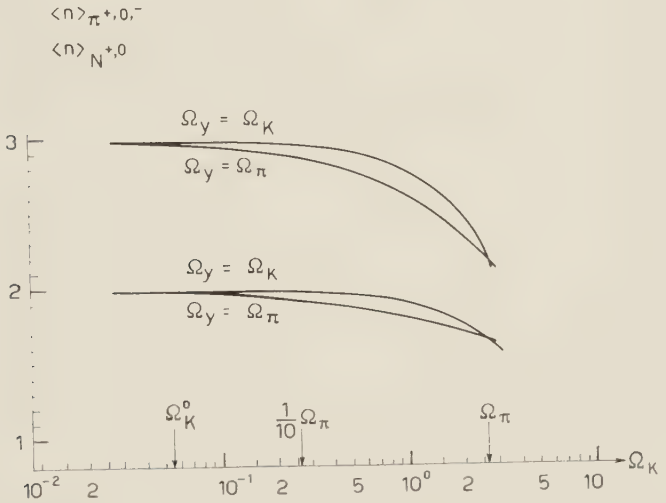

Fig. 13. – Mean number of π and $\mathcal{N}$ per collision.

(See F. CERULUS and R. HAGEDORN: CERN 59-3, where the charge distribution at another energy is carried through. A calculation to do the same in the present case is in progress).

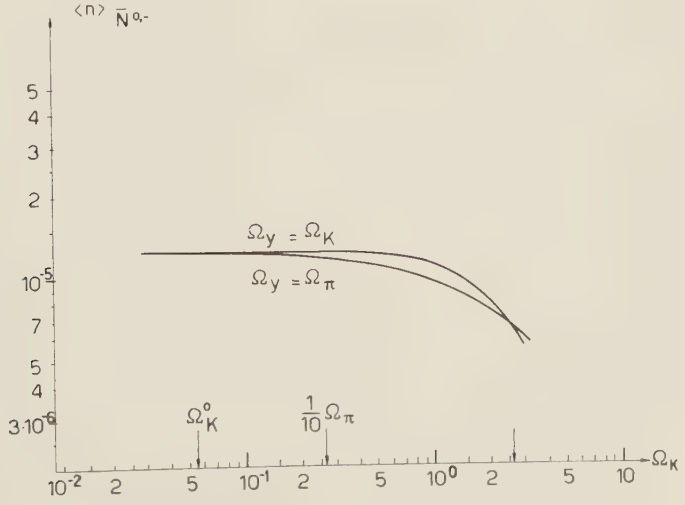

Fig. 14. – Mean number of $\bar{\mathcal{N}}$ per collision.

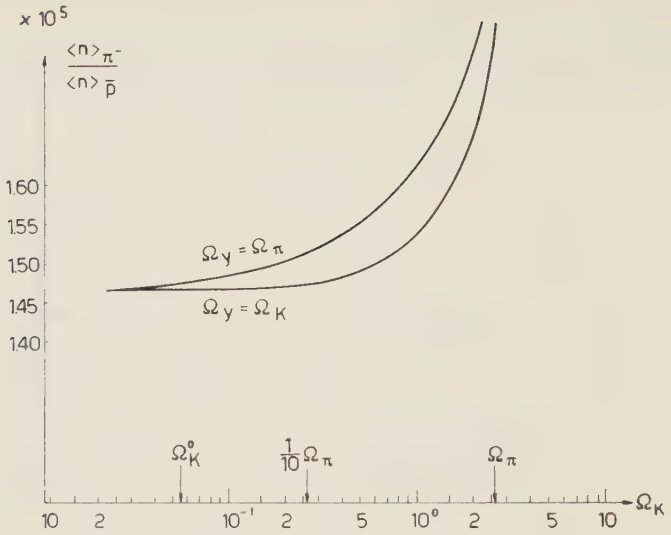

Fig. 15. – Ratio of $\pi^-/\overline{\mathrm{p}}$.

In all figures Ω_K is the varying variable and the curves show the dependence of the particle numbers on Ω_K. In all cases where the assumptions

(i) $$\Omega_Y = \Omega_\pi ,$$

and

(ii) $$\Omega_Y = \Omega_K ,$$

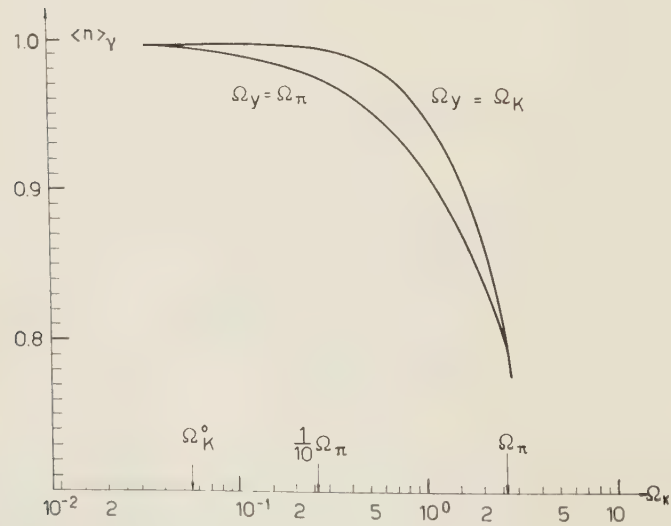

Fig. 16. – Total γ number from π^0 and Σ^0 decay per collision.

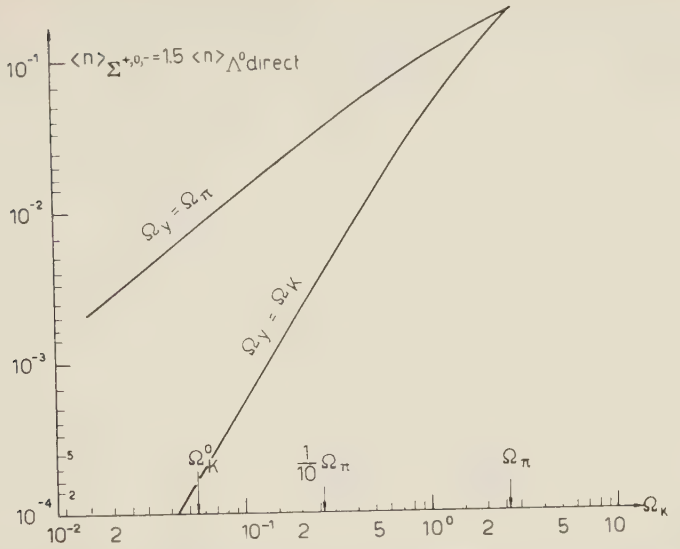

Fig. 17. – Total Σ and Λ number per collision: the total number of $\Sigma^+ + \Sigma^0 + \Sigma^-$ equals approximately $\frac{3}{2}$ of the number of directly produced Λ^0. If the masses of Σ and Λ were equal, one would expect a factor 3, but the reduction in phase space of the states with Σ, because of its higher mass, gives almost exactly a factor 1.5. The curves represent therefore simultaneously the mean number of $\Sigma^{+,0,-}$ and the mean number of $\Lambda^0_{direct} + \Sigma^0$, which equals the total number of observed Λ^0.

show different results, two curves are given. When only one curve is drawn, it means that both assumptions lead to the same result.

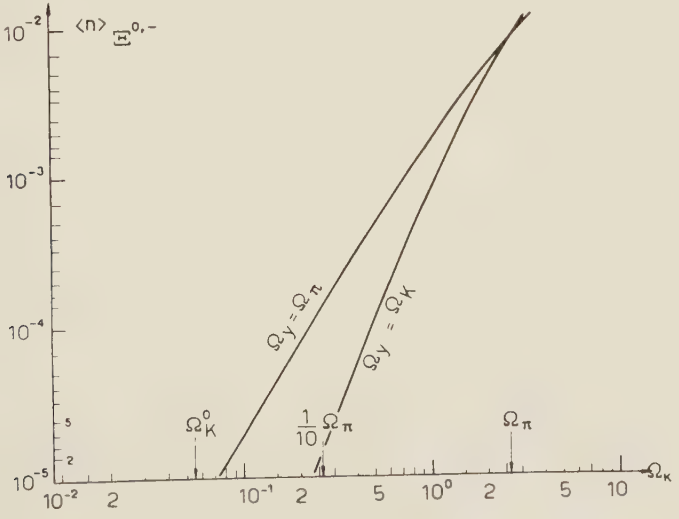

Fig. 18. – Total number of $\Xi^{0,-}$ per collision.

Obviously both assumptions give nearly the same result for those quantities, which anyway hardly change with Ω_K, namely, the numbers of π, $\mathcal{N}$, $\overline{\mathcal{N}}$ and γ from π^0 and Σ^0 decay. There we show these numbers in a linear scale.

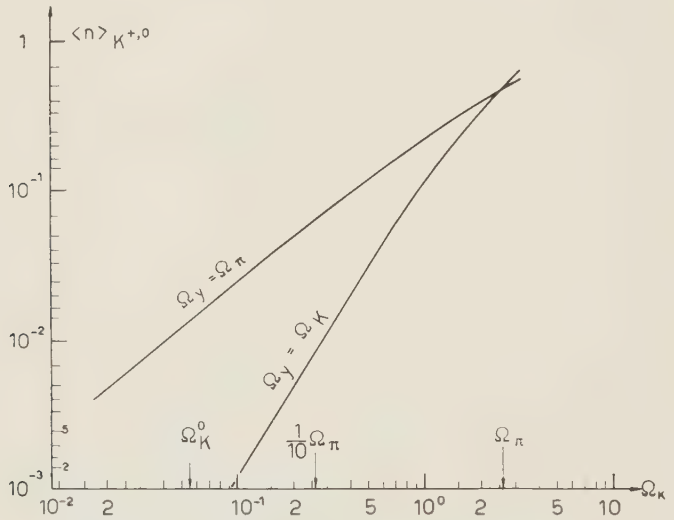

Fig. 19. – Total K-production per collision.

The numbers of hyperons and K-mesons depend strongly on Ω_K and in a different way for each assumption, they are shown in a logarithmic scale.

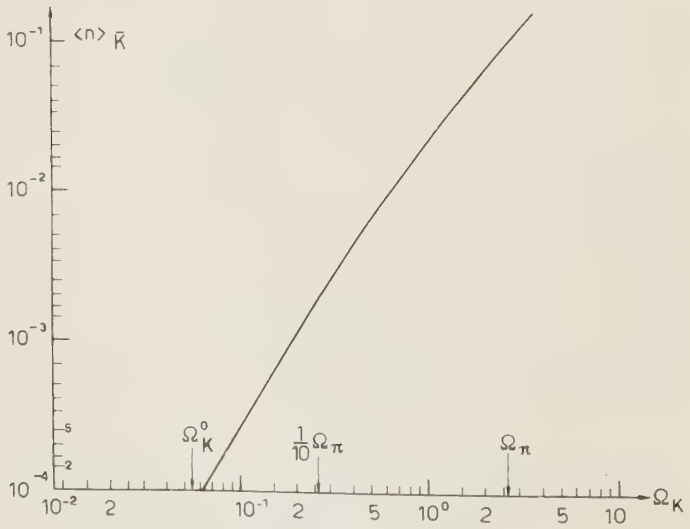

Fig. 20. – Total $\overline{K}$-production per collision.

We would expect that assumption (i) $\Omega_Y = \Omega_\pi$ with a value of Ω_K between $\frac{1}{10}\Omega_\pi$ and $\frac{1}{15}\Omega_\pi$ should give agreement with experiments. This would agree

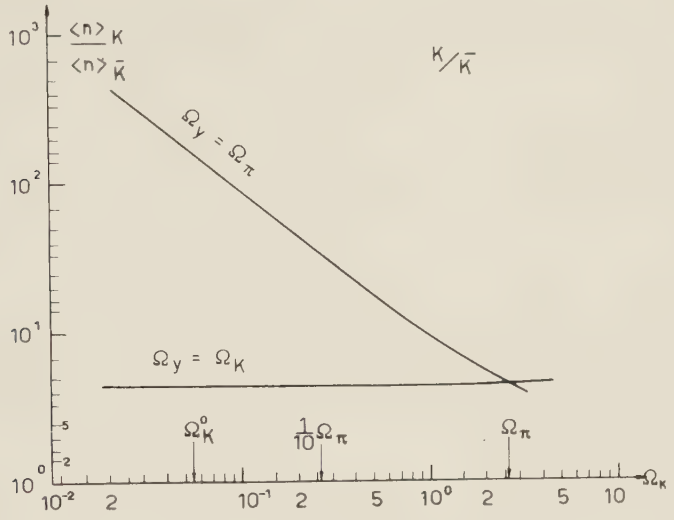

Fig. 21. – The ratio $K/\bar{K} \approx K^+/K^-$. Since the K-mesons are produced in associated ($\mathcal{N}+\mathcal{N} \to Y+K+n\pi$) *and* in pair production ($\mathcal{N}+\mathcal{N} \to K+\bar{K}+n\pi$), whereas the $\bar{K}$ are produced only in the latter reaction, this ratio is >1. In fact, it rather strongly depends on Ω_K in the «global symmetry» version and is constant in the version $\Omega_Y = \Omega_K$. If the experiment shows that $K/\bar{K} \gg 1$, then this definitely rules out the version (ii) $\Omega_Y = \Omega_K$ in favour of the other one.

in a loose sense with global symmetry and a coupling strength for the K-mesons which is smaller by about one order of magnitude than that of the π-mesons.

Appendix II

The total probability for an event in which an $\mathcal{N}\mathcal{N}$-pair is created, is proportional to:

$$\text{(A.1)} \qquad \varrho^*(E_0; m_1 \dots m_n; \sum \boldsymbol{p} = 0) = \int \mathrm{d}\boldsymbol{p}_1 \dots \mathrm{d}\boldsymbol{p}_{n-2}\, \mathrm{d}\boldsymbol{\pi}_1\, \mathrm{d}\boldsymbol{\pi}_2\, \delta(E_0 - \sum_{i=1}^{n} \varepsilon_i)\, \delta(\sum_{i=1}^{n-2} \boldsymbol{p}_i + \boldsymbol{\pi}_1 + \boldsymbol{\pi}_2)\,.$$

Here $\boldsymbol{\pi}_1$ is the momentum of the $\bar{\mathcal{N}}$ and $\boldsymbol{\pi}_2$ that of the $\mathcal{N}$ of the pair. ($\varepsilon_{n-1} = \sqrt{\pi_1^2 + 1}$; $\varepsilon_n = \sqrt{\pi_2^2 + 1}$; $M = 1$). Correspondingly,

$$\text{(A.2)} \qquad \mathrm{d}\boldsymbol{\pi}_1\, \mathrm{d}\boldsymbol{\pi}_2 \int \mathrm{d}\boldsymbol{p}_1 \dots \mathrm{d}\boldsymbol{p}_{n-2}\, \delta(E_0 - \sum_{i=1}^{n} \varepsilon_i)\, \delta(\sum_{i=1}^{n-2} \boldsymbol{p}_i + \boldsymbol{\pi}_1 + \boldsymbol{\pi}_2)\,,$$

would be proportional to the probability of the same event but with the $\overline{\pi}$ having a momentum near to $\boldsymbol{\pi}_1$ and the π having it near to $\boldsymbol{\pi}_2$. We can therefore single out all those events in which these two particles have less than a certain relative momentum, simply by integrating $\boldsymbol{\pi}_1$ and $\boldsymbol{\pi}_2$ not over all values but only over a restricted region fulfilling the wanted condition.

To this end we return to (A.1) and write it in a different way, using the identity

$$\text{(A.1')} \qquad \varrho^* = \int \mathrm{d}E\, \mathrm{d}\boldsymbol{P} \int \mathrm{d}\boldsymbol{p}_1 \ldots \mathrm{d}\boldsymbol{p}_{n-2}\, \delta\Big(E_0 - E - \sum_{i=1}^{n-2} \varepsilon_i\Big)\, \delta\Big(\sum_{i=1}^{n-2} \boldsymbol{p}_i + \boldsymbol{P}\Big) \cdot$$

$$\cdot \int \mathrm{d}\boldsymbol{\pi}_1\, \mathrm{d}\boldsymbol{\pi}_2\, \delta(E - \varepsilon_{n-1} - \varepsilon_{n-2})\, \delta(\boldsymbol{P} - \boldsymbol{\pi}_1 - \boldsymbol{\pi}_2).$$

By integrating over E and $\boldsymbol{P}$ this gives back (A.1). After having thus separated off the pair, we may easily carry out the above idea by introducing the coordinates one usually takes in two-body systems. That amounts to putting

$$\text{(A.3)} \qquad \left.\begin{array}{ll} \boldsymbol{P}' = \boldsymbol{\pi}_1 + \boldsymbol{\pi}_2; & \boldsymbol{\pi}_1 = \boldsymbol{p}' + \tfrac{1}{2}\boldsymbol{P}' \\ \boldsymbol{p}' = \tfrac{1}{2}(\boldsymbol{\pi}_1 - \boldsymbol{\pi}_2); & \boldsymbol{\pi}_2 = \boldsymbol{p}' - \tfrac{1}{2}\boldsymbol{P}' \end{array}\right\} \quad \text{with} \quad \frac{\partial(\boldsymbol{\pi}_1 \boldsymbol{\pi}_2)}{\partial(\boldsymbol{p}' \boldsymbol{P}')} = 1\,.$$

Introducing further $\cos(\boldsymbol{p}', \boldsymbol{P}') = \xi$ one sees that

$$\varepsilon_{n-1} = \sqrt{\pi_1^2 + 1} = \sqrt{p'^2 + P' p' \xi + \tfrac{1}{4} P'^2 + 1}\,,$$

$$\varepsilon_n \;\; = \sqrt{\pi_2^2 + 1} = \sqrt{p'^2 - P' p' \xi + \tfrac{1}{4} P'^2 + 1}\,.$$

After integration over $\boldsymbol{P}'$, we have, on account of the δ-function

$$\text{(A.4)} \qquad \int \mathrm{d}\boldsymbol{\pi}_1\, \mathrm{d}\boldsymbol{\pi}_2 \ldots =$$

$$= 2\pi \int p'^2\, \mathrm{d}p'\, \mathrm{d}\xi\, \delta\left(E - \sqrt{p'^2 + Pp'\xi + \frac{P^2}{4} + 1} - \sqrt{p'^2 - Pp'\xi + \frac{P^2}{4} + 1}\right).$$

Now, p' is half the relative momentum and P the total momentum of the pair. We wish to single out cases in which the relative momentum p is small. Then, for small P, the 1 is the leading term and we may develop the square roots by which the term $Pp'\xi$ drops out:

$$\sqrt{p'^2 + Pp'\xi + \frac{P^2}{4} + 1} + \sqrt{p'^2 - Pp'\xi + \frac{P^2}{4} + 1} \approx$$

$$\approx 2\left[1 + \frac{1}{2}\left(p'^2 + \frac{P^2}{4}\right)\right] \approx 2 \cdot \sqrt{1 + p'^2 + \frac{P^2}{4}}\,.$$

If, on the other hand P is large, $1+P^2/4$ is the leading term and

$$\left| \sqrt{p'^2 + Pp'\xi + \frac{P^2}{4} + 1} + \sqrt{p'^2 - p'P\xi + \frac{P^2}{4} + 1} \right| \approx$$

$$\approx 2 \cdot \sqrt{1 + \frac{P^2}{4}} \cdot \left(1 + \frac{p'^2}{2 \cdot (1 + (P^2/4))}\right) \approx 2 \cdot \sqrt{1 + p'^2 + \frac{P^2}{4}} \,.$$

So we may write as a good approximation

$$\delta\left(E - \sqrt{p'^2 + Pp'\xi + \frac{P^2}{4} + 1} - \sqrt{p'^2 - Pp'\xi + \frac{P^2}{4} + 1}\right) \approx$$

$$\approx \delta\left(E - 2 \cdot \sqrt{1 + \frac{P^2}{4} + p'^2}\right).$$

Inserting this into (A.4) and (A.4) into (A.1′), we find after integrating over E

$$\text{(A.1}'') \qquad \delta\varrho^* \simeq 4\pi \int_0^{p_0'} p'^2 \,\mathrm{d}p' \int \mathrm{d}\boldsymbol{p}_1 \ldots \mathrm{d}\boldsymbol{p}_{n-2} \,\mathrm{d}\boldsymbol{P} \cdot$$

$$\cdot \delta\left(E_0 - \sqrt{4 + 4p'^2 + P^2} - \sum_{i=1}^{n-2} \varepsilon_i\right) \delta\left(\sum_{i=1}^{n-2} \boldsymbol{p}_i + \boldsymbol{P}\right).$$

This, since we integrate only up to p_0', is proportional to the number of events where the $\pi\,\overline{\pi}$ pair comes out with a relative momentum $p_{\mathrm{rel}} \leqslant 2p_0'$. Finally we put $p = 2p'$ and have

$$\text{(A.1}''') \qquad \delta\varrho^* = \frac{\pi}{2} \int_0^{p_0} p^2 \,\mathrm{d}p \int \mathrm{d}\boldsymbol{p}_1 \ldots \mathrm{d}\boldsymbol{p}_{n-2} \,\mathrm{d}\boldsymbol{P} \cdot$$

$$\cdot \delta\left(E_0 - \sqrt{(4 + p^2) + P^2} - \sum_{i=1}^{n-2} \varepsilon_i\right) \delta\left(\sum_{i=1}^{n-2} \boldsymbol{p}_i + \boldsymbol{P}\right).$$

Now the second integral is nothing else than $\varrho^*(E_0, m_1 \ldots m_{n-2}, m^*, \sum \boldsymbol{p} = 0)$, that is the ϱ^* for the $n-2$ first particles plus one more particle (namely the $\pi\,\overline{\pi}$-pair) with mass

$$m^* = \sqrt{4 + p^2} \approx 2 + \frac{p^2}{4} \,,$$

which has the obvious meaning of a particle consisting of two nucleons plus the kinetic energy of their relative motion (remember $m = 1$).

Therefore

$$\delta\varrho^* = \frac{\pi}{2}\int_0^{p_0} p^2\,\mathrm{d}p\cdot\varrho^*(E_0, m_1 \ldots m_n, m^*(p)) \ . \tag{A.5}$$

To this we add the further factor $(\sigma_{\text{annihil}}/\sigma_{\text{total}})(p)$, to account for the experimental fact that not all low-energy p-$\bar{\text{p}}$ collisions result in annihilation. The $\varrho^*(E_0, m_1 \ldots m_{n-1}, m^*)$ is then computed with the usual Monte Carlo method for four different $m^*(p)$ and the integral is calculated by Simpson's formula. We call $\Delta\varrho^*$ the integral (A.5) including the σ_a/σ_t-factor.

We choose $p_0 = 1$, since this is the order of magnitude which corresponds to the $\mathcal{T}$ and $\mathcal{T}$ staying together nearer than a pion Compton wavelength for longer than one elementary time.

The value of p_0 and the factor $(\sigma_{\text{annihil}}/\sigma_{\text{total}})(p)$ are of course somewhat doubtful. However, the contributions to $\Delta\varrho^*$ coming from $p \leqslant \frac{1}{4}$ and $p \geqslant \frac{1}{2}$ are not important; for the small p the p^2 decreases too strongly and for the larger p the $m^*(p)$ takes away too much energy, hence $\varrho^*(E_0, m_1 \ldots m_{n-1}, m^*(p))$, becomes small. Consequently, if the rate of the « recombination » of $\mathcal{T}$-$\mathcal{T}$ pairs immediately after the collision is a smoothly varying function, one can account for the portion of $\mathcal{T}$-$\mathcal{T}$ pairs which scatter without annihilating, by introducing a suitable factor (<1) multiplying $\delta\varrho^*$. In the present case we took for this factor σ_a/σ_t, which is nearly $\frac{1}{2}$ over the whole range of p we have to consider here. Between $p = 0$ and the lower limit of the experiment, we assumed a $1/r$ behaviour of σ_a, but the contribution of this region to $\Delta\varrho^*$ is quite unimportant. Because of the vanishing of ϱ^* for large p, it is also unimportant (in the present case where the $\mathcal{T}$ can have only a small kinetic energy) where we put the limit p_0, as long as $p_0 \geqslant \frac{1}{2}$, which seems a reasonable value.

We still have to account for the fact that there are three nucleons with which the antinucleon may annihilate, whereas our calculation has tacitly assumed that only the last one could. Let us visualize $\Delta\varrho^*$ and ϱ^* as volumes. Then in ϱ^* there are one antinucleon, three nucleons and may be other particles. If there were only one nucleon and one antinucleon, then $\mathcal{T}\cdot(\Delta\varrho^*/\varrho^*)$ would be the number of $\mathcal{T}$ that would annihilate. In other words: if the nucleon is in $\Delta\varrho^*$, annihilation takes place and $\Delta\varrho^*/\varrho^*$ is the probability for finding the nucleon in $\Delta\varrho^*$.

This is a situation well known in elementary statistical gas theory: we have n particles (nucleons) in a box of volume ϱ^*. Inside there is a smaller box of volume $\Delta\varrho^*$ and we just have calculated the probability to find a definite nucleon in $\Delta\varrho^*$ no matter where the others are. This, however, is not what we need, since annihilation will take place *as soon as at least one* of the n nucleons is in $\Delta\varrho^*$. In complete analogy to the elementary statistics we find that the probability for this is equal to

$$1 - [\text{probability that no nucleon is in } \Delta\varrho^*] = 1 - \left(1 - \frac{\Delta\varrho^*}{\varrho^*}\right)^n .$$

Hence the total number of annihilated antinucleons will be

$$\mathcal{N} - \overline{\mathcal{N}}\left|1 - \left(1 - \frac{\Delta\varrho^*}{\varrho^*}\right)^n\right|,$$

if n nucleons are present.

In our case $n = 3$. If there are other particles (pions, etc.) present, then these three nucleons may be considered as independent and the above consideration is correct. That is true for slightly higher energies than ours. Here we have no other particles and therefore we will have a correlation between the nucleons, because the sum of their momenta must vanish. So only two nucleons are really free, though not completely independent. It will be probably not a bad approximation to account for the correlations of the nucleons by considering two of them as completely free in the volume ϱ^* and the third to be completely fixed by the position of the first two. That amounts to put $n = 2$ instead of 3 as one would do if the mesons could balance the momentum. This yields the formula quoted in the main text.

There remains the correction of the $\mathcal{N}$-spectrum. We have done this in a rather unsatisfactory way and some steps taken are not proved in detail. We think, however, that it allows at least a good qualitative guess.

Suppose again, for a moment, that only one of the three nucleons can annihilate with the antinucleon. We wish to calculate the spectrum of those $\mathcal{N}$, which then would annihilate, *i.e.* that $\Delta\mathcal{N}$ spectrum which had to be subtracted from the $\mathcal{N}$-spectrum in order to yield the observable $\mathcal{N}_{\text{obs}}$-spectrum.

The $\mathcal{N}\mathcal{N}$-pair with relative momentum p_r has been shown to be equivalent to a single particle with mass $m^* = \sqrt{4 + p_r^2}$. In the calculation of $\varrho^*(E, \ldots m^*)$ the spectrum of this fictitious particle m^* is also computed and using the subprogramme for the decay of this m^* particle into two particles of $m = 1$ one obtains a spectrum which is just the spectrum of the $\mathcal{N}$ and of the $\mathcal{N}$ under the present restrictions on their relative momentum, *i.e.* in particular the spectrum of the annihilating $\overline{\mathcal{N}}$.

Therefore one had for each p_r to calculate the corresponding $\mathcal{N}$-spectrum and add them up by Simpson's rule, thus obtaining a total $\Delta\mathcal{N}$-spectrum. This has been done.

Now comes the difficulty: this would be correct for the case that one single nucleon is available for annihilation with the $\overline{\mathcal{N}}$. In fact there are three and our above argument concerning the overall effect of annihilation should now be applied to the integrand for every value of p_{rel}. But here the correlation must be taken into account and the question becomes much more complicated as in the overall effect. We do therefore an approximation: the $\Delta\overline{\mathcal{N}}$-spectrum is calculated along the lines given above *as if* only one nucleon were present. Then it is renormalized such that its norm equals the overall $\Delta\mathcal{N} = \overline{\mathcal{N}}[1 - (1 - \Delta\varrho^*/\varrho^*)^2]$. Then the original $\mathcal{N}$-spectrum is normalized to $\overline{\mathcal{N}}$ and the $\Delta\mathcal{N}$-spectrum is subtracted from it. The resulting spectrum is considered as the « observable $\mathcal{N}$-spectrum ». The philosophy behind this is that the most important effect is not so much, that at the same time more that one nucleon can be near $\overline{\mathcal{N}}$ (inside $\Delta\varrho^*$), but rather that the probability to find just one has become larger because there are three nucleons each of which is able to enter in $\Delta\varrho^*$. Therefore the spectrum of the annihilating $\mathcal{N}$'s is given mainly by those states in which only one nucleon comes near to $\mathcal{N}$

(that is, what we have in fact calculated first), but this happens much more often than our calculation gives; hence we correct it by renormalizing the spectrum of the annihilating $\mathcal{N}$ to have a norm equal to the total $\Delta\bar{\mathcal{N}}$.

If, on the other hand, the probability of two, or more, nucleons being in $\Delta\varrho^*$ becomes large, then the effect of there being more than one nucleon will turn out to be different for different relative momenta and such an over-all renormalization is certainly wrong. We may be just on the border line.

RIASSUNTO (*)

La teoria di Fermi per la produzione di particelle viene usata in forma rigorosa e raffinata allo scopo di calcolare gli spettri e i numeri medi di particelle per tutte le particelle prodotte (cioè $\mathcal{N}$, π, $\bar{\mathcal{N}}$ e particelle strane) in urti p-p a 6.2 GeV (sistema cinetico del laboratorio).

(*) *Traduzione a cura della Redazione.*

Large Amplitude Waves in a Collision-Free Plasma.
I. - Single Pulses with Isotropic Pressure (*).

A. Baños jr. and R. Vernon

Department of Physics, University of California - Los Angeles, Cal.

(ricevuto il 13 Ottobre 1959)

Summary. — We consider an infinite expanse of low density, fully ionized plasma, magnetically immobilized in a constant and uniform field of magnetic induction. In the absence of collisions we assume that the ion and electron motions take place in planes perpendicular to the magnetic field. We then transform to a « shock » frame of reference moving at constant speed at right angles to the magnetic field, and then we search for the class of non-trivial, time-independent, one-dimensional, self-consistent solutions of the Maxwellian set and of the equations of motion of the charged particles; that is, we study the propagation of transverse pulses and waves whose characteristic length is much smaller than the collision mean free path. Upon making appropriate simplifications, we are led to a system of equations in which collisions are neglected, charge neutrality is assumed, and both ions and electrons behave like two-dimensional fluids obeying isentropic relations with $\gamma=2$ and exhibiting rigorously isotropic pressure tensors. With these simplifications and assumptions, the system of equations can be solved completely by a simple numerical quadrature. Both symmetric pulses and periodic waves are obtained, with characteristic lengths of the order of the plasma « skin depth », or mean gyromagnetic radius for particles traveling with the Alfvén speed. In this paper, Part I, we describe the solitary pulses, which are the only solutions satisfying the conditions of the undisturbed plasma ahead of the wave train. Two basic parameters are required for a complete specification of the problem: the Alfvén Mach number α, which gives a measure of the speed of propagation, and the ratio β of the total plasma pressure to the magnetic pressure, which specifies the initial state of the plasma. It is shown that, for given β, stationary solutions exist only for a limited range of speeds α.

(*) Supported in part by the U.S. Atomic Energy Commission through the University of California Lawrence Radiation Laboratory, Berkeley and Livermore.

1. – Introduction.

The problem of the one-dimensional shock in a collision free plasma furnishes the principal motivation for the present study. As things stand today (1), it has not been established, theoretically or experimentally, whether or not a shock-like phenomenom exists in the absence of collisions or other dissipative mechanisms. But it is known (2), that in the absence of collisions there exist non-trivial steady-state solutions which may serve as a guide to the whole question of one-dimensional shocks. In this paper we consider a two-dimensional plasma magnetically immobilized by a constant and uniform field of magnetic induction. We then transform to a « shock » frame of reference moving at constant speed at right angles to the magnetic field and inquire into the existence of stationary, one-dimensional, self-consistent solutions of the Maxwellian set and of the equations of motion of the charged particles. Among the steady-state solutions (in the shock frame of reference), we find solitary pulses and periodic solutions.

In this paper, Part I, we describe the structure of large amplitude solitary pulses and their domain of existence for a plasma supposed to be endowed with rigorously isotropic pressure. In this respect, our results constitute an extension of earlier work by ADLAM and ALLEN (3) and by DAVIS, LÜST and SCHLÜTER (4), who consider only the zero temperature case.

In the sequel to this paper, Part II, we propose to discuss the structure of large amplitude periodic solutions (waves) and their relation to the solitary pulses, again for a plasma with isotropic pressure. There is a close connection between our work, in both Parts I and II, with that of MORAWETZ (2) in the absence of the friction term, which will become apparent in the course of this discussion. We are at present extending this work to include the non-isotropic components of the pressure tensor for the special case of equal masses. These results will be reported separately in Part III.

2. – Fundamental equations.

The model that we consider here envisions an infinite expanse of neutral plasma consisting of singly-ionized ions and electrons in thermal equilibrium, embedded in a constant and uniform field of magnetic induction parallel to

(1) C. S. GARDNER, H. GOERTZEL, H. GRAD, C. S. MORAWETZ, M. H. ROSE and H. RUBIN: *Hydromagnetic Shock Waves in High Temperature Plasmas*, NYO-2538, Inst. Math. Sci., N.Y.U., January 30, 1959.

(2) C. S. MORAWETZ: *Magneto-Hydrodynamic Shock Structure Using Friction*, NYO-8677, Inst. Math. Sci., N.Y.U., January 12, 1959.

(3) J. H. ADLAM and J. E. ALLEN: *Phil. Mag.*, **3**, 448 (1958).

(4) L. DAVIS, R. LÜST and A. SCHLÜTER: *Zeits. f. Naturf.*, **13***a*, 916 (1958).

the z-axis of a laboratory Cartesian frame of reference. Because we neglect collision phenomena altogether, it is convenient to assume that the charged particles execute circular orbits in planes perpendicular to the magnetic field, thus giving rise to what we might term a two-dimensional, collision-free plasma. Next, we make a Lorentz transformation to a *shock* frame of reference moving at constant speed u_0 in the *negative* x direction, with respect to the laboratory frame, and then we look for the class of non-trivial time-independent (stationary), one-dimensional solutions of the Maxwellian set and of the equations governing the motion of the charged particles. To simplify the notation we adopt here the convention of designating ion quantities with capital letters and electron quantities with the corresponding lower case letters.

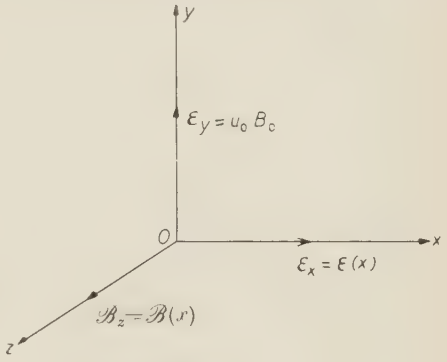

Fig. 1.

Accordingly, the electromagnetic field vectors $\mathcal{E}$ and $\mathcal{B}$ (see Fig. 1), and the ion and electron fluid velocities $\boldsymbol{V}$ and $\boldsymbol{v}$ exhibit respectively, in the shock frame of reference, the components

$$\begin{aligned}
\mathcal{E} &= [\mathcal{E}(x),\ u_0 B_0,\ 0] \to (0,\ u_0 B_0,\ 0) \\
\mathcal{B} &= [0,\ 0,\ \mathcal{B}(x)] \quad\ \to (0,\ 0,\ B_0) \\
\boldsymbol{V} &= [V_x(x),\ V_y(x),\ 0] \to (u_0,\ 0,\ 0) \\
\boldsymbol{v} &= [v_x(x),\ v_y(x),\ 0] \to (u_0,\ 0,\ 0)
\end{aligned}$$

which reduce to the indicated limiting forms as $x \to -\infty$ (boundary conditions), and where u_0 is the speed of the shock frame and B_0 is the magnitude of the original field of magnetic induction.

In the adopted notation, the fundamental equations for the present one-dimensional stationary case can be listed as follows [5]:

Maxwell's equations, in rationalized mks units, reduce to

$$\varepsilon(\mathrm{d}\mathcal{E}/\mathrm{d}x) = e(N - n)\,, \tag{1}$$

and

$$\mathrm{d}\mathcal{B}/\mathrm{d}x = \mu e(nv_y - NV_y)\,, \tag{2}$$

[5] For the derivation of the equations in general form see, for example, H. Grad: *Notes on Magneto-Hydrodynamics. I. General Fluid Equations*, NYO-6486, Inst. Math. Sci., N.Y.U., August 1, 1956.

where e is the electronic charge, N and n are the number densities of ions and electrons, respectively, and $\mu\varepsilon = c^{-2}$.

The continuity equations (conservation of mass) for ions and electrons, which can be integrated at once, yield respectively

$$NV_x = \text{constant} = n_0 u_0 , \tag{3}$$

and

$$nv_x = \text{constant} = n_0 u_0 , \tag{4}$$

where n_0 is the number density of ions and of electrons as $x \to -\infty$.

The equations of motion (conservation of momentum) for ions and electrons, become respectively, for the x component of momentum,

$$NMV_x(\mathrm{d}V_x/\mathrm{d}x) = -\mathrm{d}P/\mathrm{d}x + Ne(\mathscr{E} + V_y\mathscr{B}) , \tag{5}$$

$$nmv_x(\mathrm{d}v_x/\mathrm{d}x) = -dp/\mathrm{d}x - ne(\mathscr{E} + v_y\mathscr{B}) , \tag{6}$$

and for the y component of momentum,

$$NMV_x(\mathrm{d}V_y/\mathrm{d}x) = Ne(u_0 B_0 - V_x\mathscr{B}) , \tag{7}$$

$$nmv_x\ (\mathrm{d}v_y/\mathrm{d}x) = -ne(u_0 B_0 - v_x\mathscr{B}) . \tag{8}$$

Furthermore, assuming that the pressure tensors for ions and electrons remain rigorously isotropic, which is equivalent to saying that the respective distribution functions behave, in the course of the phenomenon, as *local* Maxwellian distributions with number densities and temperatures which vary only as functions of x, we obtain the second moment equations [6]

$$\mathrm{d}(V_x P)/\mathrm{d}x = -P(\mathrm{d}V_x/\mathrm{d}x) , \tag{9}$$

and

$$\mathrm{d}(v_x p)/\mathrm{d}x = -p\,(\mathrm{d}v_x/\mathrm{d}x) , \tag{10}$$

which we can integrate at once to yield

$$PV_x^2 = \text{constant} = p_0 u_0^2 , \tag{11}$$

and

$$pv_x^2 = \text{constant} = p_0 u_0^2 , \tag{12}$$

[6] L. SPITZER jr.: *Physics of Fully Ionized Gases* (New York, 1956), Appendix.

where p_0 is the pressure of ions and of electrons as $x \to -\infty$. We observe, therefore, that both fluids satisfy the isentropic relation for ideal gases with $\gamma = 2$.

In addition to the immediate integrals (3), (4,) (11), and (12), which result from the stationary one-dimensional character of the problem, we have also, quite generally, the classical integrals of the motion which arise from the conservation laws of momentum and energy for the whole plasma [5]. In the present instance we have, for the x component of momentum

$$(13) \qquad (NMV_x^2 + P) + (nmv_x^2 + p) - \tfrac{1}{2}\varepsilon\mathscr{E}^2 + (\mathscr{B}^2 - B_0^2)/2\mu = 2p_0 + n_0(m+M)u_0^2 ,$$

and for the y component of momentum

$$(14) \qquad NMV_xV_y + nmv_xv_y - \varepsilon u_0 B_0 \mathscr{E} = 0 .$$

Finally, the conservation of energy for the whole plasma yields, in the present case,

$$(15) \qquad [\tfrac{1}{2}NM(V_x^2 + V_y^2) + 2P]V_x + [\tfrac{1}{2}nm(v_x^2 + v_y^2) + 2p)]v_x + \\ + u_0 B_0(\mathscr{B} - B_0)/\mu = 4p_0u_0 + \tfrac{1}{2}n_0(m+M)u_0^3 .$$

3. – Charge neutrality.

The set of equations (1) through (10) constitutes a closed system in the ten dependent variables $\mathscr{E}$, $\mathscr{B}$; N, n; V_x, v_x; V_y, v_y; and P, p. The solution of this system as listed is intractable by analytic methods and extremely cumbersome (if not impossible) by numerical methods because of its complexity and because of the recognized smallness of the charge separation,

$$(16) \qquad |N - n| \ll n ,$$

which appears in Poisson's equation (1). As shown in Section **8**, this condition is satisfied to a high degree of accuracy in most cases of interest. Therefore, to achieve a practical solution of the original system we *assume*, at the outset, that the plasma remains electrically neutral throughout the phenomenon,

$$(17) \qquad N = n ,$$

as a consequence of which (3) and (4) yield

$$(18) \qquad V_x = v_x ,$$

while the integrals (11) and (12) then give

$$P = p. \tag{19}$$

Thus, to this approximation, ions and electrons go hand in hand with identical horizontal velocities and identical pressures and temperatures.

Further reduction of the system is achieved by noting that eqs. (7) and (8), making use of (17) and (18), yield at once upon addition

$$MV_y + mv_y = 0\,, \tag{20}$$

which, in conjunction with (14), makes it evident that the assumption of charge neutrality (17) is tantamount to letting $\varepsilon \to 0$ (or $c \to \infty$) in (1), (13) and (14). Thus, with the aid of (18), (19), and (20) we can express the ion quantities in terms of corresponding electron quantities, and with the aid of (3) and (4) we can eliminate the number densities

$$N = n = n_0 u_0 / v_x\,. \tag{21}$$

In this manner we reduce the original system of ten equations to the following five:

$$Mv_x(\mathrm{d}\mathscr{B}/\mathrm{d}x) = \mu e n_0 (m + M) u_0 v_y\,, \tag{22}$$

$$Mv_x(\mathrm{d}/\mathrm{d}x)\left[v_x + 2p/n_0(m + M)u_0\right] = -\,e v_y \mathscr{B}\,, \tag{23}$$

$$mv_x(\mathrm{d}v_y/\mathrm{d}x) = e(v_x\mathscr{B} - u_0 B_0)\,, \tag{24}$$

$$v_x(\mathrm{d}p/\mathrm{d}x) = -\,2p(\mathrm{d}v_x/\mathrm{d}x)\,, \tag{25}$$

$$2Me\mathscr{E} = (M - m)[Mv_x(\mathrm{d}v_x/\mathrm{d}x) - e v_y \mathscr{B}]\,. \tag{26}$$

Thus, (22) through (25), constitute a closed set in the *four* dependent variables $\mathscr{B}$, v_x, v_y, and p; once this system is solved, eq. (26) yields the longitudinal electric field. We note that we could readily make use of (25) to eliminate p from (23), but we choose not to do so at this juncture for reasons that will become apparent in Section 5.

In addition to the basic equations listed above we have the integrals corresponding to the conservation laws of momentum and energy. Thus, making the same substitutions as before, the x component of momentum (13) can now be written as

$$n_0 u_0 (m + M)(v_x - u_0) + 2(p - p_0) + (\mathscr{B}^2 - B_0^2)/2\mu = 0\,, \tag{27}$$

while the conservation of energy (15) reduces to

$$(28) \qquad \tfrac{1}{2}n_0u_0(m+M)[r_x^2+(m/M)r_y^2-u_0^2]+4(pr_x-p_0u_0)-u_0B_0(\mathscr{B}-B_0)/\mu=0\,.$$

Finally, we add the integral of (25), which we interpret as the conservation of entropy and which reads, in accordance with (11) and (12), as

$$(29) \qquad pv_x^2=\text{constant}=a^3p_0u_0^2\,,$$

where $a\geqslant 1$ is a convenient parameter that we introduce here for ulterior reasons (Section 5) and which must assume the value $a=1$ for solutions which satisfy the boundary conditions as $x\to-\infty$.

4. – Reduction to dimensionless form.

To facilitate the solution of the preceding equations it is useful to express the field vectors $\mathscr{E}$ and $\mathscr{B}$ in terms of the dimension-free variables

$$(30) \qquad E=\mathscr{E}/u_0B_0 \qquad \text{and} \qquad B=\mathscr{B}/B_0\,,$$

and to express the horizontal and vertical components r_x and r_y of the electron fluid velocity in terms of the variables

$$(31) \qquad u=v_x/u_0 \qquad \text{and} \qquad v=(v_y/u_0)(m/M)^{\frac{1}{2}}\,.$$

In addition, we replace p, wherever it appears in the preceding equations, by the product pp_0, where *now* p is a dimension-free variable and p_0 is the pressure of ions and electrons at minus infinity. Finally, instead of the element of length $\mathrm{d}x$, we introduce the dimension-free element

$$(32) \qquad \mathrm{d}\xi=\mathrm{d}x/r_m\,, \qquad r_m=(mM)^{\frac{1}{2}}u_0/eB_0\,;$$

that is, we express lengths in terms of the *geometric mean* gyromagnetic radius r_m for ions and electrons at the mean speed and magnetic field prevailing at minus infinity.

To further facilitate the reduction to dimensionless form we introduce Alfvén's Mach number

$$(33) \qquad \alpha=u_0/v_A\,, \qquad v_A^2=B_0^2/\mu n_0(m+M)\,,$$

where c_A is Alfvén's phase velocity for the conditions of the plasma at minus infinity, and the parameter

$$\beta = 2p_0/(B_0^2/2\mu) , \tag{34}$$

which gives the ratio of the total ion and electron pressure to the magnetic pressure. Thus, the entire problem is expressed in terms of the two parameters α and β, which measure respectively the shock strength and the initial temperature of the plasma. For numerical purposes we combine the two parameters in the ratio

$$\nu^3 \equiv \beta/\alpha^2 = 4p_0/[n_0(m+M)u_0^2] , \tag{35}$$

where ν^3 is a convenient parameter which expresses the square of the ratio of the sound speed to the shock speed.

Making use of the dimension-free variables and parameters listed above, the system of four non-linear, first-order differential equations (22) through (25) now becomes

$$u(\mathrm{d}B/\mathrm{d}\xi) = \alpha^2 v , \tag{36}$$

$$u(\mathrm{d}/\mathrm{d}\xi)(u + \tfrac{1}{2}\nu^3 p) = -vB , \tag{37}$$

$$u(\mathrm{d}v/\mathrm{d}\xi) = uB - 1 , \tag{38}$$

$$\mathrm{d}(up)/\mathrm{d}\xi = -p(\mathrm{d}u/\mathrm{d}\xi) , \tag{39}$$

to which we must add the integrals (27), (28), and (29), corresponding respectively to the conservation laws of momentum, energy, and entropy, that now read

$$u - 1 + \tfrac{1}{2}\nu^3(p-1) + (B^2-1)/2\alpha^2 = 0 , \tag{40}$$

$$u^2 + v^2 - 1 + 2\nu^3(pu-1) + 2(B-1)/\alpha^2 = 0 , \tag{41}$$

$$pu^2 = \text{constant} = a^3 . \tag{42}$$

Finally, the longitudinal electric field, as deduced from (26), becomes in dimensionless form

$$E = \tfrac{1}{2}(M-m)(mM)^{-\frac{1}{2}}[u(\mathrm{d}u/\mathrm{d}\xi) - vB] = \tag{43}$$

$$= -(M-m)(mM)^{-\frac{1}{2}}vB(1 - \tfrac{1}{2}\nu^3 p/u)/(1 - \nu^3 p/u) ,$$

wherein the second form is obtained by eliminating the term $u(\mathrm{d}u/\mathrm{d}\xi)$ with the aid of eqs. (37) and (39). We observe that, in the special case of equal

masses ($M = m$), the condition of charge neutrality (17) becomes rigorous and the longitudinal electric field vanishes identically.

5. – Singular points of the differential equations.

The singularities of the system of differential equations (36) to (39) occur where [2]

$$uB = 1 \qquad \text{and} \qquad v = 0 \,. \tag{44}$$

According to (40), (41) and (42), there are three such singular points, one of which occurs for negative values of u and is therefore immediately discarded. The remaining two singularities are respectively a saddle point and a focal point.

The saddle point occurs when $v = 0$ and

$$u = 1 \,, \quad B = 1 \,, \quad a = 1 \,, \quad \text{and hence} \quad p = 1 \,, \tag{45}$$

which are in fact the boundary conditions prescribed as $\xi \to -\infty$. The nature of the singularity is readily ascertained by expanding the solution, in its vicinity, in the form

$$\begin{cases} B = 1 + B_1 \exp\,[\Lambda\xi] \\ u = 1 + u_1 \exp\,[\Lambda\xi] \\ p = 1 + p_1 \exp\,[\Lambda\xi] \\ v = v_1 \exp\,[\Lambda\xi] \,, \end{cases} \tag{46}$$

where Λ is the characteristic exponent and B_1, u_1, p_1, and v_1 are the coefficients of the first variation. As is well known, upon substituting the expansions (46) into the primitive set of differential equations (36) through (39), there results a homogeneous system of algebraic equations in the coefficients of the first variation whose determinant must vanish, giving rise, in this instance, to a quadratic secular equation in Λ^2 with roots

$$\Lambda^2 = 0 \qquad \text{and} \qquad \Lambda^2 = \alpha^2 - (1 - \nu^3)^{-1} \,. \tag{47}$$

The pair of zero roots corresponds merely to the trivial solution in which all derivatives vanish and the variables retain their values fixed by (45). The second pair leads to real roots, which is what we are after in accordance with

(46), provided the Alfvén Mach number α satisfies, for a given ν (or, alternatively, for a given β), the inequality

$$\alpha \geqslant \alpha_- , \qquad \alpha_-^2 = (1 - \nu^3)^{-1} = 1 + \beta , \tag{48}$$

which fixes the lower bound of α. This analysis establishes the saddle-point character of the singularity provided (48) is satisfied.

The focal point occurs where $v = 0$ and

$$u_f B_f = 1 , \qquad a = a_f , \qquad \text{and hence} \qquad p_f = a_f^3/u_f^2 , \tag{49}$$

where, in accordance with (40), (41), and (42), we must have

$$u_f = 1/B_f = \tfrac{1}{3}[1 + 2(1 + \beta)/\alpha^2] \leqslant 1 , \tag{50}$$

and

$$\tfrac{1}{2}(\nu a_f)^3 = [1 + \tfrac{1}{2}(1 + \beta)/\alpha^2]u_f^2 - u_f^3 - 1/2\alpha^2 ; \tag{51}$$

that is, the co-ordinates of the focal point correspond to the same momentum and energy as the saddle point, but exhibit a higher entropy ($a_f > 1$). In the words of a hydromagnetic analogue, this is the state that would be obtained behind the shock from the familiar Rankine-Hugoniot relations. Proceeding as before, we now expand the solution in the vicinity of the focal point by using expansions similar to (46), obtaining a corresponding quadratic in Λ^2 with roots

$$\Lambda^2 = 0 \qquad \text{and} \qquad \Lambda^2 = B_f[\alpha^2 - B_f^2/(u_f - \nu^3 p_f)] . \tag{52}$$

The pair of zero roots again corresponds to a trivial solution, and the second pair, it can be shown, leads for all permissible values of the parameters to pure imaginary roots. That is, in the infinitesimal neighborhood of the focal point (49), our system of equations admits periodic solutions, which thus establishes the character of the singularity. We return to these periodic solutions in the sequel to this paper, Part II.

It is evident that the complete numerical solution of the problem can be obtained from the integrals of the motion (40), (41), and (42). Thus, making use of (42) with $a = 1$, and assigning suitable values to u, as explained in Section 7, we can compute B from (40); then, making use of (41) we can compute the corresponding values of r. In this manner, with $a = 1$, we obtain the *solitary pulse* illustrated by plotting v *vs.* $(B - 1)$ as shown in the pseudo-

phase diagram of Fig. 2. Proceeding similarly for $1 < a < a_f$, one obtains the closed curves or *periodic solutions* (waves) shown in the diagram. Finally, putting $a = a_f$ merely yields the focal point, which may be regarded as the condensation point of periodic solutions as $a \to a_f$. In this paper, Part I, we discuss in detail the structure of the large amplitude solitary pulses for all permissible values of the parameters, and we reserve for the sequel to this paper, Part II, a thoroughgoing discussion of the structure of the periodic solutions or stationary waves, which is a somewhat more complicated matter. For example, we have discovered that the periodic solutions do not necessarily exist for all values of the Alfvén Mach number α for which the solitary pulses do exist.

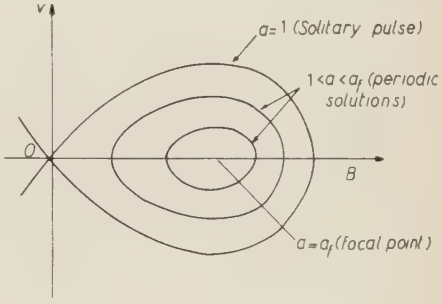

Fig. 2.

6. – Upper bound on Alfvén's Mach number.

As stated in eq. (48), the Alfvén Mach number α must exceed the lower bound α_- in order to obtain the solitary pulse solutions described above. We will now show that for a given ν (or, alternatively, for a given β), the value of α must not exceed the upper limit

$$\alpha_+^2 = 4/(1 + 3\nu - 4\nu^3) , \tag{53}$$

beyond which the solution of the system breaks down because of multiple-valued solutions in ξ; that is, beyond which solutions of the postulated type do not exist.

For the purpose, making use of (42) with $a = 1$, we rewrite (40) and (41) in the convenient forms

$$\eta(u; \nu) \equiv (B^2 - 1)/2\alpha^2 = 1 - u - \tfrac{1}{2}\nu^3(u^{-2} - 1) , \tag{54}$$

$$\zeta(u, v; \nu) \equiv 2(B - 1)/\alpha^2 = 1 - u^2 - 2\nu^3(u^{-1} - 1) - v^2 . \tag{55}$$

We note that (54) expresses η (or B) *qua* function of u, for a given ν ($0 \leqslant \nu \leqslant 1$), and that η (or B) attains a maximum when

$$u = \nu . \tag{56}$$

Thus, we argue that the significant range of values of u, for a given v, lie in the segment

$$v \leqslant u \leqslant 1 , \tag{57}$$

and that, to obtain a solitary pulse solution (see Fig. 2), it is necessary for (55), regarded as an equation for v^2, to have at least one root (other than $u = 1$, $B = 1$) in the range (57). It then becomes clear that the maximum value of α, $\alpha = \alpha_+$, must abide when $v^2 = 0$ and $u = v$ in (54) and (55) simultaneously; that is, when (55) has a double root for v^2 at $u = v$.

To determine this value of α we first compute from (54) and (55), putting $u = v$ and $v = 0$,

$$\eta(v; v) = (B_m^2 - 1)/2\alpha_+^2 = 1 - \tfrac{3}{2}v + \tfrac{1}{2}v^3 = \tfrac{1}{2}(1 - v)^2(2 + v) , \tag{58}$$

$$\zeta(v, 0; v) = 2(B_m - 1)/\alpha_+^2 = 1 - 3v^2 + 2v^3 = (1 - v)^2(1 + 2v) , \tag{59}$$

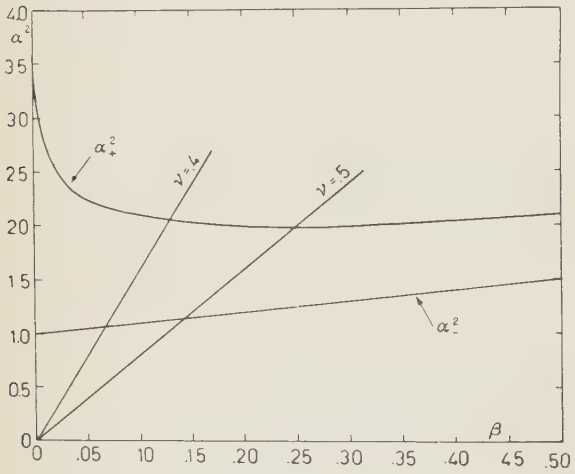

Fig. 3.

from which, by division, we readily compute the upper limit, for a given v, to the maximum value of B,

$$B_m = 3/(1 + 2v) . \tag{60}$$

Inserting this value of B_m in (59) we now solve for α^+ obtaining

$$4/\alpha_+^2 = (1 - v)(1 + 2v)^2 = 1 + 3v - 4v^3 , \tag{61}$$

which is equivalent to (53). Thus, we have shown that the solitary pulse solutions exist, for a given v (or, alternatively, for a given β) in the range

$$\alpha_- \leqslant \alpha \leqslant \alpha_+ , \tag{62}$$

where α_- is given by (48) and α_+ by (53). This allowed range is illustrated in Fig. 3 which exhibits α^2 *vs.* β, from $\beta = 0$ to $\beta = \frac{1}{2}$. In this diagram the locus of $v =$ constant is given by a set of half-lines emanating from the origin.

7. – Numerical results.

As already explained (Section 5), the complete solution of the problem can be obtained from the conservation integrals (40) and (41), or alternatively, from (54) and (55). That is, the procedure of assigning values to u and computing B and r, for $a = 1$, leads numerically to the pseudo-phase diagrams of Fig. 2. To exhibit the dependence of the several variables *qua* function of ξ (or x), we need to perform a quadrature. Because u is a convenient variable of (numerical) integration we return to (37), and making use of (39) to eliminate p with $a = 1$, we obtain

$$(u - v^3/u^2)(\mathrm{d}u/\mathrm{d}\xi) = -vB\,, \tag{63}$$

which we can at once integrate in the form

$$-\xi = \int_{u_-}^{u} [(u - v^3 u^{-2})/v(u)B(u)]\,\mathrm{d}u\,, \tag{64}$$

where $B(u)$ is determined from (54) and $r(u)$ from (55). Here the lower limit of integration u_-, which must lie in the range (57), corresponds to the maximum value of B (Fig. 2) which, according to (36), occurs when $r = 0$. This value of u_-, for a given v and a given α *within* the range (62), must be determined numerically as a root of (55), with $r = 0$. However, for $\alpha = \alpha_+$, we have simply as we have seen $u_- = v$. At the lower limit, then, we have $r(u_-) = 0$, which however, is an integrable singularity behaving as $(u - u_-)^{-\frac{1}{2}}$, except when $\alpha = \alpha_+$, $u_- = v$, in which case the integrand remains finite. At the upper limit, on the other hand, as $u \to 1$, we have $r \to 0$, but this time as $(1 - u)^{-1}$, giving rise to a logarithmic infinity in accordance with the exponential behavior (46). Since, for a given u, r assumes either positive or negative values (see Fig. 2), it is clear that, depending on the sign of r in (64) we obtain either branch of a symmetric pulse starting at $-\infty$ with the prescribed boundary values (45) and returning to these very same values as $\xi \to +\infty$.

Before describing our numerical results for specific values of α and β, it is well to observe that our chosen unit of length defined by (32) depends on the magnetic field and hence on the shock strength α. Therefore, to compare properly curves corresponding to different values of α, it is desirable to employ a unit of length first proposed by ADLAM and ALLEN [3], and independently by ROSENBLUTH [7], which is a property of the plasma, but independent of

[7] M. ROSENBLUTH: *Dynamics of a Pinched Gas*, in *Magnetohydrodynamics* (Palo Alto, 1957; edited by R. K. M. LANDSHOFF), p. 57.

the magnetic field. To this end, we define the normalized dimensionless element of length $d\xi_n$ defined as follows:

$$(65) \qquad dx = r_m d\xi = r_A d\xi_n , \qquad r_A = (mM)^{\frac{1}{2}} v_A / e B_0 = r_m / \alpha ,$$

whence we have $d\xi_n = (r_m/r_A)\, d\xi = \alpha\, d\xi$, with r_m as previously defined by (32).

We present results for three temperatures corresponding to $\beta = 0$, $\beta = 1/49$, and $\beta = 1/4$. For each temperature we display the profiles of the pertinent dimensionless variables B, u, v, and $[(mM)^{\frac{1}{2}}/(M-m)]E$ as functions of the normalized distance ξ_n, for the upper bound α_+ of Alfvén's Mach number, as computed from (61), and for the two higher temperatures we also present the corresponding profiles for an intermediate value of α in the range (62).

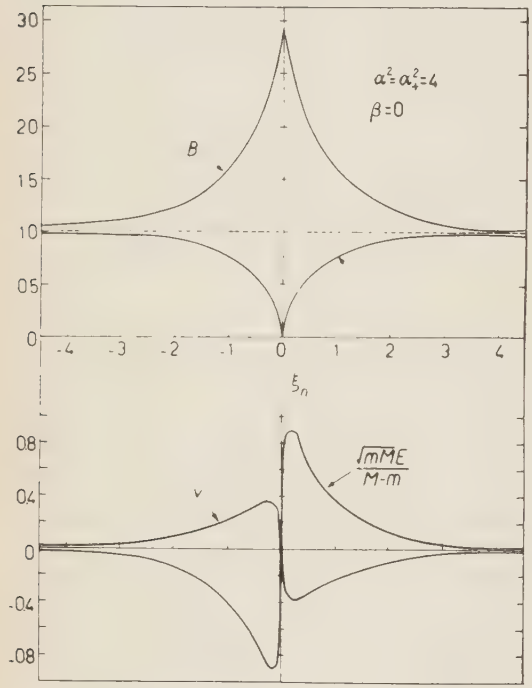

Fig. 4.

Fig. 4 exhibits the familiar results for the zero temperature case, with $\alpha = \alpha_+ = 2$, which ADLAM and ALLEN [3] had already published and which a number of other investigators had at various times obtained. We include these results here for comparison purposes and because our results include the zero temperature limit as a special case ($\nu = 0$). We note that, in Fig. 4, B attains a maximum $B_m = 3$, and u a minimum $u_- = 0$, but that in both cases the curves have a discontinuous derivative with cusps which exhibit vertical tangents. To show quite generally that, for $\alpha = \alpha_+$, the curve of u *vs.* ξ exhibits a cusp at $\xi = 0$, we simply compute the derivative $du/d\xi$ from (63) after putting $u = \nu(1+\delta)$, $\delta \ll 1$, and expanding in powers of δ. In this manner we obtain, with $\alpha = \alpha_+$, which implies $u_- = \nu$,

$$(66) \qquad (du/d\xi)_{\xi=0} = \mp \{(1-\nu)/\nu\}^{\frac{1}{2}}/(1+2\nu) \xrightarrow[\nu \to 0]{} \mp (\nu)^{-\frac{1}{2}} ,$$

the double sign arising from the sign of r (see Fig. 4) before taking the limit $\delta \to 0$. Thus, in the zero temperature case ($\nu = 0$), the curve of u *vs.* ξ exhibits

at $u = u_- = 0$ a cusp with vertical tangents. The fact that $u = 0$ for $\xi = 0$, when $v = 0$ means in accordance with (36) that the profile of B also exhibits a cusp in this case. These are the familiar results which we associate with the upper bound $\alpha_+ = 2$ at zero temperature, and which are interpreted by saying that an increase in α beyond α_+ would produce looping orbits whith the consequent breakdown of the present solutions.

Figs. 5 and 6 display, for $\alpha = \alpha_+$, the corresponding profiles of B, u, v, and E *vs.* ξ_n for the two higher temperatures chosen. This time, however, the curves of u *vs.* ξ exhibit cusps at $u = u_- = v > 0$ with *finite* tangents in accordance with (66). As a consequence because $u_- > 0$, the corresponding profiles of B *vs.* ξ are continuous with a continuous first derivative everywhere and in particular at $\xi = 0$. Increasing the value of α beyond α_+ again results in a breakdown of our mathematical solutions, but this time it is not sufficient to merely invoke as a physical reason the appearance of looping orbits, since the plasma has an initial temperature and a fraction of the orbits would be looping in any case. The breakdown of the solution appears to come from the fact that, for $\alpha > \alpha_+$, the horizontal velocity u would become multiple-valued in ξ, which of course has no physical meaning, indicating that in this case we would probably set up some turbulent regime leading to solutions *not* included in our one-dimensional stationary flows.

Another important feature which is evident in Figs. 5 and 6 is the fact that the longitudinal electric intensity E is *discontinuous* at $\xi = 0$, in contrast to the continuous curve of E *vs.* ξ in the zero temperature case (Fig. 4). To show how this discontinuity comes about we return to (43), which exhibits the longitudinal electric field in terms of the (discontinuous) derivative $du/d\xi$ of (66). Thus, putting, $u = v(1+\delta)$ wtih $\delta \ll 1$ we compute from (33) the values of E at $\xi = 0$ after letting $\delta \to 0$. In this manner we obtain, for the discontinuity in E,

$$\Delta E = E(0+) - E(0-) = (M-m)(mM)^{-\frac{1}{2}}[(1-v)v]^{\frac{1}{2}}/(1+2v)\,, \tag{67}$$

which vanishes for $v = 0$ as illustrated in Fig. 4. These results indicate, as discussed further in the next Section, that for $\alpha = \alpha_+$ the assumption of charge neutrality breaks down completely in the vicinity of the cusp.

Figs. 7 and 8 correspond to the same values of β as Figs. 5 and 6, respectively, but display the profiles belonging to intermediate values of α, $\alpha_- < \alpha < \alpha_+$. The essential feature to observe is that all the curves have continuous derivatives and that the cusps have disappeared. Thus, for any α *within* the specified range and for $a = 1$ in eq. (29), the solutions are solitary pulses with the characteristic symmetric behavior depicted in Figs. 7 and 8.

Finally, to exhibit the changes brought about by an increase in temperature while keeping $\alpha = \alpha_-$, which in turn depends on the temperature in

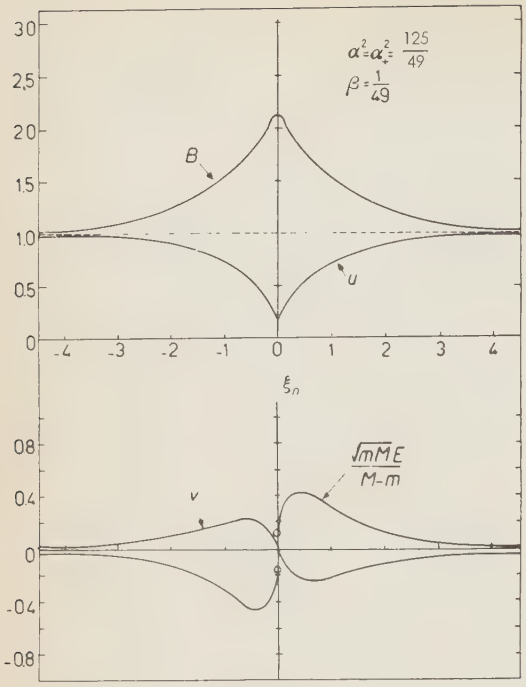

Fig. 5.

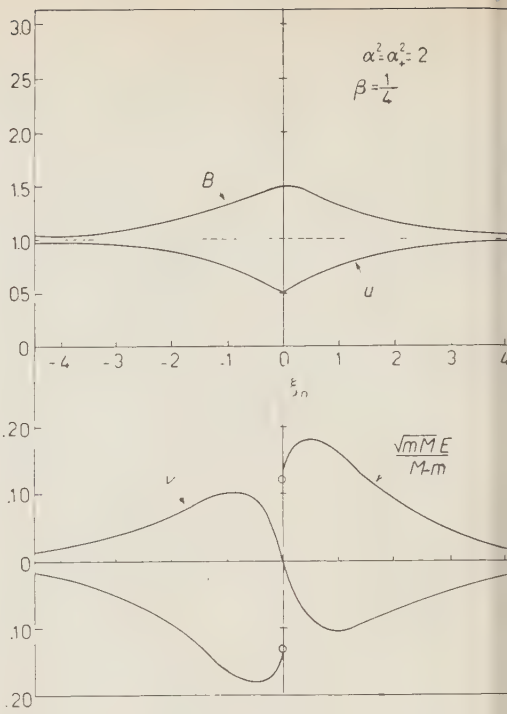

Fig. 6.

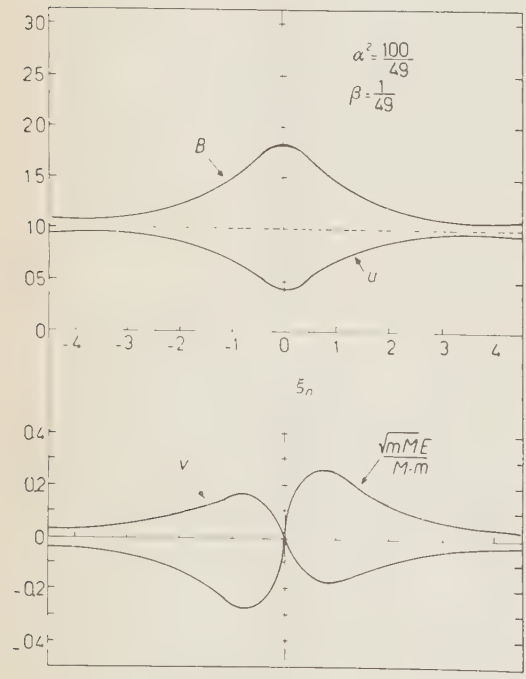

Fig. 7.

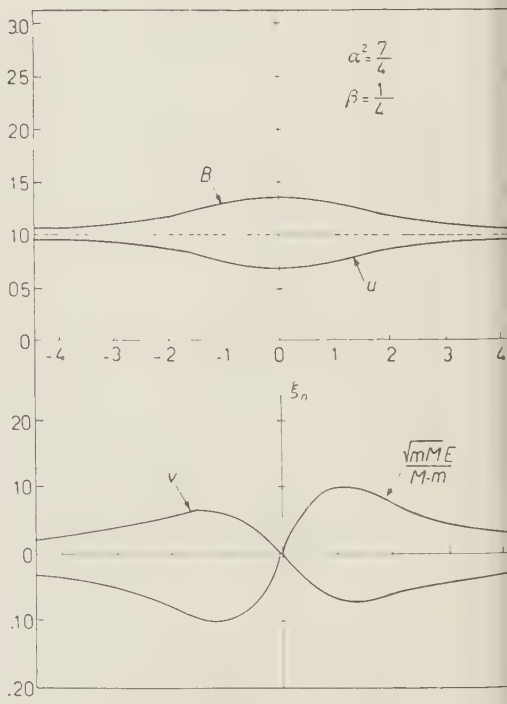

Fig. 8.

accordance with (53), we have plotted in Fig. 9 the behavior of B and u *vs.* ξ_n, for the three chosen values of β: $\beta = 0$, $\beta = 1/49$ and $\beta = 1/4$. Similarly, Fig. 10 shows the behavior of v and E for the same values of β. It is readily seen, in agreement with (67), that initially at least, the discontinuity of the electric

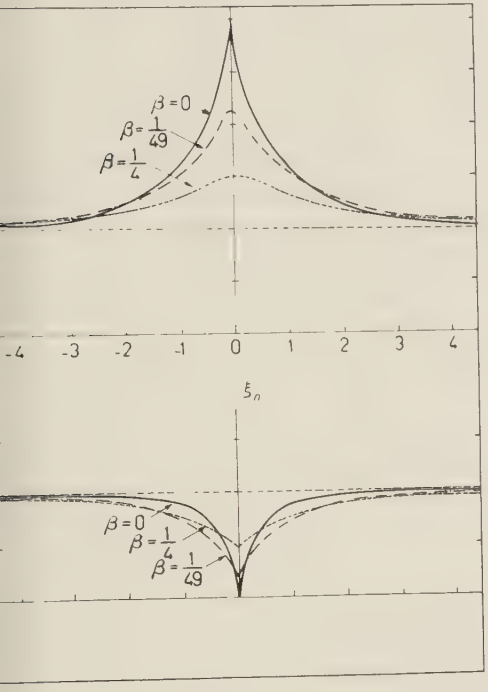

Fig. 9.

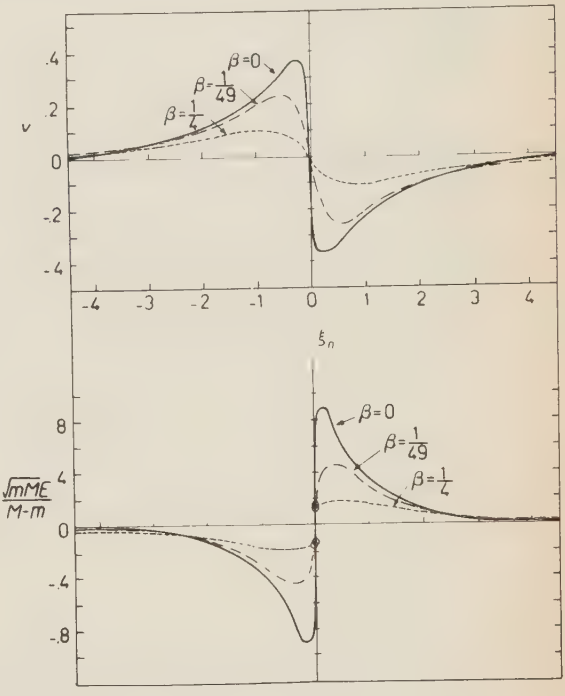

Fig. 10.

intensity at the cusp increases with the plasma temperature. This peculiar behavior suggests that we should re-examine our assumption of charge neutrality.

8. – Charge separation.

Returning to Poisson's equation (1) and expressing it in dimensionless form we obtain for the fractional charge separation, making use of (43),

$$(68) \qquad (N-n)/n_0 = (m+M)(mM)^{-\frac{1}{2}}(v_A/c)^2(\mathrm{d}E/\mathrm{d}\xi) = \\ = \tfrac{1}{2}[(M^2-m^2)/mM](v_A/c)^2(\mathrm{d}/\mathrm{d}\xi)[u(\mathrm{d}u/\mathrm{d}\xi) - vB]\,,$$

and it is clear that, as long as $\mathrm{d}u/\mathrm{d}\xi$ behaves properly, that is, as long as the derivative $\mathrm{d}u/\mathrm{d}\xi$ is continuous, the fractional charge separation is essentially

governed by the numerical factor

$$[(M^2 - m^2)/mM]\,(v_A/c)^2 \doteq (10^{19}/n_0)B_0^2 \qquad \text{in mks units}\,, \tag{69}$$

which, except for very low densities and extremely high magnetic fields, is considerably less then unity. Therefore, our fundamental inequality (16) is generally well satisfied provided we keep away from the singular behavior of E in the vicinity of the cusp for $\alpha = \alpha_+$.

On the other hand, our assumption of charge neutrality, as already pointed out, completely breaks down when $\alpha = \alpha_+$. In this case E is actually discontinuous at $\xi = 0$, see eq. (67), with the result that the fractional charge separation becomes infinite in the vicinity of the cusp. In fact, putting $\alpha = \alpha_+$ and $u = v(1+\delta)$, $\delta \ll 1$, and going to the limit as $\delta \to 0$, we obtain from (68), for the fractional charge separation at the cusp, the limit

$$(N - n_0)/n_0 \xrightarrow[\delta \to 0]{} [(M^2 - m^2)/mM](v_A/c)^2 \{(1-v)/(1+2v) \pm [(1-v)v]^{\frac{1}{2}}\}/3\delta v^2\,, \tag{70}$$

which becomes infinite as $1/\delta v^2$; that is, the more so as the initial plasma temperature is lowered ($v \to 0$).

9. – Discussion.

We have obtained solutions with the desired property that the characteristic length r_A can be much smaller than the mean free path. Furthermore, owing to the fact that the lower bound of u is v, which decreases toward zero as B_0 increases, there is no upper limit on the possible amplitudes of the density and pressure. The magnetic field, on the other hand, never exceeds three times its initial value B_0. The pulses connect two identical equilibrium states and therefore do not correspond to hydromagnetic shock waves. This is a consequence of the conservation of entropy (29) which, in turn, follows from the neglect of all possible dissipative mechanisms. In Part II we shall examine the consequences of relaxing this restriction, and obtain the conditions under which these waves can develop into stationary shocks connecting two unlike states.

Our present results constitute the simplest possible extension of the zero temperature work [3,4] to include thermal motions of the particles. We observe that, in general, our equations and results reduce to the zero temperature case if we simply set β or v equal to zero. The outstanding exception is the breakdown of the assumption of charge neutrality in the vicinity of α_+. The factor $(u^3 - \frac{1}{2}v^3)/(u^3 - v^3)$, appearing in (43) making use of (29), which governs

the behavior of $(N - n)$ near $u = v$, is simply unity if we set $v = 0$ from the start. We also observe that the approach to the limit $\beta - 0$ is rather steep so that the behavior even for fairly small β differs considerably from the idealized case $\beta = 0$.

Examination of the effect of charge separation appears to be a fruitful subject for further study. Our formulation may be regarded as the zero-order approximation from an expansion in powers of $(v_A/c)^2(M^2 - m^2)/Mm$. Higher-order terms can be obtained by inserting the charge separation (68) in our original equations. The breakdown of our charge neutrality assumption is not responsible, however, for the failure to find solutions for $\alpha > \alpha_+$. This failure is a result of the appearance of physically meaningless double-valued solutions which do not extend to $x \to +\infty$. Before returning to the question of charge separation, therefore, we shall discuss, in Part III, an extension of our equations to include the non-isotropic components of the pressure tensor, eliminating the question of charge separation by considering the case $M = m$.

In the zero temperature case, failure to find solutions for $\alpha > 2$ is explained by the appearance of « looping » orbits which will make all solutions dependent on the time. When $\beta > 0$ the picture is more complex, since a fraction of the orbits will always be looping. We simply say that time-independent solutions do not exist for B_0 so small that $\alpha > \alpha_+$, and this is not surprising because in the absence of a magnetic field such solutions do not exist at all. Waves will broaden continuously until finally collisions establish a steady state with characteristic length of the order of a mean free path. In a given plasma we find that waves of the type described in this paper can propagate with any arbitrary velocity greater than the sound speed, provided B_0 exceeds some limiting value. We have placed the burden of maintaining the steady state upon the magnetic field. It must be strong enough to accomplish the task.

* * *

Part of the work reported here was started while one of us (A.B.) enjoyed a sabbatical leave of absence in 1958 at the Istituto di Fisica Guglielmo Marconi dell'Università, Roma. We wish to express our thanks to Professors Enrico Persico and Edoardo Amaldi for their generous hospitality at the Istituto, and to the John Simon Guggenheim Memorial Foundation and the U.S. Fulbright Commission for fellowship grants which made possible the leisurely prosecution of these studies. In addition, we are indebted to Drs. Theodore C. Northrop and Marvin Mittleman, of the U.C. Lawrence Radiation Laboratory, and to Drs. Harold Grad and Cathleen Morawetz, of the N. Y. U. Institute of Mathematical Sciences, A.E.C. Computing and Applied Mathematics Center, for many illuminating discussions on the subject.

RIASSUNTO (*)

Consideriamo una estensione infinita di plasma a bassa densità, completamente ionizzato, magneticamente immobilizzato in un campo costante ed uniforme di induzione magnetica. In assenza di collisioni, supponiamo che i movimenti degli ioni e degli elettroni abbiano luogo in piani perpendicolari al campo magnetico. Poi passiamo ad un sistema di riferimento di « urto » che si muova a velocità costante in direzione normale al campo magnetico, e ricerchiamo la classe di soluzioni non banali, indipendenti dal tempo, ad una dimensione e autocongruenti delle equazioni di Maxwell e delle equazioni del moto delle particelle cariche, cioè, studiamo la propagazione degli impulsi trasversali e delle onde la cui lunghezza caratteristica sia molto minore del cammino libero medio. Facendo delle opportune semplificazioni, arriviamo ad un sistema di equazioni in cui si trascurano gli urti, si presuppone la neutralità della carica, e sia gli ioni che gli elettroni si comportano come fluidi bidimensionali che seguono le relazioni isoentropiche con $\gamma = 2$ e presentano tensori di pressione rigorosamente isotropici. Con queste semplificazioni e presupposti, il sistema di equazioni può essere risolto completamente con una semplice quadratura numerica. Si ottengono impulsi simmetrici e onde periodiche, con lunghezze caratteristiche dell'ordine della profondità dello strato superficiale del plasma, ossia del raggio giromagnetico medio per particelle che si muovono alla velocità di Alfvén. In questo articolo, parte I, descriviamo gli impulsi unici, che sono le sole soluzioni che soddisfino le condizioni del plasma non perturbato in posizione anteriore al treno d'onde. Per una completa determinazione del problema si richiedono due parametri fondamentali: il numero di Mach di Alfvén, che dà una misura della velocità di propagazione, ed il rapporto β fra la pressione totale del plasma e la pressione magnetica, che determina lo stato iniziale del plasma. Si dimostra che per un dato β esistono soluzioni stazionarie solo per un limitato campo di valori della velocità α.

(*) *Traduzione a cura della Redazione.*

IL NUOVO CIMENTO Vol. XV, N. 2 16 Gennaio 1960

The Analytic Properties of Perturbation Theory - I (*).

J. C. Polkinghorne

Trinity College - Cambridge

G. R. Screaton

Emmanuel College - Cambridge (**)

(ricevuto il 26 Ottobre 1959)

Summary. — A general method is given for locating the complex singularities of the contributions from Feynman diagrams regarded as functions of the external scalar products. The method is illustrated by application to the third-order vertex function.

1. – Introduction.

In recent years it has been noticed that many functions of physical interest possess powerful properties when regarded as functions of complex variables. As part of the programme for exploiting these properties investigations have been made of the analyticity of the terms of perturbation theory regarded as functions of energy, momentum transfer, etc. The earlier work on this subject [1-6] was largely concerned with the singularities occurring for real

(*) Supported in part by the U.S. Air Force, European Office, Research and Development Command.

(**) Now at: Tait Institute of Mathematical Physics, University of Edinburgh.

(1) Y. Nambu: *Nuovo Cimento*, **6**, 1064 (1957); K. Symanzik: *Prog. Theor. Phys.*, **20**, 690 (1958).

(2) R. Karplus, C. M. Sommerfield and E. H. Wichman: *Phys. Rev.*, **111**, 1187 (1958); **114**, 376 (1959).

(3) S. Mandelstam: *Phys. Rev.*, **115**, 1741, 1752 (1959).

(4) J. G. Taylor: to be published.

(5) J. C. Taylor: to be published.

(6) L. D. Landau: *Proceedings of the International Conference on High Energy Nuclear Physics, Kiev* (1959).

values of the arguments. However, since the motivation for much of this work is an interest in Mandelstam's conjecture [7] on the analytic properties of the scattering amplitude, it is also essential to determine the positions of the complex singularities. The very informative example of the third-order vertex function has been completely discussed by OEHME [8] using the explicit expressions obtained by KÄLLÉN and WIGHTMAN [9], but no general method has so far been given for investigating these complex singularities.

It is our purpose in this paper to develop such a method (*). It is based on an approach used by EDEN [10] for a discussion of the analytic properties of perturbation theory, but the method is applied in our case not to the integrations over internal momenta but to the integrations over Feynman parameters that remain when symmetric integration has removed these internal momenta. The final form of the answer is the same as that given by LANDAU [6] for the real singularities. Indeed he seems to state that this form should determine the complex singularities also, but no discussion is given.

2. – Functions defined by perturbation theory.

The contribution from an arbitrary graph in perturbation theory is of the form

$$\lim_{\varepsilon \to 0+} \int_0^1 \mathrm{d}\alpha_1 \dots \mathrm{d}\alpha_n \int \mathrm{d}^4 k_1 \dots \mathrm{d}^4 k_m \frac{\delta(\alpha_1 + \dots + \alpha_n - 1)}{[F(\alpha_i;\, k_j;\, p_k) + i\varepsilon]^n}\,, \tag{1}$$

where

$$F(\alpha_i;\, k_j;\, p_k) = \sum_{i=1}^{n} \alpha_i (q_i^2 - m_i^2)\,. \tag{2}$$

The variables $\alpha_1 \dots \alpha_n$ are the Feynman parameters used to write the contributions from the n lines of the graph in the form of a single denominator. Each line is associated with momentum q_i and mass m_i. The variables k_j

(*) While this work was being written up we were shown a preprint by Mr. J. TARSKI in which essentially the same method as that given here is used to discuss the special case of contributions from graphs with only one internal loop. Mr. TARSKI does not, however, discuss the peculiar complications that arise from the multiple integrations over Feynman parameters (see Section **4**).

(7) S. MANDELSTAM: *Phys. Rev.*, **112**, 1344 (1958).

(8) R. OEHME: *Nuovo Cimento*, **13**, 778 (1959).

(9) G. KÄLLÉN and A. S. WIGHTMAN: *Mat. Fys. Skr. Dan. Vid. Selsk.*, **1**, no. 6 (1958).

(10) R. J. EDEN: *Proc. Roy. Soc.*, A **210**, 388 (1952).

are some set of independent internal momenta associated with the graph. They may be conveniently chosen by selecting a set of independent closed loops specifying the structure of the graph. The variables p_k are the external momenta. The case of all Bose particles is discussed for the sake of simplicity: no new difficulties arise from the introduction of Fermi particles.

It is assumed that some procedure of regularization has made the integral (1) convergent for the k-integrations. These are now performed by the technique of symmetric integration giving a function of the external scalar products $p_{jk} = p_j \cdot p_k$, of the form

$$f(p_{jk}) \equiv \lim_{\varepsilon \to 0^+} \int_0^1 \mathrm{d}\alpha_1 \dots \mathrm{d}\alpha_n \frac{\varphi(\alpha_i)\,\delta(\alpha_1 + \dots + \alpha_n - 1)}{[F'(\alpha_i;\, p_{jk}) + i\varepsilon]^{n-2m}} . \tag{3}$$

Numerical multiplicative factors have been omitted. The function F' is obtained from the function F by eliminating the k_j by use of the equations summarized in vector form by

$$\frac{\partial F}{\partial k_j} = 0 , \qquad j = 1, \dots, m. \tag{4}$$

The fact that F' is obtained from F by taking its stationary values with respect to the integration variables has been particularly emphasized by MATHEWS [11]. The function $\varphi(\alpha_i)$ is a simple algebraic function of the α's which is relevant for our considerations only if it vanishes at some critical value of the α's.

The presence of the $i\varepsilon$ term in (1) permits the use of symmetric integration. It tells us that for real values of p_{jk} the physically important function is that obtained by letting the masses associated with the internal lines tend to the real axis from the lower half plane. Since the method we discuss below is easily extended to discuss analytic continuation in these internal masses we shall omit the $i\varepsilon$ term and consider the function of the complex variables z_{jk} defined by

$$f(z_{jk}) \equiv \int_0^1 \mathrm{d}\alpha_1 \dots \mathrm{d}\alpha_n \frac{\varphi(\alpha_i)\,\delta(\alpha_1 + \dots + \alpha_n - 1)}{[F'(\alpha_i;\, z_{jk})]^{n-2m}} . \tag{5}$$

In order to discuss the singularities of this function it is convenient to establish a lemma suggested by the work of EDEN [10].

---

[11] J. MATHEWS: *Phys. Rev.*, **113**, 381 (1959).

3. – Lemma.

Consider a function $f(\zeta)$ defined by

$$f(\zeta) = \int_C F(u, \zeta)\, \mathrm{d}u \,. \tag{6}$$

ζ may stand for several complex variables. Then $f(\zeta)$ is certainly a regular function of ζ in the domain Z such that for all $\zeta \in Z$, $F(u, \zeta)$ is a regular function for all u lying on the contour C. We wish to show that $f(\zeta)$ can be continued along a path from Z to any point ζ'' lying outside Z provided this path does not pass through certain exceptional points ζ^*, defined below.

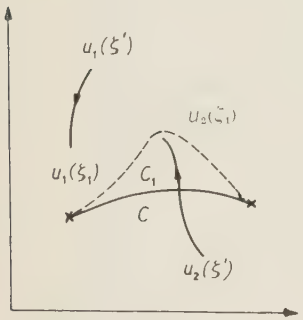

Fig. 1. – Paths of singularities in the u-plane.

The functions $F(u, \zeta)$ with which we shall be concerned are all such that in general as ζ varies along a path from some point $\zeta' \in Z$ to the point ζ'' then the singularities of $F(u, \zeta)$ describe paths in the u-plane in a continuous fashion. No singularity crosses C until we leave Z. When we have reached some point ζ_1 outside Z the singularities, $u_i(\zeta)$, may have described some such paths in the u-plane as are depicted in Fig. 1. The contour C_1 is such that the function

$$f_1(\zeta) = \int_{C_1} F(u, \zeta)\, \mathrm{d}u \,, \tag{7}$$

is regular at $\zeta = \zeta_1$. Successive points along the path define successive contours in this way with the property that the contours define functions regular at the point in question and coinciding in some neighbourhood with the functions associated with neighbouring points along the path. The contours are obtained by continuous deformation of the original contour C away from the direction of the advancing singularities. The associated functions provide a continuation of $f(\zeta)$ to the point ζ''.

The method may, however, fail for one of three reasons:

i) A singularity may pass through one of the end points of C in which case no useful deformation can avoid it. We shall call this case an end-point singularity.

ii) Two singularities *coming from opposite sides of the contour* may coincide for the same ζ, say ζ^*, as in Fig. 2. The contour is then « pinched » and no further useful deformation is possible. We shall refer to this as a case of coincident singularities, though it is important to notice that only singularities tending to coincidence from *opposite* sides of the contour give rise to exceptional points. The situation illustrated by Fig. 3 is quite harmless.

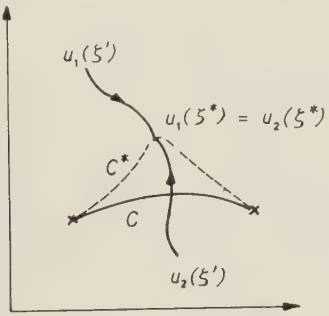

Fig. 2. – Coincident singularities.

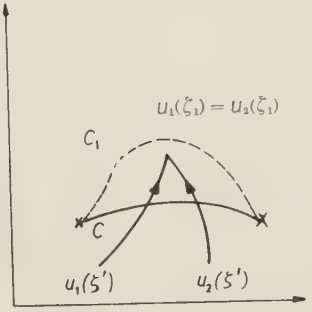

Fig. 3. – Harmless coincident singularities.

iii) For some values of ζ one or more singularities may recede to infinity. This is best discussed by employing a transformation that brings the point at infinity into the complex plane. In general our integrands are well-behaved at infinity and only obviously coincident singularities give rise to exceptional points. These singularities are not, therefore, separately classified in what follows. (A particularly striking case of this behaviour occurs when for some ζ, $F(u, \zeta)$ becomes independent of u. All singularities have receded to infinity unless $F(u, \zeta)$ is itself singular at this point when in fact they cover the whole plane).

The exceptional points ζ^* are defined as the class of points that give rise to singularities in $f(\zeta)$ in one of these three ways.

The value of the function at the point ζ'' that we obtain by this method of continuation will depend upon the path of continuation chosen. That is to say, the function $f(\zeta)$ is in general multi-valued. It is clear from the freedom that exists in the choice of successive contours C_1 that if two paths in the ζ-space are chosen so related that one can be obtained from the other by a continuous deformation that never passes through an exceptional point ζ^*, then they will give the same value.

Finally, in our discussion so far we have assumed that the limits of our contour C are independent of ζ. In the cases to which we wish to apply the lemma this is not so. One end point is fixed but the other depends on ζ. However, its dependence is in terms of an analytic function (indeed a linear function) and so the conclusions of the lemma are not disturbed.

4. – Application to multiple integrals.

We now wish to apply the ideas of the last section to the multiple integral defined by equation (5). The δ-function must first be eliminated and so we consider the integral

$$f(z_{jk}) = \int_0^1 \mathrm{d}\alpha_1 \int_0^{1-\alpha_1} \mathrm{d}\alpha_2 \ldots \int_0^{1-\alpha_1-\ldots-\alpha_{n-2}} \mathrm{d}\alpha_{n-1} \frac{1}{[F''(\alpha_i, z_{jk})]^{n-2m}} . \tag{8}$$

F'' is obtained from F' by eliminating the variable α_n by the substitution $\alpha_n = 1 - \alpha_1 - \ldots - \alpha_{n-1}$. Although the integral (8) selects a particular ordering of the α's we shall find that our final answer can be cast into a form symmetric in the n α's.

It is tempting to suppose that f will be singular only if each integration in (8) has either an end point singularity or a coincident singularity. This in fact turns out to be the case but the argument leading to it is somewhat involved. For any particular integration in (8) the yet-unintegrated α's combine with the z_{jk} to form the ζ of the lemma. Moreover, after the α_{n-1} integration has been performed the successive integrands are in general multi-valued.

The method that must be used to deal with this problem is sufficiently illustrated by the case of two integrations. Consider the function defined by

$$\varphi(\zeta) = \int_B \mathrm{d}\beta \int_A \mathrm{d}\alpha \frac{1}{[F(\alpha, \beta; \zeta)]^n} , \tag{9}$$

A and B are the appropriate contours of integration for α and β, and $F(\alpha, \beta; \zeta)$ is assumed to be regular in the finite plane. The singularities of the integrand are therefore just the zeroes of F. Once again ζ may signify a number of complex variables.

A domain Z is assumed to exist such that for $\zeta \in Z$, $F(\alpha, \beta, \zeta) \neq 0$ for $\alpha \in A$, $\beta \in B$. The points outside Z may be singular points of $\varphi(\zeta)$ or they may be points lying on the specific cuts defined by the integral representation (9) since this representation clearly defines a one-valued function. The purpose of this investigation is to separate these two cases.

This will be done by defining a continuation of our function by deforming the contours A and B. In the α-plane we shall have to avoid the points $\alpha'(\beta, \zeta)$ which are such that $F(\alpha', \beta, \zeta) = 0$. By the lemma of Section 3 this can always be done to define a (multivalued) function regular at all β and ζ except the exceptional points $(\beta'(\zeta), \zeta)$ which are such that

either: i) $F(\alpha_0, \beta'(\zeta); \zeta) = 0$, where α_0 is an end point of A (end point singularities);

or ii) $F = \partial F/\partial\alpha = 0$, some α, and the two coincident singularities that this implies approach each other from *opposite* sides of the α-contour (coincident singularities).

It will therefore be necessary to deform β to avoid the points $\beta'(\zeta)$ as ζ varies along its assigned path.

Until ζ leaves Z no deformation of A and B is required and so in particular no $\beta'(\zeta)$ lies on B. Thereafter the contour B is deformed in a continuous way to avoid the points $\beta'(\zeta)$, in the manner of Section 3. This continuous deformation defines (in a way that is inessentially non-unique) a path linking each point on the original contour B with its corresponding point on the deformed contour B_1. In this way the original path in the ζ-plane defines a series of paths in the combined β-ζ space. These paths select the branch of the multi-valued function obtained by performing the α-integration. This function is analytic in β and ζ for every point on the contour B_1. Moreover the continuity properties of our functions and of the paths defined above ensure that the function associated with a particular β and ζ coincides in some neighbourhood with the functions associated with neighbouring β and ζ (*). Thus the contour B_1 is so arranged that the β-integrand is regular along it and so the β-integration yields an analytic function of ζ, which depends, of course, on the path of continuation in the ζ-plane. The method fails, however, if B_1 can not be deformed to avoid the points $\beta'(\zeta)$. This will happen if one of these points coincides with β_0, an end point of B, or if two points β' tend to coincidence from opposite sides of B_1. This only happens for certain values of ζ and these points are the singularities of φ. Thus we may say that the singularities of φ occur at the points ζ^* which are such that

either: i) $F(\alpha_0, \beta_0; \zeta^*) = 0$ (an end point singularity in α giving an end point singularity in β);

or ii) $F(\alpha, \beta_0; \zeta^*) = (\partial F/\partial\alpha)(\alpha, \beta_0; \zeta^*) = 0$, and the coincident singularities in α « pinch » the contour (a coincident singularity in α giving an end point singularity in β);

or iii) $F(\alpha_0, \beta; \zeta^*) = (\partial F/\partial\beta)(\alpha_0, \beta; \zeta^*) = 0$, and the coincident singularities in β « pinch » the contour (an end point singularity in α giving a coincident singularity in β);

(*) Singularities receding to infinity require a special discussion here which is best made by transforming the point at infinity into a point of the finite plane.

or iv) $F(\alpha, \beta; \zeta^*) = (\partial F/\partial\alpha)(\alpha, \beta; \zeta^*) = (\partial F/\partial\beta)(\alpha, \beta; \zeta^*) = 0$, and the coincident singularities in both α and β « pinch » their respective contours (coincident singularity in α giving a coincident singularity in β).

We note that the specification i) to iv) produces a scheme independent of the relative α, β order of integration, although that order played a part in our definition of the continuation. The final answer is what one expected: there must be an end point singularity or coincident singularity in each integration.

5. – The singularities of perturbation theory.

The ideas of the previous section can now be applied to the perturbation theory integral, equation (7). Each integration must either give rise to an end point singularity or a coincident singularity. Thus we must have

$$F''(\alpha_i; z_{jk}) = 0 \,, \tag{10}$$

together with

either: i) $\alpha_i = 0$ (lower limit end point) or
$\alpha_n = 0$ (upper limit end point);

or ii) $\partial F''/\partial\alpha_i = 0$ and the resulting coincident singularities in the α_i integration « pinch » the contour;

for $i = 1, ..., n-1$.

These conditions may now be written in a more symmetrical form. By the use of the condition

$$\alpha_1 + ... + \alpha_n = 1 \,. \tag{11}$$

$F''(\alpha_i; z_{jk})$ in (10) may be equivalently replaced by the function $F'(\alpha_i; z_{jk})$ which is homogeneous of degree one in the α's. Then the derivatives of F'' are just the derivatives of F' subject to the condition (11) and may be written

$$\frac{\partial F''}{\partial \alpha_i} = \frac{\partial F'}{\partial \alpha_i} + \lambda \,, \qquad i = 1, ..., n-1, \tag{12}$$

where λ is a Lagrange multiplier. However, Leibnitz theorem for homogeneous functions implies that

$$F'(\alpha_i; z_{jk}) = \sum_{i=1}^{n} \alpha_i \frac{\partial F'}{\partial \alpha_i} \tag{13}$$

and so the vanishing of F'' (or equivalently F') implies that under the conditions (10) $\lambda = 0$ and these conditions may be rewritten as

$$(14) \qquad \begin{cases} \textit{either} & \alpha_i = 0 , \\ \textit{or} & \dfrac{\partial F'}{\partial \alpha_i} \approx 0 , \end{cases} \qquad i = 1, \ldots, n;$$

where the symbol $\approx$ is used to denote the fact that two singularities must not only coincide but « pinch » the contour.

When account is taken of the derivation of F' from F by equations (4) and (11), the conditions (14) are seen to be just the generalization of the condition given by LANDAU (6) for the real singularities and derived by him in a different manner. From equations (2) and (4) it follows that

$$(15) \qquad \frac{\partial F'}{\partial \alpha_i} = (q_i^2 - m_i^2) + \sum_{j=1}^{m} \frac{\partial F}{\partial k_j} \frac{\partial k_j}{\partial \alpha_i} = (q_i^2 - m_i^2) ,$$

and so the conditions (14) can be interpreted that *either* a line is omitted from a diagram *or* its momentum vector is put on the mass shell. This leads to the dual diagram analysis of J. C. TAYLOR (5) and LANDAU (6) for the real singularities.

The exclusion by the condition of « pinching » in (14) of harmless coincidences of the type illustrated by Fig. 3 means that not all the points satisfying the weaker conditions:

$$(16) \qquad \begin{cases} \textit{either} & \alpha_i = 0 , \\ \textit{or} & \dfrac{\partial F}{\partial \alpha_i} = 0 , \end{cases} \qquad i = 1, \ldots, n;$$

are singular points of f on the physical sheet defined by the integral representation (8). However, when the function is continued into all its sheets then the equations (16) give the possible singular points. This is because this continuation may be achieved by considering the totality of contours joining the given end points and thus every coincident singularity « pinches » some contour. An example of how singularities can appear and disappear on given sheets is provided by the third-order vertex function discussed below. Since we are concerned in physics with particular sheets it is necessary to supplement the simple equations (16) by an analysis of whether the coincident singularities « pinch » the contour (*). This is simple in principle, but tedious in practice, for any given diagram.

(*) A most interesting illustration of this has been given by Mr. TARSKI in his discussion of the fourth-order scattering diagram.

We may note that the consequences of (16) find a particularly simple expression in the case when the diagram under discussion has only one closed loop. $F'(\alpha_i; z_{jk})$ is then a polynomial of second degree in the α_i and linear in the z_{jk} divided by a linear term in the α_i. The linear term is actually the sum of the α_i and so is just equal to one. The important term is the second degree polynomial which may be written in matrix form as

$$\sum_{i,j=1}^{n} A_{ij}(z)\alpha_i \alpha_j \,. \tag{17}$$

The condition that this form together with all its first α-derivatives vanishes for some values of the α's is that its discriminant vanishes:

$$\det [A_{ij}(z)] = 0 \,. \tag{18}$$

The other singularities, corresponding to the vanishing of one or more α's, are then given by the vanishing of the principal minors of $\det [A_{ij}]$ obtained by omitting the appropriate rows and columns. J. C. Taylor [12] has already conjectured that the location of singularities might be given by these determinantal conditions in simple cases.

6. – The third-order vertex function.

We conclude by applying our method to the third-order vertex function, or rather to the differentiated third-order vertex function which has been particularly discussed by Oehme [8]. To avoid irrelevant algebraic complication we will assume the equality of all the masses of the internal particles. In the notation of reference [8] we are concerned then with the function

$$f(Z, Z_3) = \int_0^1 \frac{\mathrm{d}\alpha\, \mathrm{d}\beta\, \mathrm{d}\gamma\, \delta(1-\alpha-\beta-\gamma)}{(m^2 - (\alpha+\beta)\gamma Z - \alpha\beta Z_3)^2} \,. \tag{19}$$

This is an example of a function associated with a single loop diagram and the conditions described by equation (18) *et. seq.* may be used to find the possible singularities. The vanishing of the determinant gives

$$Z_3[m^2 Z_3 + Z(Z - 4m^2)] = 0 \,, \tag{20}$$

[12] J. C. Taylor: private communication.

and the principal minors give

$$Z\,(Z-4m^2)=0\,, \tag{21}$$

$$Z_3(Z_3-4m^2)=0\,. \tag{22}$$

KÄLLÉN and WIGHTMAN have integrated (19) explicitly (9) obtaining

$$f(Z,Z_3)=\frac{1}{m^2Z_3+Z(Z-4m^2)}\cdot \tag{23}$$
$$\cdot\left[\frac{2Z^{\frac{1}{2}}}{(Z-4m^2)^{\frac{1}{2}}}\log\frac{1}{2m^2}\left(2m^2-Z+[Z(Z-4m^2)]^{\frac{1}{2}}\right)-\right.$$
$$\left.-\frac{Z_3-2Z}{Z_3^{\frac{1}{2}}(Z_3-4m^2)^{\frac{1}{2}}}\log\frac{1}{2m^2}\left(2m^2-Z_3+[Z_3(Z_3-4m^2)]^{\frac{1}{2}}\right)\right|.$$

Clearly the singularities of (23) lie on the curves (20)–(22).

It is also important to know when they occur on the physical sheet. The physically important function is that branch obtained by letting Z and Z_3 tend to the positive real axis from above. While Z and Z_3 both have the non-vanishing imaginary parts of the same sign the integrand in (19) cannot vanish in the region of α and β integration (*). No contour deformation is required therefore until the real axis is actually reached. The physical function will have singularities at real Z and Z_3 only if on reaching the real Z and Z_3 axes from above end-point or coincident singularities appear on the relevant parts of the α and β real axes.

For example the doubly coincident singularities associated with (20) are found to occur at

$$\alpha=\beta=\frac{m^2}{Z}\,. \tag{24}$$

Since we integrate only over real positive values of α and β such that $\alpha+\beta<1$, if Z is real and

$$Z<2m^2\,, \tag{25}$$

this singularity will not occur for the physical function. If, however, Z is real and

$$Z\geqslant 2m^2 \tag{26}$$

(*) We assume now the γ-integration done to remove the δ-function.

the corresponding values of α and β lie on the contours and a trivial calculation shows that they do indeed « pinch » them. Thus we are able to understand the sudden appearance on the physical sheet of the anomalous threshold discovered by KARPLUS, SOMMERFIELD and WICHMAN [2].

RIASSUNTO (*)

Si espone un metodo generale per la localizzazione delle singolarità complesse dei contributi dei diagrammi di Feynman considerati come funzioni dei prodotti scalari esterni. Il metodo viene illustrato con l'applicazione alla funzione vertice del terzo ordine.

(*) *Traduzione a cura della Redazione.*

LETTERE ALLA REDAZIONE

(La responsabilità scientifica degli scritti inseriti in questa rubrica è completamente lasciata dalla Direzione del periodico ai singoli autori)

The Effect of Multiple Scattering in the Photoproduction of Charged Mesons at Deuterium.

N. MacDonald

Department of Natural Philosophy. The University - Glasgow (*).

(ricevuto il 14 Dicembre 1959)

This note reports briefly on a calculation of the multiple scattering correction to the impulse approximation treatment of the photoproduction of charged pions at deuterium. One of the original aims of this work was to shed light on the process of photoproduction of negative pions at free neutrons. It is now apparent that a more fruitful approach to this problem would be along the lines of recent work by Chew and Low [1] on unstable particles as targets in scattering experiments, and such work has been reported by Anderson *et al.* [2]. However there is still some interest in the multiple scattering approach because of its relation to the problem of π-D scattering, recently treated by Bransden and Moorhouse [3], Rockmore [4] and de Alfaro and Stroffolini [5]. Also recent experimental work by Land [6] shows that the impulse approximation gives a reasonable description of the process in circumstances for which our work predicts that the multiple scattering correction is very small.

The impulse approximation has been used for this process by various authors [7] and experimental results have been analysed using their work [6,8]. In this approximation [9] the transition operator for the process is taken as the sum of transi-

(*) Present address: Atomic Weapons Research Establishment, Aldermaston, England.

(1) G. F. Chew and F. E. Low: *Phys. Rev.*, **113**, 1640 (1959).

(2) J. D. Anderson, D. C. Gates, T. L. Jenkins, R. W. Kenny and W. P. Swanson: *Bull. Am. Phys. Soc.*, **4**, 356 (1959).

(3) B. H. Bransden and R. G. Moorhouse: *Nucl. Phys.*, **6**, 310 (1958).

(4) R. M. Rockmore: *Phys. Rev.*, **105**, 256 (1957).

(5) V. de Alfaro and R. Stroffolini: *Nuovo Cimento*, **11**, 447 (1959).

(6) R. H. Land: *Phys. Rev.*, **113**, 1141 (1959).

(7) S. Machida and T. Tamura: *Progr. Theor. Phys.*, **6**, 572 (1951); Y. Saito, Y. Watanabe and Y. Yamaguchi: *Progr. Theor. Phys.*, **7**, 103 (1952); G. F. Chew and H. W. Lewis: *Phys. Rev.*, **84**, 779 (1952); M. Lax and H. Feshbach: *Phys. Rev.*, **88**, 509 (1952).

(8) R. S. White, M. J. Jacobsohn and A. G. Schultz: *Phys. Rev.*, **88**, 836 (1952); D. C. Hageman, K. M. Crowe and R. M. Friedman: *Phys. Rev.*, **106**, 818 (1957).

(9) G. F. Chew and G. C. Wick: *Phys. Rev.*, **85**, 636 (1952); G. F. Chew and M. L. Goldberger: *Phys. Rev.*, **87**, 778 (1952).

tion operators T_1 and T_2 for photoproduction at nucleons 1 and 2. The effect of of nuclear binding is ignored, except in so far as it determines the wave function for the initial and final states. The interaction of the meson and the two nucleons is also ignored. [We use the term impulse approximation to refer to the treatment which ignores both these factors, although strictly it is the failure to include the effect of binding that makes it an impulse approximation.] We continue to neglect the effect of binding and deal with the meson-nucleon interaction by allowing for successive scattering at alternate nucleons. This has been done previously for elastic production of neutral pions at deuterium by CHAPPELEAR ([10]) and at helium by STOODLEY ([11]).

We use the same, method, essentially, as CHAPPELEAR. Writing the matrix element, between states of one nucleon and one meson, of the transition operator t_i for the interaction of a meson with nucleon i as

$$(1) \qquad (\boldsymbol{q}_2|t_i|\boldsymbol{q}_1) = a_i b(q_1, q_2)\boldsymbol{q}_1\cdot\boldsymbol{q}_2 \exp\left[i(\boldsymbol{q}_2-\boldsymbol{q}_1)\cdot\boldsymbol{r}_i\right],$$

this method involves the approximation that

$$(2) \qquad \int_{-\infty}^{\infty} \frac{\mathrm{d}q\, q \exp\left[iqR\right] b(q_2, q) b(q, q_1)}{\omega(q_E) - \omega(q) + i\varepsilon} = 2\pi i \omega(q_E) b(q_1, q_E) b(q_E, q_1) \exp\left[iq_E R\right].$$

In the above a_i is a function of isotopic spin, (the effect of ordinary spin is ignored).

$\boldsymbol{q}_1, \boldsymbol{q}_2$ are the initial and final meson momenta;

$\boldsymbol{r}_i$ is the position of nucleon i;

$R = |\boldsymbol{r}_1 - \boldsymbol{r}_2|$;

$\omega(q)$ is the meson energy for momentum $\boldsymbol{q}$, and

q_E is the meson momentum on the energy shell.

If we take b in the form $b(q_1, q_2) = c(q_1)d(q_2)$ we can evaluate the correction without using the approximation (2). The form of b used, which is taken from work of VELIBEKOV and MESHCHERYAKOV ([12]), resembles that used in ref. ([5]) for the π - D problem. In this case we find that the approximation (2) is fairly good.

The use of the approximation (2) enables one to use $(\boldsymbol{q}_2|t_i|\boldsymbol{q}_1)$ in the form $a_i b(q_E, q_E)\boldsymbol{q}_1\cdot\boldsymbol{q}_2 \exp\left[i(\boldsymbol{q}_1 - \boldsymbol{q}_2)\cdot\boldsymbol{r}_i\right]$ alone, without requiring knowledge of b off the energy shell (*). We take $b(q_E, q_E)$ as

$$(3) \qquad -\frac{2\pi}{\omega(q_E)q_E^3} \exp\left[i\delta_{33}(q_E)\right] \sin\delta_{33}(q_E).$$

([10]) J. CHAPPELEAR: *Phys. Rev.*, **99**, 254 (1955).

([11]) K. D. C. STOODLEY: unpublished thesis (1957).

([12]) V. R. VELIBEKOV and V. A. MESHCHERYAKOV: *Dokl. Akad. Nauk SSSR*, **105**, 941 (1955).

(*) The approximation does not however correspond to taking scattering on the energy shell only, as has sometimes been stated. DRELL and VERLET ([13]) distinguish between these approximations.

([13]) S. D. DRELL and L. VERLET: *Phys. Rev.*, **99**, 849 (1955).

with empirical values of the $(\frac{3}{2}, \frac{3}{2})$ phase shift. For the operator T_i we take the electric dipole and dominant magnetic dipole (again corresponding to $(\frac{3}{2}, \frac{3}{2})$ state of meson and nucleon) operators of CHEW and LOW [14].

Results were obtained for 300 MeV γ s. The impulse approximation energy spectrum of mesons at a given angle is made up of two peaks. One is about the energy of the meson produced at this angle from a free nucleon, and dominates the energy spectrum except at small forward angles. On this peak the multiple scattering correction is about -5%. The second peak occurs near maximum meson energy, and is a consequence of the interaction of the residual nucleons when they have low relative momentum. We in fact include the nucleon interaction in the S-state only, and find that on this peak the correction rises to -20%. Now this situation is the nearest in our process to elastic production, so the larger correction is consistent with the fact that Chappelear found a -40% effect in elastic π^0 production.

In general comparison with experiment is hampered by the fact that most experiments have been done not with a monoenergetic γ beam but with a bremsstrahlung spectrum. However recent work by LAND [6] uses a beam with energy (292 ± 8) MeV. He detects mesons at 120°, which means he is dealing with the free nucleon peak, and in agreement with our result he finds that the impulse approximation is adequate.

In the case of π - D Scattering, DRELL and VERLET [13] estimate that double scattering provides the major part of the multiple scattering correction. This is in agreement with ROCKMORE's results [4] but not with those of DE ALFARO and STROFFOLINI [5]. The corresponding process in our case is photoproduction followed by one scattering. In our formalism we cannot estimate the contribution from this process separately. However the contributions from photoproduction followed by an odd or an even (non-zero)number of scatterings appear separately, and are of comparable magnitude. The former would be expected to predominate if the most important process were photoproduction with one scattering.

This work was carried out while the author held a maintenance grant from the Department of Scientific and Industrial Research. It forms part of a thesis submitted to the University of Glasgow. The problem was suggested by Prof. J. C. GUNN, who is thanked for his advice and encouragement. Helpful discussions of the multiple scattering formalism with Dr. K. D. C. STOODLEY are also acknowledged.

---

[14] G. F. CHEW and F. E. LOW: *Phys. Rev.*, **101**, 1579 (1956).

IL NUOVO CIMENTO Vol. XV, N. 2 16 Gennaio 1960

Cross Sections of Reactions Produced by High Energy Neutrino Beams.

N. Cabibbo and R. Gatto

Istituto di Fisica e Scuola di Perfezionamento dell'Università - Roma
Istituto Nazionale di Fisica Nucleare - Sezione di Roma

(ricevuto il 28 Dicembre 1959)

1. – The expected availability in the next future of high intensity beams of high energy particles makes it appealing to think of possible experiments to detect reactions initiated by high energy neutrinos (1). Neutrinos are known to have only weak interactions and their cross sections at low energy are indeed very small (2). Neutrino cross-sections are however suspected to grow-up very fast with energy (3).

One would argue that, in a reaction such as $\bar{\nu}+p \to e^+ + n$ the phase space volume will eventually grow-up with the square of the C.M. energy, while the matrix element derived naively from the four-linear β coupling will remain constant, thus giving a cross-section increasing with the square of the C.M. energy. This argument is obviously wrong at least because of the presence of form factors and of new couplings induced through the virtual fields of particles which interact strongly with the nucleons, such as pions, etc.

In listing the possible reactions which can be produced from high energy neutrinos one has to note that many reactions are forbidden by the lepton conservation law. Their absence would actually constitute the most direct proof of lepton con-

(1) We have learned that various physicists, namely Prof. Amaldi, Prof. Bernardini, Prof. Cocconi, Prof. Lederman, Prof. Lee, Prof. Preiswerk and perhaps many others are thinking at present on the possibility of such experiments.

(2) C. L. Cowan, F. Reines, F. B. Harrison, H. W. Kruse and A. D. Mc Guire (*Nature*, **178**, 446 (1956)) gave a cross-section $6 \cdot 10^{-44}$ for he reaction $\bar{\nu}+p \to n+e^+$.

The experiment was possible because of the high intensity of neutrinos from a thermal neutron reactor.

(3) There have already been theoretical discussions on the importance of weak interactions at high energies [see, for instance, D. I. Blokhinstev: *On the Limits of applicability of Quantum Electrodynamics*, F. 148, Joint Institute for Nuclear Research, (1958)].

servation (4). The allowed reactions are

$$\bar{\nu}+p\to e^+ + n \qquad \nu+n\to e^- + p$$

$$\bar{\nu}+p\to e^+ + n + \pi^0 \qquad \bar{\nu}+n\to e^+ + n + \pi^-$$

$$\to e^+ + p + \pi^- \qquad$$

$$\nu+p\to e^- + p + \pi^+ \qquad \nu+n\to e^- + n + \pi^+$$

$$\to e^- + p + \pi^0$$

$$\bar{\nu}+p\to e^+ + \Lambda^0$$

$$\bar{\nu}+p\to e^+ + \Sigma^0 \qquad \bar{\nu}+n\to e^+ + \Sigma^-$$

$$[\nu+n\to e^- + \Sigma^+],$$

and so on.

In all the above reactions the electron can be substituted by a muon of the same charge. We have enclosed in brackets the last reaction $\nu+n\to e^-+\Sigma^+$, because it is one of those reactions which would be forbidden if some of the present ideas on the interactions of strange particles are right (5). Such a reaction is forbidden if one excludes a weak strangeness-non-conserving current with a strangeness change opposite in sign to the sign of charge. Such a forbiddeness is directly related to the suggested forbiddeness of $\Sigma^+\to n+e^++\nu$. Most of the listed reactions can only occur incoherently on a nucleus; only reactions in which the same kind of nucleon appears in both sides of the equation (such as $\nu+p\to e^-+p+\pi^+$, etc.) can also proceed coherently.

2. – To be definite let us consider the first of the listed reactions

$$\bar{\nu}+p\to e^+ + n\,. \tag{1}$$

We shall first derive the expression for its cross section in terms of the nuclear form factors. In the next section we shall try a definite estimate of the cross-section by adopting the non-renormalization hypothesis for the vector strangeness conserving current and making use of extrapolated Stanford data on the nucleon form factors, together with some guess on the relevant axial form factor. The general expression (7), (8) that we derive is rigorous in the V—A theory (6) under one important assumption: that the behaviour of the strangeness-conserving vector and axial currents under the product operation of charge conjugation and charge symmetry is the same as that of the nucleon terms, $\bar{\psi}\gamma_\mu\tau_+\psi$ and $\bar{\psi}\gamma_\mu\gamma_5\tau_+\psi$ respec-

(4) The absence of the reaction $\bar{\nu}+{}^{37}\mathrm{Cl}\to{}^{37}\mathrm{A}+e^-$ has been discussed by R. Davis: *Bull. Am. Phys. Soc.*, **1**, 219 (1956); and by C. O. Muehlhause and S. Oleska: *Phys. Rev.*, **105**, 1333 (1957). Evidence against double β decay is discussed for instance by C. L. Cowan and F. Reines: *Phys. Rev.*, **106**, 825 (1957). The study of neutrino reactions will also offer a conclusive test of the hypothesis that the neutrino emitted with the electron is the same as that emitted with the muon.

(5) A detailed discussion can be found in R. Gatto: *Fortschr. d. Phys.*, **7**, 147 (1959).

(6) R. P. Feynmann and M. Gell-Mann: *Phys. Rev.*, **109**, 193 (1958); R. E. Marshak and E. C. G. Sudarshan: *Phys. Rev.*, **109**, 1860 (1958).

tively. Such an assumption is certainly verified for the vector current under the non-renormalization hypothesis. If it werenot verified the expression for the cross-section would become more complicated and involve two more form factors. Of course, concerning the numerical estimates that we give, we could say very little at present on how much they would be changed without the non-renormalization hypothesis for the vector current or for the case of more complicated behaviour of the currents under charge symmetry. Considering the ambiguities on the form factors any such discussion would be only academic at present. The matrix element for (1) is given by

$$\sqrt{2}G\,\frac{i}{(2\pi)^2}\,\delta(\nu+p-e-n)(j\cdot l)\,, \tag{2}$$

where

$$j_\mu=(2\pi)^3\langle n\,|\,j_\mu^{(V)}(0)+j_\mu^{(A)}(0)\,|\,p\rangle\,, \tag{3}$$

and

$$l_\mu=\left(v(\bar{\nu})\,\gamma_\mu\tfrac{1}{2}(1+\gamma_5)v(e^+)\right)\,. \tag{4}$$

In (3) $j_\mu^{(V)}(x)$ and $j_\mu^{(A)}(x)$ are the strangeness-conserving vector and axial currents respectively. In (3) G is the vector coupling constant for β-decay, as defined in [6], $G\cong 1\cdot 10^{-5}\,M^{-2}$, M being the nucleon mass, and ν, n, p, e are the four-momenta. Under the above explained assumption about the behaviour of such currents under the charge symmetry operation, j_μ takes the form [7].

$$j_\mu=\bar{u}(n)\,[H_1(k^2)\gamma_\mu\gamma_5+iH_2(k^2)k_\mu\gamma_5+F_1(k^2)\gamma_\mu+\frac{\mu}{2M}\,F_2(k^2)\sigma_{\mu\nu}k_\nu]\,u(p)\,, \tag{5}$$

where H_1, H_2, F_1 and F_2 are form factors depending on k^2, with $k_\mu=(p-n)_\mu$, μ is a numerical constant, and $u(n)$, $u(p)$ are free particle spinors. The definition of the form factors in (5) is such that

$$F_1(0)=F_2(0)=1\,,\qquad H_1(0)=\frac{G_A}{G}\,. \tag{6}$$

where G_A is the axial β-decay coupling constant. The term proportional to H_2 does not contribute if the electron mass can be neglected. From (2), (4) and (5) one derives the following expression for the differential cross-section for reaction (1) in the laboratory frame

$$\sigma(\theta)\,\mathrm{d}(\cos\theta)=\frac{G^2}{\pi}\,\mathscr{E}^2\Sigma(\theta,\mathscr{E})\,\mathrm{d}(\cos\theta)\,, \tag{7}$$

[7] M. GOLDBERGER and S. B. TREIMAN: *Phys. Rev.*, **110**, 1478 (1958).

with

$$(8)\quad \Sigma(\theta,\mathscr{E}) = \left(1+\frac{2\mathscr{E}}{M}\sin^2\frac{\theta}{2}\right)^{-3}\left\{\cos^2\frac{\theta}{2}\left\{F_1^2(k^2)+\right.\right.$$

$$\left.+\frac{k^2}{4M^2}\left[2\left(F_1(k^2)+\mu F_2(k^2)\right)^2\operatorname{tg}^2\frac{\theta}{2}-\mu^2F_2^2(k^2)\right]\right\}+$$

$$+H_1^2(k^2)\left[1+\sin^2\frac{\theta}{2}+2\frac{\mathscr{E}^2}{M^2}\frac{\sin^4(\theta/2)}{1+2(\mathscr{E}/M)\sin^2\theta/2}\right]-$$

$$\left.-H_1(k^2)\left[F_1(k^2)+\mu F_2(k^2)\right]\frac{4\sin^2(\theta/2)}{1+2(\mathscr{E}/M)\sin^2(\theta/2)}\left(M\mathscr{E}+\mathscr{E}^2\sin^2\frac{\theta}{2}\right)\right\}.$$

In (7) and (8) $\mathscr{E}$ is the neutrino energy in the laboratory system, θ is the scattering angle in the laboratory system, and M is the nucleon mass. For the process $\nu+n\to e^-+p$ the cross section has the same form except for a change of sign of the interference term (the last term inside the bracket in (8)).

One verifies easily that with constant form factors the total cross-section increases linearly with the laboratory energy $\mathscr{E}$, when $\mathscr{E}\gg M$, *i.e.* it is proportional to the square of the C.M. energy.

If, on the other hand, the form factors are essentially equivalent to a cut-off for $k^2=a^2$ the total cross-section at high energies increases as

$$(9)\quad \sigma_{\text{total}}\propto(\text{C.M. energy})^2\,\Delta\omega\,,$$

where $\Delta\omega$ is the « allowed » solid angle, defined by $k^2\leqslant a^2$, which gives

$$\Delta\omega\propto(\text{C.M. energy})^{-2}\,.$$

The cross-section will then tend to a constant value rather than increase indefinitely. Of course, any definite statement about the high energy behaviour of the cross-section is impossible, as it is bound to a knowledge of the form factors for high momentum transfer. A study of μ-capture reactions can give information on the form factors for $k^2\simeq(100\text{ MeV})^2$. If one uses the non-renormalization hypothesis the form factors F_1 and F_2 can be taken from electron scattering experiments.

3. – To make an estimate of the cross-section and of its behaviour with energy we have used the non-renormalization hypothesis for the vector strangeness-conserving current. In this case $\mu=\mu_p-\mu_n=3.7$, and $F_1(k^2)$ and $F_2(k^2)$ can be taken from the analysis of electron and muon scattering on nucleons — it can be easily seen that they are given as differences of proton and neutron form factors. The Stanford results suggest

$$(10)\quad F_1(k^2)\simeq F_2(k^2)\simeq\frac{1}{(1+k^2/a^2)^2}\,.$$

In the absence of any information on $H_1(k^2)$ we make the simplest choice

$$(11)\quad H_1(k^2)=\frac{G_A}{G}\frac{1}{(1+k^2/a^2)^2}\,.$$

The total cross-section from (8), (9), (10) and (11) can then be derived analytically and it takes the form

$$(12)\qquad \sigma_{\text{total}} = \frac{G^2 a^2}{6\pi}\left\{A^{(0)}(\alpha)\left[\frac{G_A^2}{G^2}+1\right] + A^{(1)}(\alpha)\frac{a^2}{M^2}\left[\frac{\mu^2}{8} - \frac{M}{4\mathscr{E}}\left(1+\frac{G_A^2}{G^2}\right) + \right.\right.$$

$$+ \frac{M^2}{8\mathscr{E}^2}\left(\frac{G_A^2}{G^2}-1\right)\Big] + A^{(2)}(\alpha)\frac{a^4}{M^2}\left[\frac{1}{16\mathscr{E}^2}\left(\mu^2+2(1+\mu)+2\frac{G_A^2}{G^2}\right) - \frac{M}{8\mathscr{E}^3}\mu^2\right] \mp$$

$$\left.\mp \frac{a^2}{2M\mathscr{E}}\frac{G_A}{G}(1+\mu)\left[A^{(1)}(\alpha) - \frac{a^2}{2M\mathscr{E}}A^{(2)}(\alpha)\right]\right\}.$$

In (12)

$$A^{(0)}(\alpha) = 1-(1+\alpha)^{-3},$$

$$A^{(1)}(\alpha) = 1+2(1+\alpha)^{-3}-3(1+\alpha)^{-2},$$

$$A^{(2)}(\alpha) = 1-(1+\alpha)^{-3}+3(1+\alpha)^{-2}-3(1+\alpha)^{-1},$$

with

$$\alpha = \frac{4E_c^2}{a^2},$$

where E_c is the C.M. neutrino energy.

In the low-energy limit the expression for σ_{total} vanishes proportionally to $\mathscr{E}^2$, and it tends to a constant limit for high energies. In (12) the upper sign holds for reaction (1), the lower sign for $\nu+n\to e^-+p$. A graph of σ_{total} as given by (12)

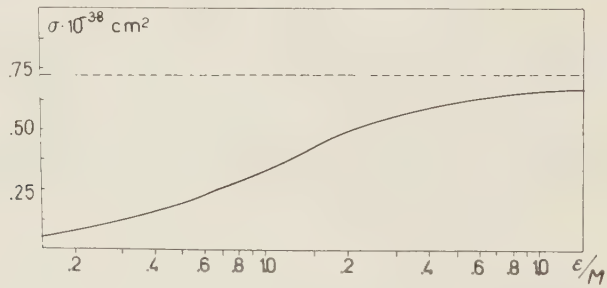

Fig. 1. – Total cross-section for $\bar{\nu}+p\to e^++n$ versus neutrino energy in the laboratory as computed from equation (12).

is reported in Fig. 1 calculated with $\mu=3.7$; $(G_A/G)^2=1.4$ and $a^2=37.5m_\pi^2$. If the three form factors are still taken of the form (10) and (11) but with different a^2 (a_1^2, a_2^2, and b^2 for H_1) the high energy limit of the cross-section is

$$(13)\qquad \sigma_{\text{total}} = \frac{1}{6\pi}G^2\left(a_1^2+\frac{\mu^2}{8}\frac{a_2^4}{M^2}\right)+\frac{1}{6\pi}G_A^2 b^2.$$

Such a limit is practically reached already for energies k slightly greater than the largest of the a's.

The high energy cross-section will thus depend very sensitively upon such parameters. One sees from Fig. 1 that the total cross-section for $\bar{\nu}+p \to e^+ + n$ predicted from our simple model is $\simeq 10^{-38}$ cm^2 for incident neutrinos of laboratory energy greater than 1 GeV. The cross section for the process $\nu + n \to e^- + p$ comes out also to be of the same magnitude at high energies because of the vanishing in that limit of the interference term.

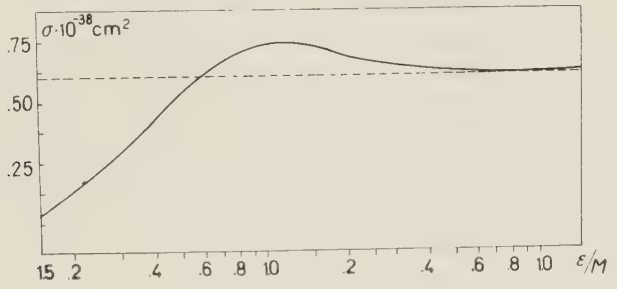

Fig. 2. – Total cross-section for $\nu + n \to e^- + p$ versus neutrino energy in the laboratory as computed from equation (12).

To obtain the total interaction cross-section one should add to such figures the value of the cross-section for the analogous processes producing muons in place of the electrons. Furthermore, one should also add the cross-sections for reactions producing pions and strange particles. We do not know any reliable method to evaluate the cross-sections for the processes

$$\nu + \mathcal{N} \to \mathcal{N} + e + m\pi \,, \tag{14}$$

leading to m final pions. When some data on multiple pion production in electron-nucleon collisions will be available at comparable energies one will be able to make some rough guess on such cross-sections, at least if the non-renormalization hypothesis holds. Statistical estimates as to the most probable number of pions that can be produced in a reaction like (14) are perhaps misleading here because of the presence of the weak leptonic vertex. If, in absence of anything better, one wants to adopt statistical models to get an idea on the most probable number of mesons that are produced in (14), then one finds at 10 GeV laboratory neutrino energy a value $\simeq 5$ for such a number, which increases to a value $\simeq 8$ at 20 GeV. We have used an interaction radius of the order of the pion wavelength and also taken approximately into account the indistinguishability for the final pions. Considering the different final channels that are available one may hope that the total interaction cross-section may turn out to be much larger than the cross-section that we have estimated here for $\nu + \mathcal{N} \to e + \mathcal{N}$. Coming back to the question of the high energy behaviour of the cross-sections we should perhaps stress the fact that we are not making any statement — neither rigorous nor approximate — as to the true high energy limit. The energies we are considering are only those practically available nowadays. The possible presence of a structure [8] for the weak interactions — for

[8] T. D. Lee and C. N. Yang: *Phys. Rev.*, **108**, 1611 (1957); S. Bludman and A. Klein: *Phys. Rev.*, **109**, 550 (1958); N. Cabibbo and R. Gatto: *Phys. Rev.*, **116**, n. 4 (1959).

instance if they were mediated by a heavy meson — would also influence the discussion of the high energy limit.

To conclude our discussion we may also remark that other interesting reactions are

$$\bar{\nu} + e^- \to \bar{\nu} + e^- , \tag{15}$$

$$\to \bar{\nu} + \mu^- , \tag{16}$$

and similar reactions with ν. One would expect that form factors, as arising for instance from virtual gammas, do not play an important role in the energy range we are considering. If so the cross-sections will increase with the square of the C.M. energy. However because of the very low mass of the target in reactions like (15) and (16), the C.M. energy is still too small to give a measurable cross-section even at $(20 \div 30)$ GeV. The cross section for (15), for example, is given, already for energies of the order of a few MeV by [6]

$$\sigma \simeq 8 \cdot 10^{-42} \mathscr{E} \text{ cm}^2 , \qquad (\mathscr{E} \text{ in GeV}),$$

and is still $= 10^{-40}$ cm^2 at 10 GeV.

LIBRI RICEVUTI E RECENSIONI

Handbuch der Physik, Band XVII *Dielektrika*, con 198 figure, 406 pagine in 8°. Edizioni Springer, 1956.

Il volume consta di tre lunghi ed aggiornati articoli. Nel primo, scritto con ammirevole chiarezza da W. Fuller Brown jr., l'autore dopo avere definiti i principali problemi della teoria dei dielettrici e richiamato i concetti di elettrostatica, di meccanica quantistica e di meccanica statistica di cui intende servirsi, affronta lo studio del comportamento dei dielettrici reali. Si occupa dapprima del comportamento dei dielettrici in campi costanti o lentamente variabili e la trattazione procede dai sistemi più semplici (gas rarefatti) a quelli via via più complessi (gas densi, fasi condensate e soluzioni). Indi discute il comportamento dei dielettrici alle frequenze ottiche, anche qui cominciando dall'esame del comportamento dei gas rarefatti per passare in seguito al caso più difficile dei gas densi e delle fasi condensate. Tratta infine il comportamento dei dielettrici a frequenze intermedie con particolare riferimento ai processi di rilassamento ed ai meccanismi suscettibili di rivelare le proprietà molecolari. La discussione di quest'ultimo aspetto del problema viene ripresa e sviluppata nell'ultimo capitolo dell'articolo. Nel penultimo capitolo dell'articolo sono esposti i metodi sperimentali di misura, con brevi ma sostanziose ed aggiornate descrizioni dei circuiti e delle tecniche.

Nel secondo articolo, opera del Prof. Walter Franz, l'autore si occupa del meccanismo delle scariche nei dielettrici solidi e liquidi e dei processi di ionizzazione interna per urti elettronici. Espone dapprima la situazione nel campo degli studi sulla scarica « calda », portante a zone fuse o gasificate nel dielettrico, ed indi passa ad occuparsi più a lungo della « scarica elettrica pura » in termini della statistica degli elettroni nei materiali isolanti.

Nel terzo articolo l'autore Peter Forsbergh jr. tratta della piezoelettricità, dell'elettrostrizione e della ferroelettricità ed antiferroelettricità. Ad una introduzione di carattere generale sui fenomeni in oggetto, corredata da una serie di bellissime fotografie di domini ferroelettrici e delle relative frontiere, fa seguito la trattazione dettagliata della piezoelettricità, della ferroelettricità e dell'antiferroelettricità. La trattazione è completata da un gran numero di figure e di grafici. Il penultimo capitolo tratta della termodinamica dei cristalli elettromeccanici, ed alla fine di esso viene delineata una teoria fenomenologica capace di porre in relazione tutte le « osservabili » macroscopiche, elettriche meccaniche e termiche, che sono le derivate parziali dei potenziali termodinamici. L'ultimo capitolo abbozza, per quanto è a tutt'oggi possibile, una teoria microscopica statistica della ferroelettricità.

Leggendo l'opera abbiamo avuto l'impressione che il primo articolo sia senz'altro al livello dei migliori fra gli altri

articoli comparsi nei volumi dell'*Handbuch* a tutt'oggi pubblicati. Il secondo articolo invece ci lascia con la sensazione che si sarebbe potuto chiarire meglio la portata del problema ed i suoi rapporti coi problemi della fisica dello stato solido. Buono il terzo articolo anche se, a nostro avviso non vi è sufficientemente sviluppata la parte teorica.

F. Gaeta

Numerische Mathematik. Springer-Verlag, Berlin-Göttingen-Heidelberg.

Si tratta di una nuova rivista pubblicata dall'Editore Springer, con la collaborazione di un Comitato di redazione costituito su base internazionale. Essa è destinata a raccogliere lavori originali nel campo dell'analisi numerica e dei metodi di programmazione per le moderne macchine calcolatrici.

Durante il 1959 sono apparsi i 5 fascicoli che costituiscono il 1° volume di 320 pagine e contenente 24 lavori; si tratta di lavori molto interessanti dovuti ai migliori specialisti della materia. Per la pubblicazione di lavori nella rivista occorre rivolgersi ad uno dei membri del sopraddetto Comitato di redazione; riteniamo perciò opportuno segnalare che il membro italiano è il Prof. A. Ghizzetti dell'Università di Roma.

A. Ghizzetti

W. Pauli – *Teoria della Relatività*, traduzione italiana di *Relativitätstheorie*, a cura di Paolo Gulmanelli. Editore Paolo Boringhieri, Torino, 1958, pag. xvi-327.

La prima edizione del libro fu stampata nel 1921 con lo scopo di dare una rassegna sui lavori della teoria della relatività fino allora pubblicati.

In occasione del cinquantenario della teoria della relatività (1955) era proposito di Pauli come egli stesso dice nella prefazione all'ultima edizione, aggiornare il libro in modo da estendere il carattere di rassegna fino alla nuova data. Tuttavia Egli rinunciò all'idea per la gran mole di lavoro che l'aggiornamento avrebbe comportato e anche perchè reputava quasi superfluo, accanto ai numerosi trattati sulla Relatività comparsi attorno a quell'anno, averne un altro costruito mediante la completa trasformazione di un libro che già aveva un carattere di « documento storico ».

Sicchè Pauli in definitiva preferì lasciare il vecchio testo nella primitiva forma con alcune aggiunte e note che contengono gli sviluppi più importanti avuti dopo il 1921 e alcune considerazioni sulle teorie unitarie di campi che, più che altro, esprimono il parere, invero molto scettico, di Pauli sulle possibilità di successo di siffatte teorie.

Il libro si articola su otto capitoli alternando e compenetrando fatti sperimentali e formalismi in modo da avere una sintesi molto equilibrata che riesce utilissima sia per lo sperimentale che per il teorico. In esso si ha un panorama molto vasto che va dalla relatività ristretta a quella generale, mettendo l'accento oltre che sugli aspetti più comunemente noti di queste teorie (meccanica, elettromagnetismo, ottica, campo gravitazionale e teorie unitarie di Einstein, Mie e Weyl) anche su altri aspetti altrettanto importanti, ma generalmente non posti nella giusta luce in altri trattati sulla relatività; mi riferisco particolarmente ai capitoli dedicati agli sviluppi della relatività ristretta concernenti la termodinamica e la statistica e alle teorie delle particelle elementari cariche.

Sono da segnalare, per il rigore e la chiarezza, alcuni argomenti formali riguardanti le trasformazioni infinitesimali e i teoremi variazionali. Inoltre si possono considerare di viva attualità le considerazioni sui limiti del concetto

classico di campo che si trovano nel capitolo sulle particelle elementari.

Ora che l'Autore è scomparso non si può fare a meno di riportare il giudizio lodevolissimo dato da EINSTEIN nella recensione di questo libro: « Chi legga quest'opera densa e dalla solida struttura non può certamente sospettare che l'autore è un giovane di ventun anni. Non si sa che cosa ammirare di più: se la capacità di cogliere le connessioni fra le idee, la sicurezza della deduzione matematica, il profondo intuito fisico, la chiarezza e la sistematicità dell'esposizione, la conoscenza della letteratura sull'argomento, la completezza della trattazione o la sicurezza del senso critico ... Questo libro andrebbe consultato da chiunque faccia lavoro di ricerca nel campo della relatività e da chiunque desideri un sicuro orientamento su questioni di principio ».

Ottima la traduzione e la veste tipografica.

R. LIOTTA

E. PERSICO – *Gli atomi e la loro energia*. Zanichelli, Bologna, 1959. Lire 5500, pag. 490.

Questo libro del Prof. PERSICO viene in aiuto a quanti desiderano avvicinarsi alla fisica nucleare di oggi, avendo a disposizione pochi elementi (o ricordi) di fisica generale e qualche elemento di calcolo infinitesimale. Perciò finalmente abbiamo il libro che consiglieremo agli ingegneri ed ai chimici che per necessità professionali o per loro diletto ci chiedono spesso un libro del genere. Invece esso non ci sembra molto adatto per gli studenti, per il carattere un poco enciclopedico e di ottimistica facilità con cui gli argomenti vengono necessariamente presentati.

Il libro è diviso in due parti: la prima dedicata all'atomistica e la seconda alla fisica nucleare. La prima parte ci sembra qualche volta non completamente omogenea come livello degli argomenti trattati (ad es. la natura del calore e la struttura dei liquidi sono trattati ad un livello liceale, mentre gli spettri atomici sono portati quasi al livello universitario). La seconda parte è invece più omogenea, chiarissima, e veramente preziosa per l'attualità degli argomenti e la quantità delle informazioni. Infine un'appendice sulle fondamentali esperienze di Fisica Nucleare e soprattutto sulle apparecchiature più usate e più citate, aggiunge a questo libro il carattere di vademecum del non-specialista in Fisica Nucleare.

G. CARERI

Ecole d'été de physique theorique, Les Houches, 1958. *The many-body problem*. Ed. Dunod, Paris, pagine 675, 6900 franchi.

In questo grosso volume sono raccolte le lezioni tenute a Les Houches sulla Fisica Teorica dei sistemi di particelle, argomento di grande attualità che accomuna campi diversi, come la struttura del nucleo, il problema dell'elio liquido e molti aspetti della Fisica dei solidi. Si tratta di una quindicina di corsi, tutti tenuti da specialisti che hanno recentemente contribuito in questi stessi argomenti; e tutti i corsi sono tenuti ad un livello piuttosto elevato. Anzi più che una serie di lezioni si può anche parlare di una serie di seminari che gli autori hanno tenuto sul loro stesso lavoro.

Un primo gruppo di lezioni, circa la metà del volume, si riferisce alla teoria della struttura del nucleo ed alle proprietà della materia nucleare; gli autori ne sono: HUGENHOLTZ, BRUECKNER, BLOCH, DE DOMINICIS, MOTTELSON, WEISSKOPF, STRANTINSKY, LIPTIN, BELIAEV. Un secondo gruppo è invece diretto verso i fluidi costituiti da bosoni

e fermioni e gli autori ne sono: Bohm, Pines, Schrieffer, Lynton, Huang. Per rendere la raccolta più accessibile alle possibilità economiche di molti lettori, l'editore ha anche fornito un'edizione di prezzo circa metà per le due parti separate.

Non c'è dubbio che si tratta di una raccolta di notevole interesse e di grande attualità e che lo sforzo della Scuola di Les Houches va ancora una volta ricordato e lodato. Tuttavia questa raccolta, considerata come un libro a se stante, non è scevra di lacune e risente del carattere frammentario dei diversi articoli.

G. Careri

Advances in Semi-Conductor Science. General Editor: H. Brooks, Pergamon Press (pagg. 553, prezzo 100 s.).

Il volume contiene i lavori presentati al Congresso mondiale sui semiconduttori, tenutosi nello Stato di New York dal 18 al 22 agosto 1958.

I lavori sono in numero di 132 e sono divisi per sessioni ognuna delle quali raggruppa ricerche sullo stesso argomento riproducendo fedelmente l'andamento del Congresso; ad ogni lavoro sono aggiunte le discussioni che ne hanno seguito la presentazione. Una sessione speciale riassuntiva è dedicata a 5 conferenze che hanno lo scopo di fare il punto della situazione e di sintetizzare alcuni dei risultati più salienti presentati.

Una delle cose che risultano subito evidenti è che, mentre il Congresso di Amsterdam del 1954 aveva rivelato una tecnica completamente nuova per la misura delle masse efficaci, questo Congresso presenta pochissimi lavori sulla risonanza ciclotronica, quasi questa tecnica sia stata momentaneamente abbandonata. La ragione è probabilmente nella limitazione imposta dalla necessità di avere per tali esperienze materiali con un lungo tempo di rilassamento per le collisioni dei portatori di carica. Il problema attuale sembra quello di superare tale limitazione.

L'enfasi di questo Congresso è posta principalmente su argomenti più tradizionali quali gli effetti dovuti alla superficie, l'assorbimento eccitonico e studi di mobilità nei semiconduttori più noti e nei composti intermetallici.

I risultati sugli effetti di superficie sono ancora di natura piuttosto qualitativa ma permettono di mettere in evidenza l'esistenza di livelli elettronici accettori alla superficie. Questi sono dovuti all'interruzione della periodicità alla superficie e sono stati previsti da Tamm nel 1932 sulle basi di un semplice modello unidimensionale; essi vengono chiamati « stati veloci » a causa del breve tempo di rilassamento. Oltre ad essi, altri livelli elettronici sono presenti per il trattamento che la superficie ha subito e sono probabilmente localizzati sulla superficie esterna del gas adsorbito: essi vengono chiamati « stati lenti ». Di qui la necessità di distinguere tra superfici ideali o « pulite » e superfici « reali ». Tra i lavori su superfici pulite sono particolarmente notevoli quelli di Fansworth, Missman e Handler.

Due intere sezioni del Congresso sono dedicate a lavori su eccitoni. Il concetto tradizionale dell'eccitone come uno stato legato di elettrone e buca fa pensare che ci si dovrebbero aspettare transizioni del tipo idrogenoide. Una serie di misure di Gross e di Nikitine in alcuni composti semiconduttori, quali il Cu_2O, rivela in effetti tali transizioni, delle quali viene anche determinato l'effetto Stark e l'effetto Zeeman. Negli alogenuri alcalini, tuttavia, si osservano poche bande di assorbimento e una loro interpretazione teorica con il modello di Frenkel perfezionato da Wannier è tuttora incompleto. Osservazioni di assorbimento eccitonico in Germanio e Silicio sono presentate da Macfarlane e col-

laboratori e da HAYNES e collaboratori. Contributi teorici sugli eccitoni vengono presentati e discussi da HAKEN e da MUTO e collaboratori.

Tra i molti studi di trasporto vanno menzionate le ricerche sulle variazioni di mobilità di elettroni in presenza di un forte campo elettrico; una rassegna completa degli effetti associati a questi cosidetti « elettroni caldi » viene presentata da KOENIG.

Di estremo interesse sono pure i lavori di JOFFÉ e collaboratori su un gran numero di composti intermetallici; essi sembrano provare che quando si ha a che fare con semiconduttori a bassa mobilità, nei quali il libero cammino medio degli elettroni e delle buche è inferiore al parametro reticolare, i concetti statici che presiedono alla teoria del trasporto nei metalli e nei semiconduttori abituali non possono più essere usati.

Il fondamento teorico per la comprensione generale delle proprietà dei semiconduttori rimane la teoria delle bande e anche a questo Congresso due sezioni sono dedicate a calcoli di questo tipo. In alcuni lavori appare lo sforzo di svolgere calcoli sempre più precisi, e in altri lo sforzo di trovare schemi di interpolazione o approssimazioni che consentano di ragionare anche su cristalli complessi. Nello sviluppare la teoria delle bande si trascurano le correlazioni tra gli elettroni dovute alla loro repulsione coulombiana e ci si può chiedere quale sia la validità dei concetti che in tale modo si ottengono. Particolare importanza in questo senso hanno alcuni lavori di KOHN e altri che descrivono elettroni e buche come eccitazioni di funzioni d'onda a molte particelle; utilizzando il metodo dei « linked clusters », KOHN ha giustificato il concetto di massa efficace dal punto di vista del problema dei molti corpi come pure quello di costante dielettrica.

Molto rimarebbe ancora da dire ma non è purtroppo possibile commentare in modo completo un volume di questa natura. Mi limito a raccomandarlo all'attenzione di tutti i Fisici.

E. BASSANI

Vacancies and Other Point Defects in Metals and Alloys. Institute of Metals Monograph no. 23 (The Institute of Metals, London 1958), pag. 248, 40 s.

Il libro raccoglie i testi di sei lavori, aventi sostanzialmente carattere di rassegna, che furono presentati al simposio dell'Institute of Metals tenuto a Harwell nel dicembre 1957. Cinque articoli sono dedicati ai difetti puntiformi, in particolare posti reticolari vacanti, in metalli e leghe, mentre un articolo riguarda i difetti puntiformi nei solidi ionici, con particolare riferimento agli alogenuri alcalini.

I primi due articoli, dovuti a COTTRELL ed a BROOM e HAM, discutono in dettaglio gli effetti esercitati sulle proprietà fisiche dei metalli, a temperatura di autodiffusione, da difetti puntiformi introdotti in soprassaturazione mediante irraggiamento o tempra o lavorazione a freddo o (in composti intermetallici) producendo deviazioni controllate dalla composizione stechiometrica. In particolare nell'articolo di COTTRELL vengono trattati l'indurimento da irraggiamento, da lavorazione a freddo e da fatica, la determinazione delle energie di formazione e di moto di posti vacanti nei metalli mediante tecniche di tempra, ed i vari tipi di interazione fra difetti puntiformi e dislocazioni; mentre il lavoro di BROOM e HAM considera gli effetti dei difetti puntiformi su energia interna, densità e parametro reticolare ai raggi X, proprietà elettriche, termiche e magnetiche, e risonanza magnetica nucleare. L'articolo di LOMER, e quello di MCLEAN, studiano rispettivamente il ruolo dei difetti puntiformi

nella diffusione e la loro influenza sulle proprietà meccaniche, con particolare enfasi sull'ascensione delle dislocazioni. L'articolo di WILLIAMS e HAYFIELD riporta interessanti studi dello stato di disordine presso la superficie dei metalli, e di fenomeni di notevole importanza tecnica quali ossidazione e corrosione: un soggetto di recente interesse, e raramente trattato. Infine il lavoro di PRATT costituisce una valida, seppur in alcuni punti frettolosa, rassegna della vasta informazione raccolta sull'influenza dei difetti puntiformi sulle proprietà meccaniche dei cristalli ionici, e presenta le ricerche recenti sullo sforzo critico di deformazione plastica in alogenuri alcalini soggetti a vari trattamenti: appare chiaro dalla lettura dell'articolo che accanto allo studio delle proprietà plastiche sarebbe utile riprendere lo studio dell'attrito interno in questi solidi, poichè in essi l'interazione fra difetti puntiformi e dislocazioni presenta notevoli proprietà caratteristiche, assenti nei metalli.

L'assenza di un capitolo introduttivo rende il libro adatto soltanto a ricercatori già introdotti nel campo dei difetti nei solidi. Per questi il libro, opera di specialisti nel campo, apparirà di notevole interesse, e sarà utile sia come rassegna critica di risultati sperimentali e teorici per lo più dispersi in periodici specializzati, sia per la vastissima bibliografia. Sebbene la rassegna ricopra l'informazione raccolta nel periodo pre-1957, informazione su ricerche di più recente pubblicazione è contenuta nelle trentacinque pagine finali, ove sono presentati i testi delle discussioni che hanno accompagnato la presentazione dei lavori.

M. P. TOSI

Direttore responsabile: G. POLVANI

Tipografia Compositori - Bologna

Questo Fascicolo è stato licenziato dai torchi il 15-II-1960